TECHNISCHE UNIVERSITÄT MÜNCHEN

Klinik und Poliklinik für Vaskuläre und Endovaskuläre Chirurgie

Klinikum rechts der Isar der Technischen Universität München

(Univ.-Prof. Dr. H.-H. G. U. Eckstein)

Evaluation of patient specific mechano-biological interactions in abdominal aortic aneurysm wall

Fadwa Schmies

Vollständiger Abdruck der von der Fakultät für Medizin der Technischen Universität München zur Erlangung des akademischen Grades eines

Doktors der Naturwissenschaften (Dr. rer. nat.)

genehmigten Dissertation.

Vorsitzende: Univ.-Prof. Dr. G. Multhoff

Prüfer der Dissertation:

1. Univ.-Prof. Dr. H.-H. G. U. Eckstein
2. Priv.-Doz. Dr. V. Hösel (nur schriftliche Beurteilung)
   Univ.-Prof. Dr. J. Müller (nur mündliche Prüfung)
3. Univ.-Prof. Dr. A. Schober

Die Dissertation wurde am 10.12.2015 der Technischen Universität München eingereicht und durch die Fakultät für Medizin am 06.07.2016 angenommen.

Eidesstattliche Erklärung

Ich erkläre an Eides statt, dass ich die bei der promotionsführenden Einrichtung bzw. Fakultät der Medizin der TUM zur Promotionsprüfung vorgelegte Arbeit mit dem Titel:

„Evaluation of patient specific mechano-biological interactions in abdominal aortic aneurysm wall”

in der Klinik und Poliklinik für Vaskuläre und Endovaskuläre Chirugie, Klinikum rechts der Isar der Technischen Universität München unter der Anleitung und Betreuung durch Prof. Dr. med. Hans-Henning Eckstein ohne sonstige Hilfe erstellt und bei der Abfassung nur die gemäß § 6 Abs. 6 und 7 Satz 2 angegebenen Hilfsmittel benutzt habe.

Ich habe keine Organisation eingeschaltet, die gegen Entgelt Betreuerinnen und Betreuer für die Anfertigung von Dissertationen sucht, oder für mir obliegenden Pflichten hinsichtlich der Prüfungsleistungen für mich ganz oder teilweise erledigt.

Ich habe die Dissertation in dieser oder ähnlicher Form in keinem anderen Prüfungsverfahren als Prüfungsleistung vorgelegt.

Die Dissertation wurde an nachstehend aufgeführten Stellen auszugweise veröffentlicht:

> **Fadwa Tanios**, Michael W Gee, Jaroslav Pelisek, Sebastian Kehl, Jonas Biehler, Verena Grabher-Meier, Wolfgang A Wall, Hans-Henning Eckstein, Christian Reeps. Interaction of biomechanics with extracellular matrix components in abdominal aortic aneurysm. Eur J Vasc Endovasc Surg. 2015;50(2):167-174.
>
> Christian Reeps, Sebastian Kehl, **Fadwa Tanios**, Jonas Biehler, Jaroslav Pelisek, Wolfgang A Wall, Hans-Henning Eckstein and Michael W Gee. Biomechanics and gene expression in abdominal aortic aneurysm. J Vasc Surg. 2014;60(6):1640-7.
>
> **Fadwa Tanios**, Jaroslav Pelisek, Brigitta Lutz, Benedikt Reutersberg, Michael Kallmayer, Edouard Matevossian, Kristina Schwamborn, Volker Hösel, Hans-Henning Eckstein,

Christian Reeps. CXCR4: a potential marker for inflammatory activity in abdominal aortic aneurysm wall. Eur J Vasc Endovasc Surg. 2015;50(6):745-53.

Ich habe den angestrebten Doktorgrad noch nicht erworben und bin nicht in einem früheren Promotionsverfahren für den angestrebten Doktorgrad endgültig gescheitert.

Die öffentlich zugängliche Promotionsordnung der TUM ist mir bekannt, insbesondere habe ich die Bedeutung von § 28 (Nichtigkeit der Promotion) und § 9 (Entzug des Doktorgrades) zur Kenntnis genommen. Ich bin mir der Konsequenzen einer falschen Eidesstattlichen Erklärung bewusst.

Mit der Aufnahme meiner personenbezogenen Daten in die Alumni-Datei bei der TUM bin ich einverstanden.

München, den Unterschrift

My Parents

Contents

Acknowledgements

First of all I would like to thank God, whom without, none of this was possible.

I would like to express my sincere gratitude to my advisor Prof. Dr. med. Hans-Henning Eckstein for giving me the opportunity to do my doctoral thesis in his laboratory of Vascular Biology, at the Department of Vascular and Endovascular Surgery, Klinikum rechts der Isar, Technische Universität München and for the support of my PhD study and research. His wide knowledge, his logical way of thinking and his encouragement have also been of great value for my thesis.

I would like to acknowledge PD Dr. rer. nat. Volker Hösel for being my second advisor and for his time, support and collaboration during this thesis. His constructive comments and his advice have been of great help.

I am also very thankful to Prof. Dr. Johannes Müller for accepting being my second examiner.

My thanks are also addressed to my mentor PD. Dr. med. Christian Reeps for giving me the possibility to work with a very interesting and challenging topic. I am thankful for his support, the fruitful discussions and the excellent guidance through the whole period of my thesis.

My deep appreciation goes to PD. Dr. rer. nat. Jaroslav Pelisek, who provided me with the scientific advice and the enthusiasm without which this work could not be completed in a timely manner. I would like to thank him for being always there for me, for his encouragement, guidance and support throughout this research project and for his friendship and understanding.

My great thanks go to Mrs. Renate Hegenloh for her technical assistance along the way, for her encouragement, support and for making the working environment enjoyable. I owe certainly a great thank to the lab members, especially Almut Glinzer, Martina Lammel and Veronika Klaus, who contributed to the work a nice and pleasant atmosphere.

To my collaborators from the laboratory of Mechanics and High Performance Computing Group, Technische Universität München, thank you for working with me and being able to provide the mechanical testing and the FEA Simulation which are an important part of this work. Special thanks go to Prof. Dr. Ing. Michael Gee for working closely with me to discuss methodologies and results in terms of mechanics.

My deepest thanks go also to my German family for all the love and family spirit they have offered me, and for accepting me with open arms and making feel like home in Germany.

I would like to thank my parents and family in Lebanon for their endless love and support, despite of the physical distances that separated us.

Last but not least, I would like to thank my husband Tobias who has been a great source of support during these endeavours. Thank you for listening, for your encouraging words and for all the passion and love you constantly bring to me.

Munich, December 2015 Fadwa Schmies

Abstract

This thesis contributes to the field of the individualized rupture risk stratification and the analysis of patient specific mechano-biological interactions of abdominal aortic aneurysm (AAA).

So far, little is known about the relationship between extracellular matrix (ECM) proteins or expression of destabilizing inflammatory, proteolytic and structural factors and locally acting mechanical forces in the human abdominal aortic aneurysm (AAA) wall. Therefore, the aim of the thesis was to investigate various ECM components and relevant proteolytic and inflammatory factors of AAA in correlation with the corresponding geometrical parameters and material properties and loads in AAA tissue samples. Furthermore, the potential role of the chemokine receptor CXCR4 and its ligand CXCL12 was evaluated in the pathogenesis of AAA. Finally, the impact of chronic kidney disease (CKD) on patients with AAA were analysed based on the evaluation of mechanical properties and loads of the aortic wall.

For this purpose, 133 aortic wall specimens from 81 AAA patients, who underwent an elective open surgical repair of the aneurysm sac, were included in total. Tissue samples were divided for corresponding immunohistological, immunohistochemical, biological and mechanical analyses. Furthermore, clinical parameters of the study patients were collected. Collagen type I and type III, total collagen, elastin, and proteoglycans were quantified by computational image analysis from the histological staining. The gene expression of collagen type I and type III, inflammatory factors CD45 and MSR1, proteolytic enzymes matrix metalloproteinases 2 and 9 (MMP-2 and -9) and tissue inhibitor of matrix metalloproteinase 1 (TIMP-1) was analysed by SYBR-Green-based RT-PCR. Material properties of the corresponding AAA tissue samples were assessed by cyclic sinusoidal and destructive tests. Local mechanical conditions of stress and strain were determined by advanced nonlinear finite element analysis (FEA) based on patient preoperative computed tomography data and the derived three dimensional AAA models. Expression analysis of CXCR4 and CXCL12 was performed at mRNA and protein level by RT-PCR and western blot. Immunohistochemical staining of corresponding histological sections for CD3 (T-cells), CD20 (B-

cells), and CD68 (macrophages) was performed to determine the cellular localization of CXCR4 and CXCL12. All data sets were analysed with SPSS 20.0 using Mann-Whitney U test and Spearman's rank correlation coefficient.

The findings of the present thesis indicate that in AAA increased locally acting mechanical forces are strongly involved in the synthesis of ECM at both mRNA and protein level and significantly influence the mechanical stability of the AAA wall. The protein amount of collagen type I and type III, and total collagen was significantly associated with local wall stress and strain. The AAA wall failure tension exhibited a significant positive correlation with collagen type I, total collagen, and proteoglycans. The alpha-stiffness correlated significantly with collagen type I and type III and total collagen, while the beta-stiffness was associated especially with proteoglycans. In contrast, increased thrombus thickness significantly correlated with decrease of collagen type I and type III and total collagen. In addition, the AAA diameter was negatively associated with the amount of elastin. In the AAA wall, the expression of all parameters, contributing to AAA destabilization, analysed in the current thesis, was significant at the mRNA level. With respect to the mechanical properties of the AAA wall, expression of collagen type III correlated with the stiffness parameter alpha and expression of MMP-2 correlated with the stiffness parameter beta and wall strength. Furthermore, significant relationships were observed between the local AAA diameter and the expression of the surface marker for lymphocytes, macrophages and TIMP-1. No interrelation was found between local calculated wall stresses and strains and the gene expression of the destabilizing factors. In addition, the gene expression of CXCR4 and CXCL12 is significantly higher in AAAs than in non-aneurysmal aortae. Likewise, the protein level of CXCR4 was significantly increased in AAA walls, CXCL12 was however not detected. Immunohistochemical analysis revealed that CXCR4 was expressed especially in B- and T- lymphocytes and macrophages, CXCL12 was observed only in plasma cells. Patients suffering from CKD had significantly diminished AAA wall thickness and diameter. Local thrombus thickness was increased and failure tension as well as wall stress and strain of the AAA wall was significantly reduced in CKD patients compared to individuals without CKD. Further correlations were observed between blood potassium and wall strength, failure tension, beta stiffness, wall stress and strain, blood urea nitrogen and failure tension, alpha and beta stiffness and between blood sodium and wall thickness, beta stiffness, wall stress and strain and calcification of the AAA wall correlated to alpha and beta stiffness.

In conclusion, this present thesis revealed significant associations between the ECM composition and the gene expression of relevant destabilizing factors of AAA with the mechanical properties and loads of the diseased aortic wall. Increased locally acting stress and strain promote the synthesis of collagen and proteoglycans as a function of increased failure tension and enhanced gene expression is effected by geometrical and mechanical properties of the AAA wall. The chemokine receptor CXCR4 and its ligand CXCL12 seem to be involved in the AAA progression as well. In addition, mechanical properties of the AAA wall are significantly impaired in patients with CKD, suggesting higher AAA rupture risk in these patients especially at smaller AAA diameters. Hence, the thesis provides new insights into the pathogenesis of AAA. Further research will be able to shed additional light onto the personalized rupture risk stratification of the AAA patients.

Keywords:

AAA, structural proteins, biomechanics, rupture risk, elastin, collagen, CXCR4, CXCL12, CKD, wall stress, wall strain.

Zusammenfassung

Die vorliegende Arbeit stellt einen Forschungsbeitrag auf dem Gebiet der individualisierten Rupturriskostratifizierung und der Analyse der mechanobiologischen Wechselwirkungen des abdominalen Aortenaneurysmas (AAA) dar.

Bisher ist wenig über die Beziehung zwischen den extrazellulären Matrix (EZM) Proteinen oder der Expression destabilisierender inflammatorischer, proteolytischer und struktureller Faktoren mit lokal wirkenden mechanischen Kräften in der menschlichen AAA-Wand bekannt. Daher wurden verschiedene EZM-Komponenten und relevante proteolytische und inflammatorische Faktoren der AAA-Pathogenese in Korrelation mit den entsprechenden geometrischen Parametern, Materialeigenschaften und Belastungen in Gewebeproben der AAA-Wand untersucht, ebenso die mögliche Rolle des Chemokinrezeptors CXCR4 und seines Liganden CXCL12 bei der AAA-Pathogenese. Zusätzlich wurden, basierend auf der Evaluation der mechanischen Eigenschaften und Belastungen der Aortenwand, die Auswirkungen einer chronischen Nierenerkrankung (CKD) auf Patienten mit AAA ausgewertet.

Insgesamt wurden von 81 AAA-Patienten, bei denen eine offene operative Aneurysmasanierung durchgeführt wurde, 133 Aortenwandproben entnommen und für entsprechende immunhistologische, immunhistochemische, biologische und mechanische Analysen vorbereitet. Weiterhin wurden die klinischen Parameter dieser Patienten erhoben. Aus den histologischen Färbungen wurden Kollagen Typ I und Typ III, Gesamtkollagen, Elastin und Proteoglykanen mittels computergestützter Farb-Bildanalyse quantifiziert. Die Genexpression von Kollagen Typ I und Typ III, inflammatorische Faktoren (CD45 und MSR1), proteolytische Enzyme von Matrix Metalloproteinasen 2 und 9 (MMP-2 und -9) und deren Inhibitor TIMP-1 wurden durch SYBR-Grün mittels RT-PCR analysiert. Die Charakterisierung der Materialeigenschaften der entsprechenden AAA-Gewebeproben erfolgte mithilfe zyklischer und destruktiver Zugversuche. Die lokalen mechanischen Belastungen der Wandspannungen und -dehnungen wurden durch eine erweiterte, nichtlineare Finite-Elemente-Analyse (FEA), basierend auf den, aus präoperativen

Computertomographie-Daten der Patienten abgeleiteten, dreidimensionalen AAA-Modellen bestimmt. Die Expressionsanalyse von CXCR4 und CXCL12 wurde auf mRNA- und Proteinebene mittels RT-PCR und Western-Blot analysiert. Immunhistochemische Färbungen korrespondierender histologischer Schnitte für CD3 (T-Zellen), CD20 (B-Zellen) und CD68 (Makrophagen) wurden durchgeführt, um die zelluläre Lokalisation von CXCR4 und CXCL12 bestimmen zu können. Alle Daten wurden in SPSS 20.0 mit dem Mann-Whitney U-Test und dem Spearman-Rangkorrelationskoeffizienten analysiert.

Die Ergebnisse der vorliegenden Arbeit zeigen, dass in der AAA-Wand erhöhte lokal wirkende mechanische Kräfte stark an der Synthese von EZM sowohl auf der mRNA- als auch auf der Proteinebene beteiligt sind und die mechanische Stabilität der AAA-Wand wesentlich beeinflussen. Die Proteinmenge des Kollagens Typ I und Typ III und des Gesamtkollagens war signifikant mit der lokalen Wandspannung und -dehnung assoziiert. Die Grenzfestigkeit der AAA-Wand zeigte eine signifikante positive Korrelation mit dem Kollagen Typ I, dem Gesamtkollagen und den Proteoglykanen. Die Alpha-Steifigkeit korrelierte signifikant mit den Kollagenen Typ I und Typ III und dem Gesamtkollagen, während die Beta-Steifigkeit mit den Proteoglykanen assoziiert war. Bei höherer Thrombusdicke zeigte sich hingegen eine Abnahme des Kollagens Typ I und Typ III und des Gesamtkollagens. Zusätzlich wurde eine negative Korrelation zwischen dem AAA-Durchmesser und dem Elastingehalt festgestellt. Die Expression aller in dieser Arbeit untersuchten Parameter, die zur AAA-Destabilisierung führen, waren signifikant auf der mRNA-Ebene exprimiert. Bei der Betrachtung der mechanischen Eigenschaften der AAA-Wand zeigte sich, dass die Expression von Kollagen Typ III mit dem Steifigkeitsparameter Alpha und die Expression von MMP-2 mit dem Steifigkeitsparameter Beta sowie der Wandfestigkeit negativ korrelieren. Weiterhin wurden signifikante Zusammenhänge zwischen den lokalen AAA-Durchmessern und der Expression der Oberflächenmarker für Lymphozyten, Makrophagen und TIMP-1 beobachtet. Keine Korrelationen konnten zwischen der berechneten lokalen Wandspannung und -dehnung und der Genexpression destabilisierender Faktoren festgestellt werden. Darüber hinaus ist die Genexpression von CXCR4 und CXCL12 im Vergleich zur nicht-aneurysmatischen Aorta in AAA signifikant erhöht. Ebenso zeigte die Proteinexpression von CXCR4 eine erhöhte Expression in AAA, jedoch war CXCL12 nicht detektierbar. Durch die immunhistochemische Analyse konnte gezeigt werden, dass CXCR4 in der AAA-Wand, insbesondere in B- und T-Lymphozyten und Makrophagen exprimiert ist, CXCL12 jedoch nur in Plasmazellen. Patienten mit CKD haben im Vergleich zu

Patienten ohne CKD eine wesentlich dünnere AAA-Wanddicke und einen kleineren AAA-Durchmesser. Die lokale Thrombusdicke war bei diesen Patienten erhöht, Grenzfestigkeit, Spannungen und Dehnungen der AAA-Wand waren deutlich reduziert. Weitere Korrelationen wurden zwischen Blutkalium und Wanddicke, Grenzfestigkeit, Beta-Steifigkeit, Wandspannung und Dehnung festgestellt. Die Werte des Blutharnstoffstickstoffes korrelierten mit der Grenzfestigkeit und der Alpha- und Beta-Steifigkeit. Schließlich korrelierte Blutnatrium mit der Wanddicke, der Beta-Steifigkeit, der Wandspannung und der Dehnung. Die AAA-Verkalkung korrelierte mit der Alpha- und Beta-Steifigkeit.

Zusammenfassend zeigen die Ergebnisse der vorliegenden Arbeit signifikante Zusammenhänge zwischen der EZM-Komposition und der Genexpression relevanter destabilisierender Faktoren der AAA-Wand mit den mechanischen Eigenschaften und Belastungen des AAA. Erhöhte lokal wirkende Wandspannungen und -dehnungen promoten die Synthese von Kollagen und Proteoglykanen in Abhängigkeit von erhöhter Wandfestigkeit. Die verstärkte Genexpression ist durch die geometrischen und mechanischen Eigenschaften der AAA-Wand beeinträchtigt. Der Chemokinrezeptor CXCR4 und sein Ligand CXCL12 scheinen auch eine Rolle bei der Entstehung und Progression von AAA zu haben. Des Weiteren sind die mechanischen Eigenschaften der AAA-Wand bei Patienten mit CKD signifikant beeinträchtigt. Diese Patienten haben ein höheres Rupturrisiko des AAA, besonders bei kleineren AAA-Durchmessern.

Daher ermöglicht diese Arbeit neue Einblicke in die AAA-Pathogenese. Weitere Forschung kann dazu beitragen, die individualisierte Rupturrisikostratifizierung der AAA-Patienten zu verbessern.

Keywords:

AAA, Strukturproteine, Biomechanik, Rupturrisiko, Elastin, Kollagen, CXCR4, CXCL12, CKD, Wandspannung, Wanddehnung.

List of Figures

List of Tables

Abbreviations

A	cross sectional area
AAA	Abdominal aortic aneurysm
ACE	Angiotensin converting enzyme
APAAP	Alkaline Phosphatase-Anti-Alkaline Phosphatase
APS	Ammonium persulfate
ASA	Acetyl salicylic acid
b	Band
BCA	Bicinchoninic acid
BSA	Bovine serum albumin
bg	Background
C	Celsius
CD	Cluster of differentiation
cDNA	Complementary deoxyribonucleic acid
CHD	coronary heart disease
CKD	Chronic kidney disease
CT	Computer tomography
CXCL12	C-X-C motif chemokine 12
CXCR4	C-X-C chemokine receptor type 4
DM	Diabetes mellitus
Dpi	Dots per inch
DNA	Deoxyribonucleic acid
EC	Endothelial cells
ECM	Extracellular matrix
EDTA	Ethylenediaminetetraacetic acid
eGFR	estimated glomerular filtration rate
EVAR	Endovascular aneurysm repair
EvG	Elastic van Gieson
F	Force
FEA	Finite element analysis
FFPE	Formalin fixed paraffin-embedded
GAPDH	Glyceraldehyde 3-phosphate dehydrogenase
GM-CDF	Granulocyte-macrophages colony-stimulating factor
h	Hour

HDL	High density lipoprotein
Hz	Hertz
HE	Haematoxylin-Eosin
HIV	Human immunodeficiency virus
HRP	Horse radish peroxidase
hsCRP	High sensitivity C reactive protein
IFN	Interferon
IHC	immunohistochemistry
Il	Interleukin
ILT	Intraluminal thrombus thickness
LDL	Low density lipoprotein
LSAB	Labelled streptavidin-biotin
MCH	Mean corpuscular haemoglobin
MCHC	Mean corpuscular haemoglobin concentration
MCP-1	Monocyte chemotactic protein 1
MCV	Mean corpuscular volume
MHC	Myosin heavy chain
mg	Milligrams
min	Minutes
ml	Millilitres
mm	Millimetres
mM	Millimolar
MPa	Mega Pascal
MMP	Matrix metalloproteinase
mRNA	Messenger ribonucleic acid
N	Newton
NC	Nitrocellulose
NORD	Normalized local diameter
OD	Optical density
OR	Open aneurysm repair
p	Pixels
PAD	Peripheral arterial disease
PAGE	Preparation polyacrylamide gel electrophoresis
PBS	Phosphate buffered saline
PCR	Polymerase chain reaction
PVDF	Polyvinylidene fluoride
RIPA	Radio immunoprecipitation assay
RNA	Ribonucleic acid
ROI	Region of interest
Rpm	Round per minute
RT	Room temperature

RT-PCR	Reverse transcription polymerase chain reaction
s	Seconds
SDF-1α	Stromal cell-Derived factor 1 alpha
SDS	Sodium dodecyl sulphate
SEF	Strain energy function
SLRP	Small leucine rich proteoglycans
SMC	Smooth muscle cell
TA	Tunica adventitia
TBE	TRIS borate EDTA
TBS	TRIS buffered saline
TEMED	Tetramethylethylenediamine
TI	Tunica intima
TM	Tunica media
TNF	Tumor necrosis factor
TRIS	Trishydroxymethylaminomethane
V	Volt

Chapter 1 General Introduction

This chapter aims to provide a general background about abdominal aortic aneurysm (AAA), its pathophysiology, the risk factors contributing to the development, growth and rupture of aneurysms and finally the objectives of this study.

1.1 Abdominal aortic aneurysm

1.1.1 Epidemiology of AAA

The aorta is the main artery in the human body which conveys the oxygenized blood directly from the left ventricle of the heart to all parts of the body through the systemic circulation. An aortic aneurysm is a local dilatation in the aorta of more than 1.5 times the original diameter (Johnston et al., 1991). Despite the fact that aneurysms can occur in every part of the aorta, the most common site for development of the aortic aneurysms is located in the abdominal aorta (*Figure 1-1*), below the level of the renal arteries and above the aortic bifurcation to the common iliac arteries (Crawford and Cohen, 1982). A diameter of 3.0 cm or larger is generally used as indication for an AAA (Lederle et al., 1997; United Kingdom Small Aneurysm Trial Participants, 2002).

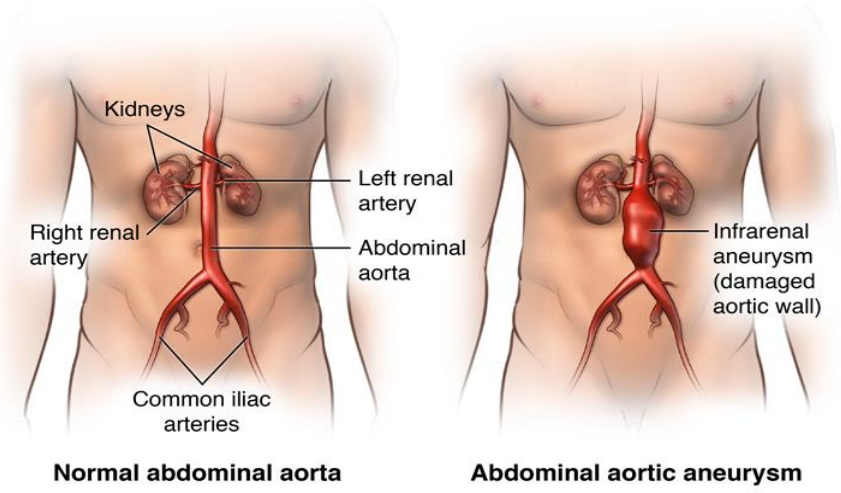

Figure 1-1: Normal abdominal Aorta (left) and abdominal aortic aneurysm (right). Image is retrieved from: http://www.hopkinsmedicine.org/healthlibrary/test_procedures/cardiovascular/abdominal_aortic_aneurysm_repair_92,P08291/

AAA occurs mostly in the elderly population. The prevalence of AAA greater than 3.0 cm for people over 65 years of age is 5.5% in men and 1.3% in women (Eckstein et al., 2009), whereas over 80% of AAA are asymptomatic (Heider et al., 2007). With increasing maximum diameter, the risk of rupture of an AAA increases exponentially (Brewster et al., 2003; Reed et al., 1997). Once an AAA has ruptured, the chances of survival without an immediate treatment are very low. Approximately 90% of all ruptured aneurysms result in death (Kniemeyer et al., 2000; Shimizu et al., 2006; Heron, 2011). Other risk factors for AAA include advanced age, male gender, smoking, hypertension, positive family history and atherosclerosis (Brewster et al., 2003; Lederle et al., 1997; Pleumeekers et al., 1995). Even though the aetiology of AAA is still poorly understood, it has been recognized to be a multifactorial and principally degenerative disease, arising from a complex interaction among different biological factors (Lederle et al., 1997; Wassef et al., 2001). If left untreated, the most AAAs progress toward further enlargement and eventually will rupture.

1.1.2 Anatomy of the AAA wall

The aortic wall consists of three layers. The tunica adventitia is the outer layer, containing connective tissue and the vasa vasorum (nurturing vessels for cells within the arterial wall). The most inner layer is named the tunica intima, in a healthy aorta consisting of a single layer of endothelial cells and a basal membrane. The tunica media represents the middle layer, consisting of smooth muscle cells (SMC) with collagen and elastic fibres. A close relationship between all these three constituents is responsible for properties of the aortic wall. It is generally accepted that AAA is a degenerative disease of the tunica media (Daugherty and Cassis, 2002). The media of an AAA is characterized by a decrease in elastin fibres (Campa et al., 1987), diminished amount of smooth muscle cells (Lopez-Candales et al., 1997) and increased infiltration of inflammatory cells (Shimizu et al., 2006), compared to a healthy aortic wall. Histological comparison shows strong differences in the composition of healthy and aneurysm wall (*Figure 1-2*). These changes affect the integrity of the aortic wall, leading to a decrease in compliance, tensile strength and a progressive dilation of the vessel.

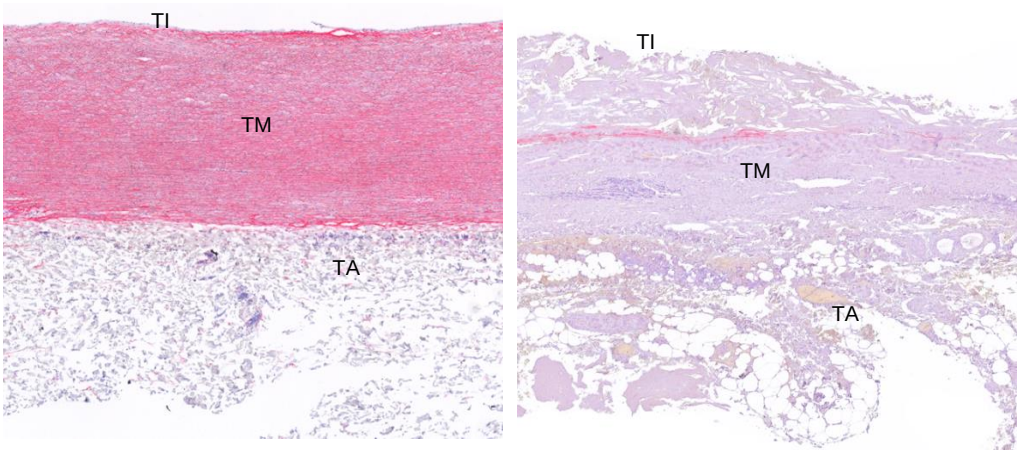

Figure 1-2: Histological staining of healthy (left) and aneurysmatic (right) aortic wall. TI is the tunica intima, TM is the tunica media and TA is the tunica adventitia. The right image of the AAA wall shows a thickened tunica intima, loss of elastin (red), an increase in vasa vasorum and infiltration of fat cells in the tunica adventitia.

1.1.3 Diagnosis and current treatment of AAA

In some cases, AAA can be already diagnosed by a physical examination in which the doctor feels the aneurysm as a soft mass in the abdomen. However, for early reliable detection to reduce the mortality rate of AAA, an ultrasound screening is necessary. This is relevant especially for men over the age of 65, and for women and men of all ages with a positive family history. Women older than 65 with a history of smoking or the presence of other cardiovascular diseases should be investigated as well (Eckstein et al., 2009; Kim et al., 2007; Thanos et al., 2008). Advantages of ultrasonography are the overall availability, the technical feasibility, the low cost, the lack of radiation exposure and a very high sensitivity and specificity of 98% (Lindholt et al., 1999; Gussmann et al., 2008). Other diagnostic methods, such as computer tomography angiography (CTA), magnetic resonance imaging (MRI) and angiography are also being used, when planning e.g. elective open repair (OR) or endovascular repair (EVAR) in AAA patients (Gussmann et al. 2008).

The maximum transverse diameter of an aneurysm, commonly used as main determinant in predicting the risk of rupture (Lederle et al., 2002; Vande Geest et al., 2006), is based on the law of Laplace, which describes a linear relationship between the lumen diameter and the wall stress inside a cylinder with constant wall thickness under luminal pressure. However, this approach fails to predict realistic loads for more complex geometries such as AAAs. Furthermore, some former studies have also demonstrated that small AAAs can also rupture (Choksy et al., 1999; Galland et al., 1998), while some of those aneurysm considered large remain stable and quiescent for years (Chaikof et al., 2009; Conrad, 2007). In addition to the diameter criterion, a high expansion rate is

usually associated with a high rupture risk. Consequently, a maximum transverse diameter of 5.5 cm for men and 4.5 to 5.0 cm for women and an expansion rate of 1 cm per year are currently the most commonly used thresholds to provide an indication for surgical or endovascular treatment (Brewster et al, 2003; Collin, 1999). Below these thresholds it is considered sufficient to perform regular checks in certain time intervals (Collin, 1999).

The main goal of AAA treatment is to exclude the diseased aortic wall from the systemic pressure, using different kinds of vascular graft. In an open repair, a regular graft is sutured to the healthy parts of the aorta by means of transabdominal or retroperitoneal surgery. This major surgical procedure has a 30-day mortality rate of about 5% (Greenhalgh et al., 2004). Endovascular repair is an established alternative to the open repair and is performed guiding a graft inside the patient's artery by a catheter. For the procedure, an incision is made in the skin at the groin, through which a catheter is passed into the femoral artery and directed to the aortic aneurysm. The catheter is used to pass the compressed stent graft to the desired location within the diseased aorta. The stent graft is then opened, creating new artificial walls through which blood then flows. Benefits of endovascular repair are a lower perioperative mortality and a shorter recovery period compared to open repair (Greenhalgh et al., 2004; Brewster et al., 1998; May et al., 1998; Zarins et al., 1999). Also, the long term results show that aneurysm-related mortality is lower for endovascular repair (Lovegrove et al., 2008). However, various complications like incomplete sealing, migration, kinking or material failure of the stent-graft may occur during the procedure as well as some time afterwards (Sandford et al., 2008; Schurink et al., 1999; Laheij et al., 2000). These circumstances lead to an elevated pressure inside the aneurysm and, in the worst case, rupture of the AAA wall (Wolters et al., 2007; Brewster et al., 2003). Therefore, patients who underwent endovascular repair remain under surveillance to follow up the status of the stent-graft over time (Sandford et al., 2008).

1.1.4 Pathogenesis of AAA

The pathogenesis of AAA formation is complex and not yet fully understood. Certain epidemiologic risk factors and comorbidities are associated with AAA development, such as male sex, smoking, advanced age, atherosclerosis, genetic predisposition, hypertension and coronary heart disease (Lederle et al., 1997; Eckstein et al., 2009). However, the relationship between these risk factors and the biological process of aneurysm formation is not clear.

It is known that AAAs are characterized by the destruction of elastin and collagen fibres in the media and adventitia (Krettek et al., 2003), loss of medial smooth muscle cells, continuously thinning the vessel wall (Henderson et al., 1999; Li et al., 1997). These processes are generally accompanied by transmural infiltration of lymphocytes, macrophages and neovascularization (Rizzo et al., 1989; Lopez-Candales et al.; 1997; Michel et al., 2011; Ailawadi et al., 2003). Atherosclerosis is a common underlying feature of aneurysms. It seems however not to be the primary driving factor in the development of AAAs (Blanchard et al., 2000; Shimizu et al., 2006). Atherosclerosis is widespread throughout the vasculature in elderly; however aneurysms only form at specific locations and only in certain individuals. Additionally, atherosclerosis is primarily a disease of the intima, whereas aneurysm formation primarily affects tunica media and adventitia (Ailawadi et al., 2003).

Moreover formation of neovessels and migration of inflammatory cells into the arterial wall appear to result from hemodynamic forces, thrombus induced hypoxia conditions, as well as destruction of medial proteins and other unknown factors. It is hypothesized that the migration of lymphocytes and release of various proteolytic enzymes such as matrix metalloproteinases (MMPs) take place due to the release of various cytokines and reactive oxygen species from these inflammatory cells. All these features lead to the destabilization of the aortic wall through the degradation of the extracellular matrix (ECM) in the tunica media and a subsequent enlargement of the aorta. Moreover, increased wall stress facilitates further remodelling and expansion in the aortic diameter. These self-reinforcing processes lead to thinning and weakening of the AAA wall, which, finally, is no longer able to withstand the hemodynamic forces and ruptures (Ailawadi et al., 2003). The predominant localization of aneurysms in the infrarenal aorta seems to be on the one hand due to a reduced elastin-collagen ratio of abdominal aorta compared to more proximal sections (Ailawadi et al., 2003), on the other hand because of the increased wall stress due to the hemodynamic forces (Moore et al., 1992). Decisive factors for the main biological pathogenesis of the aortic wall are the proteolytic degradation of the connective tissue, inflammation and immune responses, the biochemical wall stress and molecular genetic factors (Wassef et al., 2001). However, the role of these various biological processes has not yet been directly compared to the mechanical properties of AAA.

1.2 Comorbidity of abdominal aortic aneurysm

1.2.1 Overview of AAA comorbidity

There are several risk factors responsible for AAA formation, including gender, age, smoking, family history, ethnicity, cholesterol, hypertension and diabetes.

The prevalence of AAA in males is significantly increased compared to females; however, the risk of aneurysm rupture is almost four to six times higher in women than men (Morris et al, 1994; Scott et al., 1995; Lederle et al., 2001; Sweeting et al., 2012). Moreover, after the age of 60 years the risk of AAAs increases dramatically (Singh et al., 2001; Powell and Greenhalgh, 2003). Clinically relevant aneurysms (more than 4.0 cm in diameter) are present in approximately 1% of men between 55 and 64 years of age, and the prevalence increases by 2% to 4% per decade thereafter (Singh et al., 2001; Powell and Greenhalgh, 2003). In addition, AAAs develop in women approximately 10 years later than in men (McFarlane, 1991). Lederle and colleagues found that AAAs occurs more frequently in white people than in black ones (Lederle et al., 2000).

Smoking is among the major risk factors for aneurysm formation (Hirsch et al., 2006). Lederle and colleagues for instance found in their study that smoking was the most strongly associated factor with AAA (Lederle et al., 2000). The association with smoking was directly related to the number of years of smoking and the association decreased with the number of years after cessation of smoking (Lederle et al., 1997).

The effect of family history on AAA was first hypothesized by Clifton (1977) with further studies identifying the frequency of AAA in first degree relatives as 15-20% (Kuivaniemi et al., 2003), with familial AAAs more likely to occur at a younger age, often leading to rupture (Salo et al., 1999; Sakalihasan et al., 2005). A positive family history is another potential factor that significantly increases the risk of AAA (Fleming et al., 2005).

AAAs are more common in patients with atherosclerosis, with a prevalence of approximately 5% in patients with coronary artery disease, and approximately 10% in those with arteriosclerosis obliterans (Cabellon et al., 1983; Bengtsson et al., 1989). Hypertension has also been found to be associated with AAA (Lederle et al., 1997). Additionally, hypercholesterolemia has been reported to be another risk factor for AAA, with a meta-analysis of 8 studies revealing a significantly lower serum HDL cholesterol level and significantly higher serum LDL cholesterol in the AAA group

compared to controls (Takagi et al., 2010). Moreover, AAA has been found to be less common in patients with diabetes (Lederle et al., 2000). Diabetes suppresses plasmin production (an activator of MMPs) through plasminogen activator inhibitor-1 (Dua et al., 2010). This leads to a decrease in the rate of aortic wall degradation, resulting in the thicker aortic wall observed in patients with diabetes (Lederle et al., 2002). The prevalence of AAA in patients with peripheral arterial disease (PAD) is reported to be as high as 9%, with a meta-analysis of 8 studies identifying an increased risk of AAA in patients with PAD (Cornuz et al., 2004; Giugliano et al., 2012).

1.2.2 Influence of chronic kidney disease on the mechanical properties in AAA-patients

AAA has been conceded to be a serious life-threatening incidence in the elderly population that often leads to death in case of rupture (Töpel et al., 2014; Eckstein et al., 2014; Reeps et al., 2009). AAA occurs frequently in individuals with advanced atherosclerosis, leading to mechanical weakening of the aortic wall, along with degenerative ischemic alterations (Greenhalgh et al., 1998). A surgical or endovascular repair is usually performed if the AAA diameter exceeds 5.5 cm (Greenhalgh et al., 1998; Cornuz et al., 2004). However, some unexpected ruptures of smaller aneurysms may occur as well, while many larger AAAs stay stable for an extended period of time (Greenhalgh et al., 1998; Cornuz et al., 2004; Chaikof et al., 2009; Conrad et al., 2007). Therefore, the AAA diameter is not a reliable patient-specific rupture risk criterion as has already been confirmed by several studies (Reeps et al., 2013; Vande Geest et al., 2006). Moreover, haemodynamic forces act on the aortic vessel due to pulsatile blood pressure and flow. Consequently, from the biomechanical point of view, the rupture occurs when the wall stress derived from the blood pressure exceeds the wall strength within the arterial wall (Reeps et al., 2013; Vande Geest et al., 2006; Humphrey et al., 2008; Raghavan et al., 2000; Marini et al., 2012).

Nevertheless, the patients' medical history may also influence the AAA development and consequently the risk of rupture. Recently, our group has provided evidence that patients with chronic kidney disease (CKD) had significantly reduced AAA wall failure tension (Reeps et al., 2013). Patients with CKD have often increased atherosclerotic burden, augmented arterial stiffness and higher prevalence of cardiovascular disease (Moody et al., 2013; Keith et al., 2004; Pelisek et al., 2011). Thereby, CKD might be also considered as a risk factor of AAA (Reeps et al., 2013).

So far, the direct impact of CKD on the prevalence and progression of AAA as well as rupture risk is still unclear and there is no direct comparison of the material properties of AAA wall in patients with and without CKD. Therefore, it is considered to be very beneficial to test the hypothesis that patients with CKD might have an increased risk of rupture of AAA in order to gain more insights in terms of the rupture risk evaluation of AAA.

1.3 Rupture risk stratification of abdominal aortic aneurysm

1.3.1 Clinical criteria for AAA rupture

For the determination under what circumstances an AAA necessitates a surgical intervention, the risk of AAA rupture must be weighed cautiously against the risks associated with surgery and the patient's pre-existing conditions and medical history. In current clinical practice, the risk of rupture is based on the maximum anterior-posterior diameter and an elective repair procedure is recommended when the diameter reaches 5.5 cm or when the diameter grows more than 1 cm per year (Greenhalgh et al., 1998).

An autopsy study (Darling et al., 1977) analysed 24,000 non-specific reports and found 473 non-resected AAA's, of which 118 were ruptured. Of the 265 aneurysms smaller than 5.0 cm in diameter, 34 (12.8%) were ruptured, demonstrating that for a remarkable number of small AAAs, the elective repair threshold of 5.5 cm in diameter was not a sufficient criterion. Moreover, other studies showed that small aneurysms can also rupture with an association mortality rate up to 50 % (Valentine et al., 2000), where the 12-year follow up of the UK Small Aneurysm Trial reports an overall mortality of 67.3% for the surveillance group (Powell et al., 2007). Nevertheless, Lederle et al. (2002) studied rupture rate of large AAA's in patients refusing or unfit for elective repair. The 1-year incidence of rupture was 9% for AAA's with diameters between 5.5-5.9 cm. This increased to 33% for AAA's greater than 7 cm. Although the 1-year incidence is significantly high for AAA's over 5.5 cm in diameter, the majority of patients with large aneurysms may not experience rupture. Such patients would be subjected to unnecessary surgical risks in case of elective AAA repair. These findings revealed that the maximum diameter of AAA is not a reliable criterion to assess AAA risk of rupture. For more accurate rupture risk stratification, patient-specific parameters, other than the diameter, have to be considered.

Besides the maximum diameter, it is advised to include the aneurysm expansion rate in the decision for AAA repair (Wolf et al., 1994). When a patient is known to have an AAA, follow-up is in most cases done by ultrasound examination to evaluate the maximum diameter and the diameter growth. The AAA progression is believed to increase with the initial diameter of the AAA (Stonebridge et al., 1996; Vega de Céniga et al., 2008). However, a large variation in growth rate is found between AAAs. While some AAAs stay stable for a considerable period of time, others show a strong enlargement in diameter in a short time period or grow irregularly, with alternating periods of growth and non-growth (Kurvers et al., 2004; Vega de Céniga et al., 2006). Moreover Limet et al. (1991) linked the risk of rupture of AAAs with aneurysm expansion rate and different studies reported an increased mean expansion rate in patients with ruptured AAAs (Lederle et al., 2002; Brown et al., 2003).

Prediction of the future expansion rate of an AAA in an early stage can be used to optimize the follow-up schedule and intervention plans for each patient. So far, both aneurysm rupture and growth are unpredictable by the diameter alone. Better predictors for rupture and growth are required and may be found in a more extended patient-specific analysis, based on biomarker and biomechanical information. This may lead to an optimization of both the follow-up plan and the right moment of aortic repair.

1.3.2 Biomechanical analysis of AAA rupture risk

From a biomedical engineering point of view, biomechanical determinants such as stress distribution and strength play a role in the rupture of the AAA wall. It is generally recognized that an AAA ruptures, when the stress acting on the AAA wall, caused by the blood pressure, exceeds the strength of the wall (Raghavan and Vorp, 2000; Maier et al., 2010). The maximum diameter criterion, based on the law of Laplace, states that the wall stress in a thin-walled cylinder linearly increases with increasing diameter and transmural pressure, and decreases for increasing wall thickness. However, due to the complex geometry of most AAAs, the wall stress is determined by the local AAA geometry and wall thickness, and can therefore not be predicted by the law of Laplace alone, or be based on other simplified geometrical models (Hua and Mower, 2001; Reeps et al., 2009). Therefore, for a better estimation of AAA risk of rupture, a non-invasive computational method based on patient-specific AAA geometry reconstruction from medical

imaging and finite element analysis (FEA) have been increasingly performed to calculate the stresses of the vessel wall.

Recently several research groups have focussed on wall stress as a clinical measure for rupture risk and showed that peak wall stress in AAAs is a more reliable parameter than the maximum diameter for aneurysm rupture prediction (Fillinger et al., 2002; Papaharilaou et al., 2007; Truijers et al., 2007; Venkatasubramaniam et al., 2004). Fillinger et al. (2002) found that peak wall stress for ruptured and symptomatic AAAs was significantly higher than for electively repaired AAAs. The same group concluded that peak wall stress was superior over the maximum diameter for predicting AAA rupture (Fillinger et al., 2003). Truijers et al. (2007) found peak aortic wall stress at patient-specific blood pressure to be higher for ruptured AAAs than for asymptomatic AAAs. The previously mentioned studies were based on patient group statistics, and a large overlap existed in wall stress of the ruptured and asymptomatic patient groups. Sensitivity and specificity are therefore still low for AAA wall stress as a personalized predictor for rupture risk. Additionally, AAA wall stress studies so far are based on labour-intensive manual segmentation of the AAAs from the CTA data. Such a procedure requires a considerable amount of user variability. Heng et al. (2008) studied the reproducibility and the variation in the peak wall stress, based on manual segmentation, and found that peak wall stress had only a temperate reproducibility and was vulnerable to the experience and background of the individual operator.

Nevertheless, it is important to emphasize that wall stress alone is not sufficient to predict rupture risk; regional estimations of wall strength would also be relevant (Vande Geest et al., 2006). Recently, it has been shown that wall strength differs remarkably from patient to patient and within the same aneurysmal sac (Vallabhaneni et al., 2004; Vande Geest et al., 2006; Wang et al., 2002). Additionally, another study (Di Martino et al., 2006) showed that the strength of the aneurysmal wall from ruptured AAA cases is significantly lower than that selected for elective repair. Hereof, Vande Geest and colleagues (Vande Geest et al., 2006) have proposed a statistical model to estimate non-invasively the wall strength distribution in AAA taking into consideration factors such as age, sex, family history, AAA size and local intraluminal thrombus (ILT) thickness.

As in every model, assumptions and simplifications are made concerning factors that are difficult or impossible to measure. These factors include initial wall stress, intraluminal thrombus and aortic calcifications and it is not clear to what extent these simplifications influence the patient-

specific wall stress. As AAA imaging is generally performed without cardiac triggering, the AAA is subjected to a time-averaged blood pressure and a certain amount of wall stress. Ignoring this initial stress not only leads to an overestimation of the AAA volume, but also to an underestimation of the wall curvature and the wall stress (De Putter et al., 2007). However, this initial stress may have different implications for the wall stress of different AAAs. Recently, material properties of thrombus were studied with compression and shear experiments, leading to far lower elastic module than previously assumed for thrombus (Ashton et al., 2009; Hinnen et al., 2007; van Dam et al., 2008). Re-evaluation of thrombus in wall stress analyses in the light of the recently obtained material properties may give more insight in the mechanical effect that thrombus has on patient-specific wall stress. The location of aortic calcifications can be identified from the CTA data (Siegel et al., 1994). Implementation of these calcifications in patient-specific AAA models can give information on the effect of calcifications on the resulting wall stress.

Nevertheless, despite the promising outcomes of the above mentioned computational studies, one problem is still unsolved, i.e. a standardized method for the AAA model generation and the performance of the FE analysis between different research groups. Another more relevant issue is that patient-specificity, particularly regarding the mechanical properties and biological processes within the AAA wall, which is still lacking in computational FE models. Consequently, the proper consideration of patient-specific variations in mechanical AAA wall properties and biological processes by means of non-invasive techniques would be essential to improve rupture risk stratification.

1.4 Extracellular matrix proteins in AAA

The extracellular matrix (ECM) is a complex assembly of fibrillar proteins and associated glycoproteins embedded in a hydrated ground substance made of glycosaminoglycans and proteoglycans (Raines, 2000). In the vascular system as in any connective tissue, in addition to providing the architectural framework for the artery wall that conveys mechanical and viscoelastic properties, the ECM offers an optimal structural and chemical environment to the resident cells (Gurvan et al., 2010). In recent years, the ECM macromolecules have been shown to play a decisive role through their recognition by integrin and associated proteins at the cell surface in cell proliferation, survival and programmed cell death, as well as in gene expression. They also operate by their capacity to modulate the availability of soluble signalling molecules such as growth factors

and cytokines. Furthermore, proteolytic parts of ECM proteins or ambiguous domains may have distinct functions in various processes (Sakalihasan et al., 2011).

1.4.1 Composition of the ECM

As mentioned above, the aorta is made of three components: the tunica intima, made of a single layer of ECs lining the lumen; the tunica media consisting of multiple layers of smooth muscle cells, lamellar units rich in collagen and elastic fibres, and the tunica adventitia made of a loose collagen-rich tissue containing fibroblasts and vascularised by vasa vasorum.

The main structural components of the aorta are collagen and elastin fibres. These fibrillar structures deposited by SMC in the media are the major components of the arterial wall that contribute to its mechanical properties and provide the elastic recoil required in a closed circulatory system (Wagenseil et al., 2009). The medial lamellar units are formed of two parallel thick lamellae of elastic fibres enveloping SMC with numerous resistant intralamellar protrusions rich in elastin. Most of the fibrillar collagen, type I, III and V are concentrated in compact fibres, concentrically oriented, closely associated with the elastic lamellae and decorated with small patches of biglycan, a small leucine rich proteoglycan (SLRP). The intralamellar matrix contains many microfibrils rich in fibrillin-1 and collagen, type VI. Versican, a large chondroitin sulphate proteoglycan that can associate with hyaluronic acid, is found in the interstitial space and is presumably aimed at sustaining the compression generated by pulsatile forces (Dingemans et al., 2000). Although collagen and elastic fibres largely contribute to the mechanical performance, the associated proteoglycans and glycoproteins, although less abundant, are also significant players in the vessel maintenance as indicated by the vascular pathologies related to their alterations or dysfunction as observed e.g. fibrillin in Marfan's syndrome. Production of a mechanically competent matrix with adequate signalling and mechanical properties, involves large number of biosynthetic steps and post-transcriptional modifications that are under the control of regulatory mechanisms issued from the environment matrix as well as soluble factors (Lapiere et al., 2008).

Three processes play a key role in the formation and progression of AAA: inflammatory and oxidative stress, degradation of the ECM of the aortic wall and impairment of its reconstruction associated with SMC depletion and apoptosis (Hellenthal et al., 2009). A highly significant loss of elastin seems to be an early event in aneurysm formation resulting in elastic lamellae disruption and medial refraction without any substantial loss of collagen. The adventitial tissue that

predominantly contains collagen may provide mechanical resistance to the aorta in the absence of competent medial ECM. Collagen degradation seems to be the ultimate cause of rupture. The aneurysmal tissue is characterised by a large production of ECM-degrading enzymes (MMPs), proinflammatory cytokines and chemokines by the lympho-monocytic infiltrates and resident vascular wall cells, SMCs and fibroblasts.

1.4.2 ECM remodelling and biomechanical properties in AAA wall

ECM is a dynamic structure with continuous turnover whereby existing structural proteins are replaced with newly synthesized proteins. Therefore, any change in the vascular environment can be reflected in the ECM composition that attempts to maintain a homeostatic environment for optimal function. Collagen fibres in the aortic wall provide the tensile strength required for the inflation of the wall during cardiac systole without rupture, while elastin lamella controls the recoil property of the aorta which is needed during cardiac diastole (Basu and Kassiri, 2013).

So far, the interaction of biomechanical and biological factors in the pathogenesis of AAA is often proposed but not quantitatively confirmed and still has to be elucidated. It is hypothesized that out-of-balance vessel wall remodelling together with non-physiological mechanical conditions exerted by blood pressure are leading to progressive vessel expansion, aneurysm development and finally rupture (Newma et al., 1994; Henderson et al., 1999; Töpel et al., 2014; Trenner et al., 2013). Increased mechanical stress and strain in the vessel wall per se may induce biological alterations in ECM turnover and remodelling of the aortic wall. Thereby, not only degenerative but also compensatory changes in the vessel wall may be expected. For other cardiovascular disorders such processes have already been shown in vitro (Evans et al., 2013) but at present not in the human vessel wall and in particular not in AAA.

Furthermore, the material properties such as stiffness, strength and failure tension of the load bearing vessel wall are determined mainly by the quantity and functionality of various extracellular matrix (ECM) components such as collagen, elastin and proteoglycans (Choke et al., 2005; Reeps et al., 2013; Daugherty et al., 2002; Limet et al., 1998). For AAA formation, an imbalance between degradation and synthesis of ECM components has already been described histopathologically (Daugherty et al., 2002). Nonetheless, due to methodical reasons, neither the role of the acting mechanical conditions in ECM composition and remodelling, nor the impact of ECM composition on the material properties of AAA wall has been evaluated so far in vivo

(Raghavan et al., 2000; Marini et al., 2012; Raghavan et al., 2011). Still, not enough is known about macroscopic mechanical behaviour of AAA wall in correlation to the composition of ECM within the vessel wall (Reeps et al., 2013). Moreover, at present it is speculated, whether mechanical stress and strain are causative for adaptive or degenerative changes in the ECM composition of AAA wall.

Meanwhile, the local mechanical loads acting on the AAA wall can be calculated realistically by finite element analysis (FEA) and macroscopic mechanical properties of AAA wall can be measured experimentally (Gasser et al., 2010; Maier et al., 2010; Reeps et al., 2010; Okamato et al., 2002; Humphrey, 2002). Therefore, to gain better insights about the rupture risk stratification of AAA, it is very important to evaluate the ECM components in correlation to the corresponding biomechanical properties and loads in the aneurysmal wall.

1.5 Inflammatory and proteolytic processes during AAA development

1.5.1 Role of inflammation and proteolytic degradation of AAA

AAA is best described as a chronic inflammatory condition with an associated proteolytic imbalance. The striking histological hallmark of AAAs is an extensive transmural infiltration by macrophages, lymphocytes and plasma cells. It is suggested that these inflammatory cells consequently release a cascade of cytokines resulting in activation of many proteases. This process results in the expression of cell adhesion molecules, increased protease expression and the release of reactive oxygen species causing degradation of the ECM through the activation of MMPs and TIMP (Shah, 1997).

The recruitment of macrophages by chemotactic agents is possibly triggered by exposed degradation products in the aortic wall. The adventitia appears to be the primary site of leucocytes infiltration and initial MMP activation. Macrophages and lymphocytes-generated cytokines are elevated in the aneurysmal aortic wall, including IL-1β, TNF-α, IL-, IL-8, MCP-1, IFN-γ and GM-CDF (Golledge et al., 2009; Wills et al., 1996; Hance et al., 2002; Koch et al., 1993; Newman et al., 1994). These inflammatory cytokines, as well as plasmin and urokinase-type plasminogen activator, induce expression and activation of many MMPs and their inhibitors TIMPs (Newman et al., 1994, Thompson and Parks, 1996; Defawe et al., 2003).

Moreover aneurysm formation involves a complex process of destruction of the aortic media and supporting lamina through degradation of elastin and collagen. Proteolytic degeneration is known to cause AAA formation and lead to disease progression. Additionally, MMPs and other proteases, derived from macrophages and SMC are secreted into the ECM in response to stimulation by the products of elastin degradation (Ailawadi et al., 2003). Furthermore, inflammatory infiltrates and invading neovessels are relevant sources of MMPs in the AAA wall and may substantially contribute to aneurysm wall instability (Reeps et al., 2009). Therefore, in AAA disease evidence suggests that the balance of vessel wall remodelling between MMPs, TIMPs and other protease inhibitors favours elastin and collagen degradation with the net pathological effect of ECM destruction.

1.5.2 Involvement of mechanical properties

Degradation of the components of the extracellular matrix (ECM) is one of the main reasons for the initiation and progression of abdominal aortic aneurysm (AAA) (Menashi et al., 1987; Hellenthal et al., 2009). Due to the depletion of collagenous and elastic fibres, the AAA wall degenerates over time. In combination with mechanical loading exerted by blood pressure, progressive vessel dilatation takes place. However, the relevance of mutual interactions between biomechanical conditions with underlying pathohistological changes leading to further AAA expansion and finally to rupture are so far poorly understood. The ability of AAA to sustain the force exerted by blood pressure is determined by the presence and proper function of ECM proteins, especially collagen (Raghavan et al., 2000; Marini et al., 2012; Reeps et al., 2013; Okamoto et al., 2002; Vande Geest et al., 2006). In particular, collagen type I and type III play a major role in the maintenance of mechanical stability of the aortic wall (Menashi et al., 1987; Rizzo et al., 1989). The destabilising role of matrix metalloproteinases (MMPs) by degradation of the ECM has already been described in AAA (Keeling et al., 2005; Thompson et al., 2006; Longo et al., 2002). In this context, MMP-2, derived from aortic smooth muscle cells, is thought to be important in the initiation of aneurysm (Longo et al., 2002; Choke et al., 2005). In contrast, MMP-9 activity is highly expressed in the wall of already established AAA and is associated with its further progression (Hellenthal et al, 2009; Choke et al, 2005). The upregulation of MMP-2 and -9, as well as of the tissue inhibitor of metalloproteinase-1 (TIMP-1), has already been shown in detail in AAA (Tamrina et al., 1997; Yamashita et al., 2001). Thereby, characteristic inflammatory infiltrates and neovessels are relevant sources of MMPs and other proteases. These cells may additionally

contribute to the degradation of the ECM and destabilisation of the AAA wall (Reeps et al., 2009; Helenthal et al., 2009, Shimizu et al., 2005). Furthermore, proteolysis of ECM proteins facilitates migration of inflammatory cells into the aortic media resulting in additional weakening of the aortic wall, which may eventually lead to outward disruption of the AAA.

However, the outcome of inflammatory and proteolytic processes on the strength and constitutive properties of the AAA wall has so far never been supported by mechanical testing of AAA tissue samples. Furthermore, it has never been evaluated, whether mechanical loads such as wall stresses and strains influence the expression of inflammatory or proteolytic processes in the aneurysmatic aortic wall. With recent advanced approaches in patient-specific finite element analysis (FEA) now allowing the accurate computation of these mechanical loads in the AAA wall (Gasser et al., 2010; Maier et al., 2010; Raghavan et al., 2005; Rausch et al., 2011), the investigation of these interrelations is possible and might approach a new aspect towards AAA rupture risk.

1.6 The role of the chemokine receptor CXCR4 in AAA

1.6.1 CXCR4-background

The expressions of chemokines and their receptors seem to be involved in cell activation, differentiation and tissue specific trafficking within both normal and inflamed tissue (Charo et al., 2006; Viola et al., 2008).

Chemokines are small proinflammatory chemoattractant cytokines that bind to specific G-proteins coupled seven-span transmembrane receptors (Viola et al., 2008, Lagerström et al., 2008, Murdoch et al., 2000). Much attention has lately been paid to one particular member of the chemokine receptor family termed CXCR4, when it was discovered as one of the co-factors required for supporting T-lymphocytes tropic HIV (human immunodeficiency virus) infection into permissive cells. As well as being important for lymphocyte activation and trafficking at sites of inflammation, it appears that CXCR4 and its sole ligand CXCL12 play an important role in many areas of immunology and human development such as organogenesis, vascularization and embryogenesis (Bleul et al., 1996; Oberlin et al., 1996; Loetscher et al., 2000). Additionally CXCR4 has been widely investigated as a key receptor in the crosstalk between tumour cells and their microenvironment (Burger et al., 2006; Teicher et al., 2010) and between immune and nervous

system (Réaux-Le Goazigo et al., 2013; Guyon, 2014). Lately, it has been supposed that CXCR4 can also play a decisive role in vascular disease such as AAA (Ocaña et al., 2008). The exact role of CXCR4 in human AAA is still in need of being elucidated.

1.6.2 State of research

It has already been acknowledged that AAA is a relatively common pathology among the elderly (Sakalihasan et al., 2005, Eckstein et al., 2014), which may lead to rupture causing severe internal bleeding and sudden death (Töpel et al., 2014; Reeps et al., 2009; Heron, 2011, Shimizu et al., 2006). The expansion of the aorta is considered to be the result of chronic inflammation, upregulation of proteolytic processes, degradation of the ECM and apoptosis of vascular smooth muscle cells (Boddy et al., 2008; Nordon et al., 2011; Henderson et al., 1999).

Inflammatory response and activation of proteolytic enzymes are extensively controlled by a plethora of various chemokines and their receptors. Our main attention has been focused especially on the chemokine receptor CXCR4 and it is ligand CXCL12. Ocaña et al. (2008) revealed that CXCR4 was expressed in infiltrating cells, especially T- and B-lymphocytes, isolated from human AAA and that the level of stromal cell-derived factor 1 alpha (SDF-1α, known as well as CXCL12) is increased in the adventitia of the human AAA wall, attributing a proinflammatory process of the SDF-1/CXCR4 axis in AAA development. Another study evaluated the expression of CXCR4/CXCL12 in aneurysmal aortic wall and during AAA progression in a mouse model (Michineau et al., 2014). In addition, shortly published studies using microarrays on human AAA (Lenk et al., 2007; Hinterseher et al., 2013) found that the expression of CXCR4 is increased in AAA tissue samples compared to control samples. However detailed analysis of CXCR4 and its sole ligand CXCL12 are still needed in order to better explore their potential role in the pathogenesis of AAA.

1.7 Objectives and outlines

The main aim of this thesis is:

To obtain a better understanding of mechano-biological interactions in abdominal aortic aneurysm wall in order to improve its rupture risk stratification.

For this purpose, biological analysis, tensile tests and finite element simulation were performed to evaluate the interactions between the ECM composition, expression of relevant genes, associated diseases and mechanical properties and loads of the AAA wall.

The key objectives were the following:

1. Evaluation of the correlations between ECM components (collagen, elastin and proteoglycans) in the AAA wall with their corresponding mechanical properties and loads in the diseased aortic tissue.

2. Exploration of the relationships between gene expression of destabilizing biological factors (such as proteases, collagen, inflammation) and mechanical properties of the AAA wall.

3. Analysis of the expression and cellular localisation of CXCR4 and its ligand CXCL12 in the AAA and evaluation of the role of CXCR4/CXCL12 in the pathogenesis of AAA.

4. Characterisation of the AAA wall with regard to its mechanical properties in patients with and without chronic kidney disease.

Chapter 2 Materials and Methods

2.1 Study group, tissue sampling and processing

Collection of human tissue samples for research purposes was conducted according to the ethical guideline of Klinikum rechts der Isar, Technische Universität München. The local ethics committee approved the study and written informed consent was given by all patients and donors.

2.1.1 Study group

A total number of 81 patients, who underwent an open repair surgery at the Department of Vascular and Endovascular Surgery of the Klinikum rechts der Isar, Technische Universität München were included in this thesis.

In total, 133 aortic wall tissue samples were harvested from 81 AAA patients, who underwent an elective open repair of the aneurysm sac. 31 patients were included for following studies: “Impact of ECM components on biomechanical properties in AAA wall” and “Gene expression and biomechanical properties in AAA”. For the study of the CXCR4 and CXCL12, a new collective of additional 32 patients were used. Finally, 18 additional patients were added to the first collective of 31 patients (total n=49) and included in the study for the evaluation of the mechanical properties of AAA patients with and without CKD. Patients with Ehlers-Danlos syndrome, Marfan syndrome, or other known vascular or connective tissue disorders were excluded from the study. Furthermore, the included patients had no evidence or medical history of any cancer disease.

Twelve non-aneurysmal aortic tissue samples, obtained from human organ donors of the Department of Transplant Surgery, Klinikum rechts der Isar, were used as healthy controls. None of the control samples showed any signs of atherosclerosis and there was no evidence or medical history of aneurysm and the other vascular disorders. Exclusion criteria also included cancer, infection, or any other immune-mediated disease, as far as these data were available.

2.1.2 Tissue sampling and processing

During an elective open surgical repair, all AAA tissue samples were obtained from the anterior or the lateral AAA sac at the maximum dilatation area of AAA leaving enough material for a full coverage of the alloplastic prosthesis in inclusion technique. The harvested tissue samples were then immediately transferred into a physiological solution (130 mmol/l sodium chloride, 5 mmol/l potassium chloride, 2 mmol/l calcium chloride, and 3 mmol/l sodium lactate) and delivered to the lab for further processing. Thereafter, the AAA-wall was divided into three different parts: one part for immunohistochemical analysis, one for mechanical testing and the last part of the specimen was immediately frozen in liquid nitrogen for biological analysis. The part for immunohistochemical analysis was fixed with 4% formalin for 24 hours (h), followed by dehydration and then embedded in paraffin. For the mechanical analysis the specimens were stored in lactated Ringer's at 4°C until the tensile tests were performed, which happened within 24h following surgery, more precisely between 10 and 20 hours after the surgical intervention. Within this time, no significant degradation of mRNA or protein is observed (Chandana et al., 2009; Lee et al., 2013). Therefore, no significant influence of enzymatic degradation within the time interval was expected. Furthermore, fresh frozen samples were used for protein extraction and quantitative western blot analyses; quantitative real-time reverse transcriptase-PCR (RT-PCR) and histological and IHC analyses were performed using the formalin-fixed-paraffin-embedded (FFPE) samples.

2.2 Histochemical staining

As described above, for histological and immunohistological staining, AAA tissue samples were fixed for 24 h in 4% formaldehyde, then the specimens were transferred into an aqueous solution saturated with EDTA for up to 7 days, dependent upon the extent of calcification. Subsequently, the tissue samples were then dehydrated, embedded in paraffin, and sectioned in 2-3 µm thin slices with the microtome HM335E (Microm international, Walldorf, Germany). The slides used for histochemical staining, were SuperFrost® (Menzel GmbH, Braunschweig, Germany). All sectioned tissue, transferred on the slides, were dried at 56°C for one hour prior to the staining procedure, then deparaffinised by incubation in xylene for 20 min, followed by isopropanol for 20 min, 96% ethanol for 10 min, 70% ethanol for 10 min, and distilled water for 10 min. The materials used for histochemical analyses were received from the Pharmacy of the Klinikum rechts der Isar.

2.2.1 Haematoxylin-Eosin staining

The haematoxylin-eosin staining (HE) is the most commonly used staining in histochemistry. Generally, the staining of nuclei by haematoxylin is blue, cytoplasm and extracellular tissue is stained in various shades of red, pink and orange.

Procedure: Following deparaffinization, nuclear staining was performed by incubating the slides with Mayer's haematoxylin for 5-10 min at room temperature (RT). The slides were then washed in tap water for 10 min, incubated with acidified eosin for 5 min, rinsed briefly in tap water and then in ascending alcohol series (70% ethanol, 96% ethanol and isopropanol) followed by xylene. The samples were mounted in hydrophobic mounting medium (DAKO, Glostrup, Denmark) and covered with cover slips (Thermo Scientific™ Cover Slips, Thickness 1, Germany).

2.2.2 Elastica van Gieson staining

The Elastica van Gieson (EvG) staining is a combination of Weigert's haematoxylin, van Gieson's picrofuchsin and the resorcin-fuchsin solution that allows differential analysis of nuclei, connective tissue, muscle and elastic fibres.

Procedure: Weigert's haematoxylin was freshly prepared by mixing Weigert's solution A and Weigert's solution B (ratio 1:1). The slides, previously dried at 56°C and deparaffinized, were incubated in Weigert's haematoxylin for 10 min and washed in warm tap water for another 10 min. Next step consisted of staining of the cytoplasm by incubation with van Gieson solution for 3 min. This step was followed by washing in distilled water and ascending alcohol series (70% ethanol, 96% ethanol and isopropanol) followed by xylene. The samples were then mounted in DAKO and covered with glass cover slides.

2.2.3 Sirius red staining

The Sirius red staining is one of the best techniques of collagen visualization. Normally, the collagenous structures are stained red and the nuclei are black/brown.

Procedure: Picro-sirius red solution was prepared by adding 0.5 g of Sirius red (Cat# 365548, Sigma-Aldrich, St Louis, MO, USA) to 500 ml of saturated aqueous solution of picric acid. Following deparaffinization, nuclear staining was performed by incubating the slides with Weigert's haematoxylin solution as described previously for 8 min at RT. The slides were then washed for 10

min in running tap water. Thereafter, the slides were stained in picro-sirius red solution for one hour and then rinsed in two changes of 5 min in 0.5% acidified water (5 ml acetic acid in 1000 ml distilled water). Then the slides were rinsed in distilled water for 5 min and ascending alcohol series (70% ethanol, 96% ethanol and isopropanol) followed by xylene. The samples were then mounted in DAKO mounting medium and covered accordingly.

2.2.4 Alcian blue staining

Alcian blue is a basic dye that has an affinity for sulphated and carboxylated acid mucopolysaccharides and sulphated and carboxylated sialomucins (glycoproteins). The blue colour is due to the presence of copper in the molecule. The acid mucins/mucosubstances (proteoglycans) are stained in blue and nuclei in reddish pink.

Procedure: Alcian blue solution was prepared by dissolving 1 g of alcian blue 8 GX (A3157, Sigma-Aldrich, St Louis, MO, USA) in 3% glacial acetic acid (3 ml acetic acid diluted in 100 ml distilled water). The pH was adjusted to 2.5 and the solution was then filtered. The slides, previously deparaffinized, were incubated in alcian blue solution for 30 min at RT, then rinsed shortly in 3% acetic acid solution and finally washed in distilled water for 5 min. Next, the nuclei were counterstained with Weigert's iron haematoxylin solution for 5-8 min. The slides were washed first in distilled water, thereafter in running tap water and finally in ascending alcohol series (70% ethanol, 96% ethanol and isopropanol) followed by xylene. The samples were then mounted in DAKO and covered with cover slides.

2.3 Immunohistochemical staining

The immunochemical procedures carried out in the present work were performed with the LSAB kit, the Dako REAL™ Detection System, peroxidase/DAB+, Rabbit/Mouse code K5001 (DAKO, Glostrup, Denmark) or APAAP kit, the DAKO REAL™ Detection System, Mouse Code No. K 5000 (DAKO, Glostrup, Denmark), following the instructions of the manufacturer.

Procedure: For the immunohistological staining, all tissue samples were dehydrated, embedded in paraffin, and sectioned in 2-3 µm thin slides as described in *section 2.2*. All sectioned tissues were mounted on glass slides (SuperFrost Plus, VWR International, Darmstadt, Germany). These slides were pre-treated with 0.1% poly-L-Lysine solution (P8920, Sigma-Aldrich, St Louis, MO, USA) and then incubated overnight (ON) at 56°C for 48h prior to the staining procedure in order to prevent

detachment of the tissue section. Subsequently slides were deparaffinized by incubation in xylene for 20 min, followed by isopropanol for 20 min, 96% ethanol for 10 min, 70% ethanol for 10 min, and distilled water for 10 min.

Additionally each antibody was used at an optimal dilution, with the appropriate blocking and antigen retrieval method shown in *Table 2-1*. Antibodies were diluted in an antibody diluent purchased from DAKO (S2022, Dako, Glostrup, Denmark).

Table 2-1: Antibodies, dilution, blocking and antigen retrieval method of IHC used in this study.

Antigen	Antibody	Dilutio	Metho	Blocking	Antigen retrieval
Collagen type I	Anti-Collagen type I, Rabbit anti-human, polyclonal, 600-401-103, Rockland, Gilbertsville, PA, USA	1:1000	LSAB		Sections were covered with Proteinase K working solution (5 µg Protease K (Sigma-Aldrich) + 5 ml TRIS-Buffer) and incubated for 20 min at RT.
Collagen type III	Anti-Collagen type III, Rabbit anti-human, polyclonal, 600-401-105, Rockland, Gilbertsville, PA, USA	1:300	LSAB		Sections were immersed in citrate buffer (pH 6) and incubated for 2x10 min in the microwave.
CD3 (T-Cells)	Anti-CD3, Rabbit anti-human, polyclonal, clone MRQ-39, 103R-95, Cell Marque, Sigma-Aldrich, Rocklin, CA, USA	1:500	LSAB		Sections were immersed in citrate Buffer (2.1 g citrate monohydrate (Merck) in 1000 ml distilled water; pH 6) and cooked for 7 min in a pressure cooker.
CD20 (B-Cells)	Anti-CD20, mouse anti-human, monoclonal, M0755, clone L26, Dako Cytomation, Glostrup, Denmark	1:500	LSAB		
CD34 (Neovessels and Endothelial cells)	Anti-CD34, mouse anti-human, monoclonal, clone QBEnd/10, 134M-14, Cell Marque, Sigma-Aldrich, Rocklin, CA, USA	1:500	LSAB		
CD45 (Leucocytes, T- and B- cells)	Anti-CD45, mouse anti-human, monoclonal, M0701, clone 2B11+PD7/26, Dako Cytomation, Glostrup, Denmark	1:200	LSAB		
CD68 (Macrophages and monocytes)	Anti-CD20, mouse anti- Human, monoclonal, M0814, clone KP1, Dako Cytomation, Glostrup, Denmark	1:2000	LSAB		
Elastin	Anti-elastin [10B8], mouse anti-Human, monoclonal, ab77804, Abcam Inc, Cambridge, UK	1:1000	APAAP		

Antigen	Antibody	Dilutio	Metho	Blocking	Antigen retrieval
VS38c (plasma cells)	Plasma cell, mouse anti-human, monoclonal, M7077, clone VS38c, Dako Cytomation, Glostrup, Denmark	1:1000	LSAB		
CXCR4	Anti-CXCR4, rabbit anti-human, polyclonal, ab2074, Abcam Inc, Cambridge, UK	1:300	LSAB	Blocking 1h with 1% goat serum (1:100 with antibody diluent from Dako).	Sections were immersed in a target retrieval buffer (S2367, Dako; pH 9) and incubated for 2x10 min in the microwave.
CXCL12/SDF-1α	Anti-SDF-1α, rabbit anti-human, polyclonal, ab9797, Abcam Inc, Cambridge, UK	1:1000	LSAB		

2.3.1 LSAB method

Labelled streptavidin-biotin immunohistochemistry assay (LSAB) method is one of the most common used immunohistochemical stainings. The LSAB method is based on the high affinity that streptavidin (streptomyces avidinii) and avidin (chicken egg) possess for biotin. In the first step, the primary antibody is added which binds to the antigen. The secondary antibody is added and the biotinylated antibody binds to the primary antibody. The streptavidin molecule binds to enzyme molecules directly and this complex is injected into the tissue section and penetrates through the site of antigen. Finally peroxidase is added in the next step to enable the detection of the enzyme location. Through this step, a brown colour reaction is then developed.

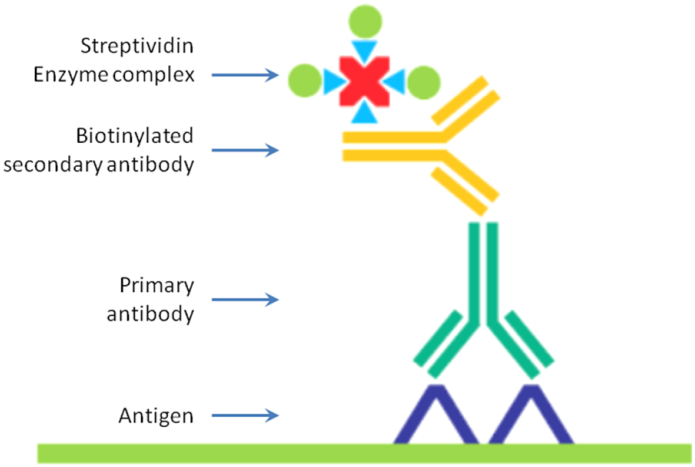

Figure 2-1: Schematic representation of the labelled streptavidin-biotin (LSAB) method. Figure is based on: http://de.slideshare.net/aalamaram/ihc-technology.

Procedure: Prior to performing the staining, a stock solution of TRIS buffer (10x) was prepared by adding 60.5 g Trizma base (Sigma-Aldrich) and 90 g NaCl (Merck) in 1 l distilled water, and adjusting the pH to 7.6 with HCl (Apotheke MRI). The TRIS buffer (1x) was then prepared by diluting a stock solution (10x) in distilled water. All following steps were performed at RT and

according to the manufacturer instructions. After antigen retrieval and in order to block the peroxidase, slides were treated and incubated for 15 min with 0.3% hydrogen peroxide (Merck) and then rinsed with TRIS buffer (1x) for 3x2 min. Upon antibody, sections were in some cases pre-treated with 1% normal goat serum (S-1000, Vector laboratories Inc., Burlingame, USA) for 60 min to block non-specific binding of immunoglobulin. Thereafter, the slides were incubated for one hour with the appropriate primary antibody (100 µl) as described in *Table 2-1*. During this procedure, all slides were kept in a humidified chamber, followed by another wash with TRIS buffer (1x) for 3x2 min. Thereafter, all the slides were incubated with biotinylated secondary antibody (solution A, pink solution) for 25 minutes and streptavidin-peroxidase (solution B, yellow solution) for another 25 minutes, and then followed by rinsing in TRIS buffer (1x) for 3x2 min, respectively. Finally, the chromogenic solution was prepared from 15 µl DAB+ (solution C) and 750 µl HRP substrate (solution D). After incubation for 3-5 min with the chromogen, samples were counterstained with haematoxylin for 20-30 seconds. Subsequently, a dehydration in alcohol series was performed (70% ethanol, 96% ethanol, isopropanol) followed by xylene. Finally, slides were mounted with Dako mounting medium and covered with the appropriate cover slips (Thermo Scientific™ Cover Slips, Thickness 1, Germany).

2.3.2 APAAP method

The alkaline phosphatase-anti-alkaline phosphatase (APAAP) method is based on an indirect reaction. The staining sequence of this technique consists of the use of an unconjugated primary antibody, a secondary antibody, the soluble enzyme-anti-enzyme complex, and substrate solution. The primary antibody and the antibody of the enzyme immune complex must be from the same species. The secondary antibody must be directed against immunoglobulins of the species producing both the primary antibody and the enzyme immune complex. Soluble enzyme-anti-enzyme immune complex techniques were named after the particular enzyme immune complex they used.

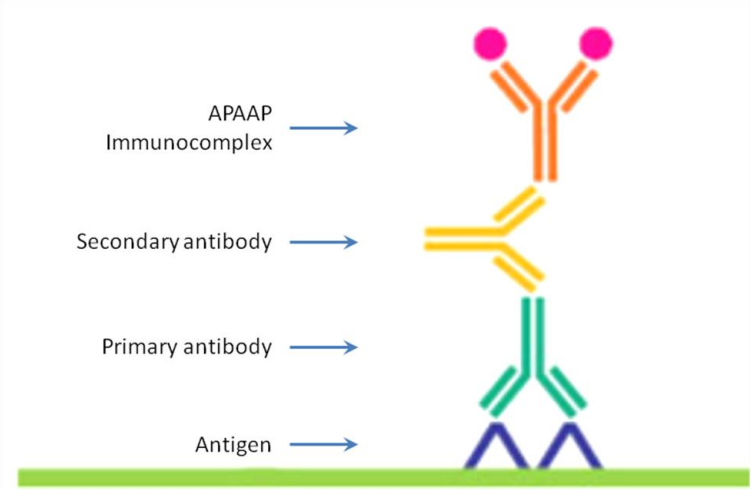

Figure 2-2: Schematic representation of the alkaline phosphatase-anti-alkaline phosphatase (APAAP) method. Figure is based on: http://www.immunohistochemistry.us/immunohistochemistry-staining.html.

Procedure: All steps of APAAP method have been performed at RT and according to the manufacturer instructions. TRIS buffer (1x) (see LSAB method) was used for washing the samples after each step of the following protocol. Primary antibody against the target protein was incubated with the samples for 1 h using optimized dilution for each antibody as shown in *Table 2-1*. The incubation with the secondary antibody (solution A) for 25 min was followed by incubation with the APAAP immunocomplex (solution B) for another 25 min. Meanwhile, the chromogen solution was prepared from 30 µl solution C, 30 µl solution D, 30 µl solution E, and 750 µl solution F (substrate solution). The chromogenic mix was incubated for 15 min, until the red colour has been observed under the microscope. Haematoxylin counterstain followed for the nuclear stain, mounting was conducted with hydrophobic mounting medium from DAKO and slides were covered with the appropriate cover slips

2.4 Microscopy and digitalization

Digital micrographs were captured with a digital image capture device-Aperio ScanScope CS2 system (Aperio, Leica Biosystems GmbH, Germany), magnified by Aperio Image Library software (Leica Biosystems GmbH, Germany) and with a Zeiss AxioCam MRc digital camera attached to a Zeiss Axio Observer Z1 microscope (Carl Zeiss Microscopy GmbH, Jena, Germany), equipped for light and fluorescence microscopy. The microscope was controlled by the AxioVision software, version 4.8.2 (Carl Zeiss Microscopy GmbH, Jena, Germany).

2.5 Histological and immunohistochemical anlaysis

2.5.1 Histochemical evaluation

The evaluation of the histological and immunohistological staining was conducted by two experienced investigators via light microscopy and characterized using a semi-quantitative scoring as described in *Table 2-2.*

Table 2-2: Description of the semi-quantitative scoring used for histological and immunohistological characterization.

-	-/+	+	++	+++
no staining	**weak staining**	**positive staining**	**moderate staining**	**Strong staining**

The HE staining was performed to evaluate the cellularity and the inflammatory infiltrates of the tissue samples. The characterization of collagen and elastin fibres was determined by the EvG staining. Additionally, this histopathological scoring was performed as well for macrophages, B and T-cells, neovascularization, CXCR4, CXCL12 and plasma cells.

2.5.2 Quantification of collagen, elastin and proteoglycans

Digital images of IHC-stained slides were obtained at 20x magnifications using a whole slide scanner (ScanScope CS, Aperio) and analysed using Adobe Photoshop CS5. First, the whole vessel area was determined as a number of pixels against the background and set as 100%. Thereafter, the stained area for each staining (collagen type I and type III, total collagen, elastin, and proteoglycans) was labelled. In all cases the proper adjustment was re-evaluated visually to ensure that only the stained area was selected. The relative area of collagen, elastin or proteoglycans was then calculated by dividing the number of pixels of the stained area by the number of pixels of the entire tissue area on the individual slide and displayed as a percentage of the ECM component in the analysed section.

As the mechanical quantities from tensile testing involve the macroscopic wall thickness, the percentile area of the stained components of ECM was multiplied by the thickness of the corresponding aortic tissue sample to obtain quantities that are mechanically meaningful to correlate.

2.6 Analysis of gene expression at mRNA level using PCR

2.6.1 RNA extraction from FFPE tissue samples

RNA (ribonucleic acid) was extracted from FFPE tissue sections corresponding to the slides used for the histological staining with the High Pure RNA Paraffin Kit (Roche Diagnostics GmbH, Mannheim, Germany) according to the manufacturer's instructions. To avoid RNA degradation, the microtome surface as well as the microtome blades and paraffin blocks were cleaned with RNase ZAP® Solution (Invitrogen, Carlsbad, USA) prior to cut. The FFPE blocks were then cut with the microtome HM335E ((Microm international, Walldorf, Deutschland).

Procedure: Two tissue slices, each of 10-20 µm thickness were placed into a 1.5 ml RNase-free reaction tube (PCR tube, Eppendorf, Germany), deparaffinized by adding 800 µl xylene, mixed by inverting, and incubated at RT for 5 min. The xylene was then removed and replaced by 400 µl ethanol absolute, mixed and centrifuged at 12,000 rpm for 4 min at RT. The supernatant was carefully removed and 1 ml ethanol absolute was added and mixed by inverting followed by centrifugation at 12,000 rpm for 4 min at RT. The supernatant was then discarded and dried for 10-15 min at 55°C.

Extraction procedure was continued according to the instruction of the manufacturer's protocol (Roche) as follows: A mix of 100 µl of Tissue Lysis buffer (Bottle 1, Roche Kit), 16 µl of 10% SDS (sodium dodecyl sulphate) and 40 µl of Proteinase K (Vial 2, Roche Kit) was prepared and added to each of the dried samples. The pre-treated samples were then incubated overnight at 55°C and 350 rpm in the Thermomixer compact (Eppendorf AG, Hamburg, Germany). The next day, additional 10 µl of Proteinase K (Vial 2, Roche Kit) was added and incubated for another hour at 55°C and 350 rpm in order to dissolve completely the tissue. Meantime the High-Pure-Filter-tube (Roche Kit), were inserted into the Collection-tube (Roche Kit). Then 325 µl of Binding buffer (Bottle 3, Roche Kit) and 325 µl of absolute ethanol were added to each sample, mixed gently by inverting and finally transferred to the High-pure-Filter-Tube. After 30 s centrifugation at 8,000 rpm, the flow-through was discarded. The centrifugation was then repeated for another 2 min at 12,000 rpm. The samples were then washed with 500 µl of Wash Buffer I (Bottle 4, Roche Kit), and centrifuged at 8,000 rpm for 15 s. The flow-through was again discarded. The washing step was again repeated twice with Wash Buffer II (Bottle 5, Roche Kit) (500 µl and 300 µl, respectively). After centrifugation of 2 min at 12,000 rpm, the flow-through was again discarded. Subsequently,

the collection-tube was removed and the High-Puffer-Filter-tube was placed into a sterile Eppi tube. The samples were then incubated at RT for 2 min with 90 µl Elution buffer (Vial 8, Roche Kit) and centrifuged for 1 min at 8,000 rpm. The High-Pure-Filter-tubes were then discarded.

As next, DNase digestion was continued by adding 1 µl of DNase I (Vial 6, Roche Kit) and 10 µl of DNAse Incubation Buffer (Vial 7, Roche Kit) to the isolated RNA. The mixture was mixed gently by pipetting up and down and incubated for 45 min at 37°C in the Thermomixer compact.

Thereafter, the RNA purification was followed by adding to each sample, 20 µl of Tissue Lysis buffer (Bottle 1, Roche Kit), 18 µl of 10% SDS and 40 µl of Proteinase K (Vial 2, Roche Kit). The mixture was then vortexed and incubated for 1 h at 55°C and 350 rpm in the Thermomixer compact. Then 325 µl of Binding buffer (Bottle 3, Roche Kit) and 325 µl of absolute ethanol was added to each sample, mixed gently by inverting and finally transferred to the High-pure-Filter-Tube. After 30 s centrifugation at 8,000 rpm, the flow-through was discarded. The centrifugation was then repeated for another 2 min at 12,000 rpm. The samples were then washed with 500 µl of Wash Buffer I (Bottle 4, Roche Kit), and centrifuged at 8,000 rpm for 15 s. The flow-through was again discarded. The washing step was again repeated twice with Wash Buffer II (Bottle 5, Roche Kit) (500 µl and 300 µl, respectively). After centrifugation of 2 min at 12,000 rpm, the flow-through was again discarded. Subsequently, the collection-tube was removed and the High-Puffer-Filter-tube was placed into a sterile Eppi tube. The samples were then incubated at RT for 2 min with 2x 30 µl Elution buffer (Vial 8, Roche Kit) and centrifuged for 1 min at 8,000rpm. The High-Pure-Filter-tubes were then discarded.

RNA was finally eluted in 60 µl of RNase-free water and quantified spectrophotometrically with the Nanodrop 200c spectrophotometer (pegLab, Erlangen, Germany). Following the measurement of RNA concentration, eluted RNA was directly used to synthesize cDNA (complementary Deoxyribonucleic acid) or stored at -80°C until analysis.

2.6.2 cDNA synthesis

The cDNA synthesis was performed with the RevertAid First Strand cDNA Synthesis Kit (Fermentas GmbH, St. Leon-Rot, Germany). The kit is using the M-MuLV Reverse Transcriptase, which is a polymerase that synthesizes DNA from RNA and the primer oligo (dT)18.

Procedure: For each reaction, a total volume of 11 µl of RNA was used. To each RNA sample 1 µl oligo (dT)18 primer was added, gently mixed, briefly centrifuged, and incubated at 65°C for 5 min. The sample was then placed on ice for at least 2 min; meanwhile a working master-mix was prepared (4 µl of 5x reaction buffer, 2 µl of 10 mM dNTPs mix, 1 µl RNase inhibitor, and 1 µl M-MuLV Reverse transcriptase). The mix was added on the sample and incubated for 1 h at 43°C. Subsequently, the reaction was terminated by heating at 70°C for 5 min. Finally, the reaction tubes contained 20 µl of cDNA in total, were then either directly used in RT-PCR applications or stored at -20°C until further use.

2.6.3 SYBR Green-based real time PCR

The real-time polymerase chain reaction (Real-time PCR), also called quantitative polymerase chain reaction (qPCR) is a method used to detect the gene expression level in a sample. The procedure follows the general principle of polymerase chain reaction. Its key feature is that the amplified DNA is detected as the reaction progresses in “real time” after each cycle, in contrast to a standard PCR approach, where the product of the reaction is detected at its end. Moreover, in real-time PCR, the amount of DNA is measured after each cycle via fluorescent dyes that yield increasing fluorescent signal in direct proportion to the number of PCR product molecules (amplicons) generated. Data collected in the exponential phase of the reaction yield quantitative information on the starting quantity of the amplification target. The change in fluorescence over the course of the reaction is measured by an instrument that combines thermal cycling with fluorescent dye scanning capability. By plotting fluorescence against the cycle number, the real-time PCR instrument generates an amplification plot that represents the accumulation of product of the duration of the entire PCR reaction (*Figure 2-3*).

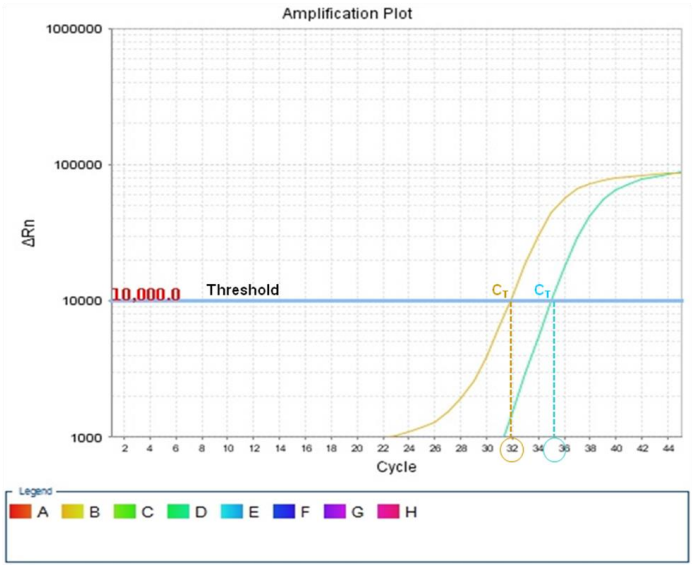

Figure 2-3: Graphical representation of an amplification plot of real- time PCR data. The x-axis presents the cycle number. The y-axis presents the magnitude of the fluorescence signal. C_T, the threshold cycle, is the cycle number at which the fluorescent signal of the reaction crosses the threshold.

The quantification of gene expression in this study was performed with SYBR Green-based-PCR (peqlab, Erlangen, Germany) using StepOnePlus Real Time PCR-System (Applied Biosystems/Life Technologies, Darmstadt, Germany) and the corresponding software 2.1.

SYBR Green I, a commonly used fluorescent DNA binding dye, binds all double-stranded DNA (dsDNA). The detection of SYBR Green I dye was monitored by measuring the increase in fluorescence throughout the individual PCR cycle. A melting curve charts the change in fluorescence observed, when dsDNA with incorporated dye molecules dissociates, or melts into single-stranded DNA (ssDNA) as the temperature of the reaction increased. For example, when dsDNA bound with SYBR Green I dye is heated, a sudden decrease in fluorescence is detected when the melting point (T_m) is reached, due to the dissociation of the DNA strands and subsequent release of the dye. The fluorescence is plotted against the temperature (*Figure 2-4*).

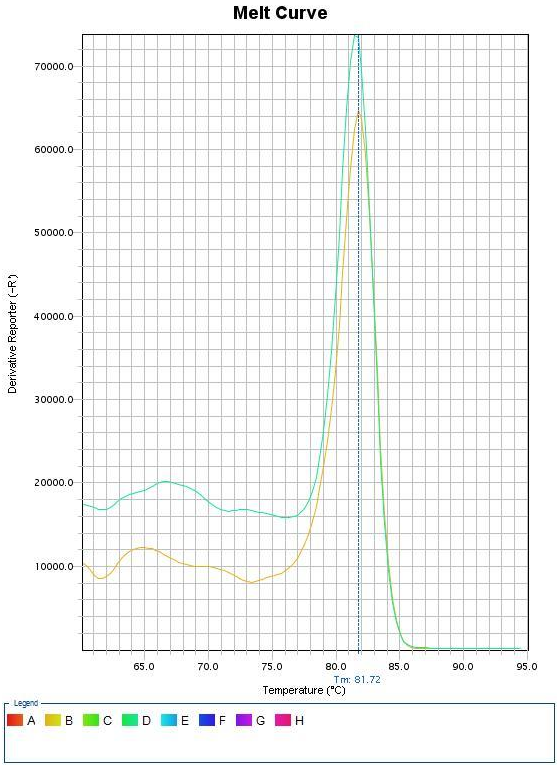

Figure 2-4: Example of a melting curve. The x-axis presents the temperature (°C), the y axis presents the derivative reporter of the fluorescence.

Procedure: In this study, the transcript levels of different genes were determined using the ready-to-use polymerase, KAPA^{TM} SYBR® FAST qPCR Master Mix Universal (peqLab, Erlangen, Germany).

First of all, a master mix solution was prepared as follow: 12.5 µl of SYBR® FAST qPCR Master Mix Universal, 8.5 µl of sterile water, 2 µl of the appropriate primer and 2 µl of cDNA. A total volume of 25 µl of each PCR reaction was then pipetted into a 96-well plate (MicroAmp® Fast Optical 96-Well Reaction Plate, Applied Biosystems, Darmstadt, Germany). Measurements were performed in duplicates for each samples and a non-template blank was served as a negative control. The PCR conditions were set as follow: initial PCR activation step for 5 min at 95°C, followed by 45 thermal cycles of denaturation for 10 s at 95°C, annealing temperature for 30 s at 60°C, extension for 10 s at 72°C, and an additional step for 15 s at 77°C to eliminate primer dimer. The mRNA levels for each target gene were standardized to the expression levels of glyceraldehyde-3-phosphate dehydrogenase (GAPDH).

The primers used in this study were all commercially purchased from Qiagen (QuantiTect Primer Assay; Hilden, Germany) as ready-to-use mix already optimized for the corresponding mRNA expression product (*Table 2-3*). The corresponding sequences are not available for these primers.

Table 2-3: Primers used for the real time PCR in this study.

Gene	Name	Amplicon (bp)	GeneGlobe Specification
GAPDH	QuantiTect Primer Assay Hs_GAPDH_1_SG	1455	NM_001256799
Col I	QuantiTect Primer Assay Hs_COL1A2_1_SG	5411	NM_000089
Col III	QuantiTect Primer Assay Hs_COL3A1_1_SG	5490	NM_000090
MMP-2	QuantiTect Primer Assay Hs_MMP2_1_SG	3558	NM_004530
MMP-9	QuantiTect Primer Assay Hs_MMP9_1_SG	2387	NM_004994
TIMP-1	QuantiTect Primer Assay Hs_TIMP1_1_SG	931	NM_003254
CD3	QuantiTect Primer Assay Hs_CD3D_1_SG	771	NM_000732
MSR1	QuantiTect Primer Assay Hs_MSR1_1_SG	2960	NM_002445
CD45	QuantiTect Primer Assay Hs_PTPCR_5_SG	5429	NM_002838
CXCR4	QuantiTect Primer Assay Hs_CXCR4_1_SG	1912	NM_001008540
CXCL12	QuantiTect Primer Assay Hs_CXCL12_1_SG	3549	NM_000609

2.6.4 Quantification of real-time PCR data

A widely used method to analyse the real-time PCR data is the comparative C_T method (also known as $\Delta\Delta C_T$). This is due to the fact that real-time PCR is not an absolute but merely a relative quantification. Therefore a co-determination of a reference or housekeeping gene is required.

First of all, a replication of reactions for each gene of interest and for the housekeeping gene (GAPDH) for each sample was performed under conditions yield to C_T values. The C_T value, called threshold cycle, is the intersection between an amplification curve and a threshold (*Figure 2-3*). To compare the gene expression between samples, $\Delta\Delta C_T$ should be calculated in the following fashion. A ΔC_T value is calculated for each sample as the difference between the C_T value for the gene of interest and the housekeeping gene in each sample. The $\Delta\Delta C_T$ value is the difference between the ΔC_T values of an experimental sample and the control sample. The fold-change in gene expression is equal to $2^{-\Delta\Delta C_T}$, if the PCR replication efficiency for all genes is 100%.

In the present work, $\Delta\Delta C_T$ and the relative expression were determined as followed:

$$\Delta\Delta C_T = \Delta C_T\left(target\,gene\right)_i - \Delta C_T\left(GAPDH\right)_i \tag{2.1}$$

where i corresponds to the number of individual samples analysed in this study.

$$relative expression = 2^{-\Delta\Delta C_T} \tag{2.2}$$

2.7 Analysis of protein expression using western blot

Western blotting is a widely used molecular biological technique to identify specific proteins from a complex mixture of proteins extracted from tissue samples or cells. The western blot technique uses three elements to accomplish this task: (i) protein separation by size using gel electrophoresis, (ii) transfer the separated proteins onto a special membrane (e.g. polyvinylidene fluoride (PVDF) or nitrocellulose (NC)), (iii) marking target protein using a proper primary and secondary antibody to visualize. Finally, using specific chemiluminescent substrate, the target protein is revealed as a band on an appropriate imaging system (e.g. blotting membrane, X-ray film or an imaging system).

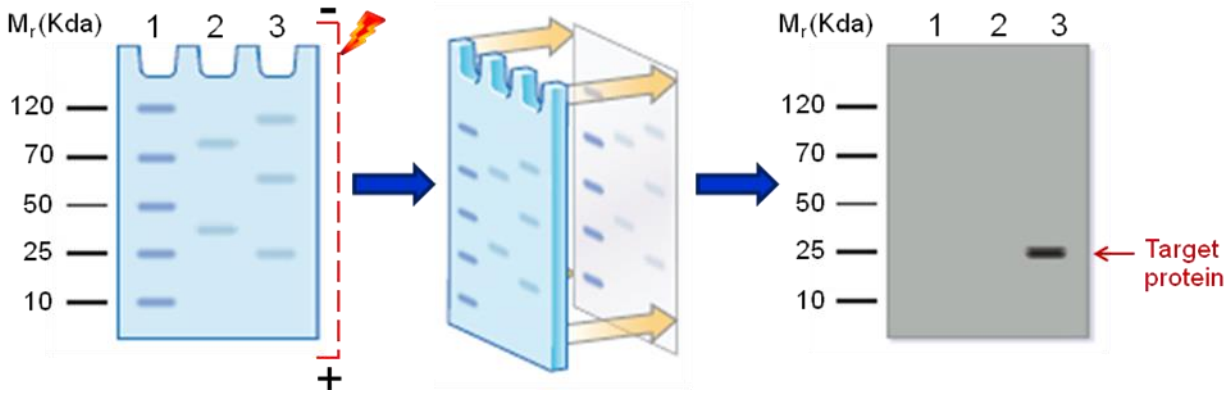

Figure 2-5: Schematic presentation of the western blot method; Separation of protein mixtures by electrophoresis; transfer to a blotting membrane; and detection of the target protein. Figure is based on: https://www.abdserotec.com/western-blotting-immunoblotting-introduction.html.

2.7.1 Sample preparation from tissue

Snap frozen samples were cut into small pieces and then crushed in liquid nitrogen in a mortar. The pulverised samples were placed into a 1.5 ml tube (Eppi tube, Eppendorf, Germany) and mixed with RIPA (radio immunoprecipitation assay) lysis buffer (50 mM TRIS-HCl (Merck) (pH=7.5); 150 mM NaCl; 1% Triton X-100; 0.5% sodium deoxycholate, 0.1 % SDS in distilled water), supplied with freshly prepared protease inhibitor mix (Roche, Mannheim, Germany). In the meantime, the homogenate was vortexed and incubated on ice for 30 min. After centrifugation for 30 min at 4°C and 12,000 rpm, the supernatants were collected in a new tube for the protein concentration and stored at -20°C until further use.

2.7.2 Protein concentration

Protein concentrations were determined using the Pierce BCA Protein Assay (23225-Pierce® BCA Protein Assay Kit, Thermo Scientific, Germany), which is a detergent-compatible formulation based on bicinchoninic acid (BCA) for the colorimetric detection and quantitation of total protein. Preparation of standards was prepared from diluted bovine serum albumin (BSA) ampoule (2mg/ml) diluted in the same lysis buffer as the samples (*Table 2-4*). The working reagent was prepared by mixing fifty parts of BCA reagent A with one part of BCA reagent B (50:1, Reagent A:B). A total volume of 10 µl of standards as well as samples (1 µl sample + 9 µl of lysis buffer) were pipetted in duplicates into a 96-well plate (96-Well Polystyrene Plates, Corner Notch, Thermo Scientific, Germany) and then 200 µl of working reagent were added to each sample and standard. After 30 min of incubation time at 37°C, the plate was measured with Photometer Asys Expert Plus Microplate Reader (Biochrom Ltd., Cambridge, UK). The absorbance at 590 nm was recorded and the protein concentration was then determined by comparison to a standard curve.

Table 2-4: Preparation of diluted bovine serum albumin (BSA) standards.

Vial	Volume of lysis buffer (µl)	Volume and source of BSA (µl)	Final BSA concentration (µl/ml)
1	0	300 of stock	2000
2	125	375 of stock	1500
3	325	325 of stock	1000
4	175	175 of vial 2 dilution	750
5	325	325 of vial 3 dilution	500
6	325	325 of vial 4 dilution	250
7	325	325 of vial 5 dilution	125
8	400	0	0 = Blank

2.7.3 Protein separation by polyacrylamide gel electrophoresis

The electrophoresis gel is usually composed of 2 different gel types, the separation gel and the stacking gel, with different concentrations in acrylamide as shown in *Figure 2-6*.

Figure 2-6: Schematic presentation of the electrophoresis gel.

Depending on the size of target proteins, different concentrations of acrylamide for the separation gel were used as described in *Table 2-5*. For the stacking gel, the composition is detailed in *Table 2-6*.

Table 2-5: Preparation of separation gel; SDS - Sodium dodecyl sulphate, APS - Ammonium persulfate, TEMED - N,N,N',N'-Tetramethylethylenediamene.

	Volume in ml for 1 gel		
Reagents	**15%**	**10%**	**6%**
TRIS-HCl (1.5 M; pH= 8.8)	2.500	2.500	2.500
Distilled water	2.400	4.100	4.900
Acrylamide 30%	5.000	3.300	2.000
SDS 10%	0.100	0.100	0.100
APS 10%	0.050	0.050	0.050
TEMED	0.005	0.005	0.005

Table 2-6: Preparation of 5% stacking gel.

Reagents	**Volume in ml for 1 gel**
TRIS-HCl (0.5 M; pH= 7.5)	1.250
Distilled water	2.750
Acrylamide 30%	0.850
SDS 10%	0.050
APS 10%	0.025
TEMED	0.005

Procedure: First, the separating gel was poured, swirled gently and then pipetted into the gel cassette (Bio-Rad GmbH, Germany). The top of the gel solution was layered with ethanol absolute and then incubated for 30 min at RT to polymerize. After polymerization, the ethanol was discarded and the top of the gel was rinsed with distilled water. With a filter paper, the excess water was carefully removed. Thereafter, the stacking gel was poured and pipetted into the gel

cassette. Finally, the comb was placed carefully. After another 30 min of polymerization, the comb was removed and the wells were rinsed with distilled water.

2.7.4 Electrophoresis procedure

Prior to start the electrophoresis procedure, a total volume of 30 µl of equal amount of protein lysates (50 µg) of each sample were mixed with 2x Laemmli buffer to a final dilution of 1x. The mixture was then heated to 95°C for 5 min, briefly centrifuged and then cooled on ice. Meanwhile, the electrophoresis chamber (Mini-Protean® Tetra Handcast Systems, Bio-Rad laboratories GmbH, Germany) was prepared and filled with the electrophoresis buffer (3.03 g Trizma base, 14.4 g glycine and 1.0 g of SDS in 1000 ml distilled water). The prestained marker IV (peqLab Biotechnologie GmbH, Erlangen, Germany) and the protein lysates were loaded onto the gel (*Figure 2-7*). The gel was running first for 20 min at 100 Volt (V) and then the voltage was increased to 200 V to finish the run in about 40-60 min.

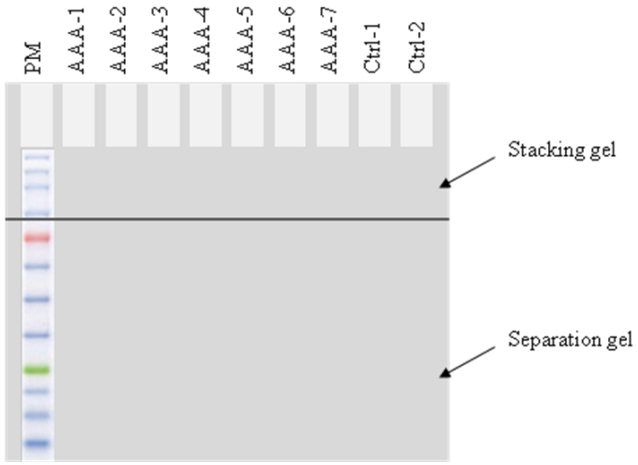

Figure 2-7: Schematic presentation of loading the prestained marker (PM) and the samples onto the gel during the electrophoresis procedure; AAA-Abdominal aortic aneurysm samples, Ctrl-Control (healthy aortic tissue samples).

2.7.5 Transferring the protein from the gel to the membrane

After the electrophoresis, the gel and the PVDF blotting membrane, activated with methanol for 5 s, were equilibrated for 30 min in the transfer buffer (3.03 g Trizma base (25 mM), 14.4 g glycine and 100 ml methanol in 1000 ml distilled water). Subsequently, the transfer sandwich consisting of paper-gel-membrane-paper wetted in transfer buffer was placed directly between cathode and anode respectively, in the semi-dry transfer cell system (Trans-Blot® SD, Bio-Rad laboratories GmbH, Germany) as shown in *Figure 2-8*. The transfer was running for 60 min at a constant voltage of 15V.

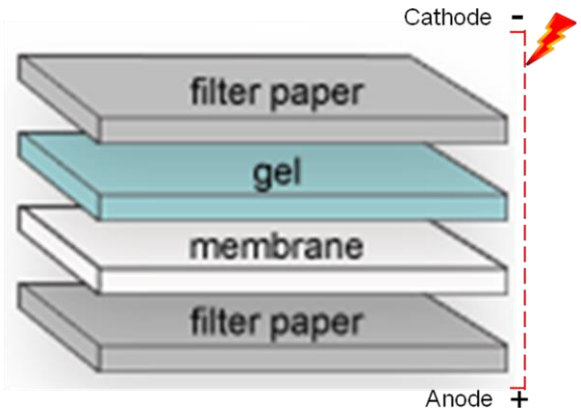

Figure 2-8: Assembling of the transfer sandwich. Figure is based on: http://www.cardio-research.com/protocols/western-blot.

To visualize, if proteins migrated uniformly and evenly, the gel was treated for 30 min with Coomassie Brilliant Blue solution (0.5 mg Coomassie brilliant blue R-250, 50 ml methanol, 10 ml acetic acid in 40 ml distilled water) following the transfer step. Moreover, the membrane was stained for 5 min with Ponceau S (Sigma-Aldrich, St Louis, MO, USA) to assess the success of the transfer. Before proceeding, the membrane was extensively rinsed with distilled water until the water is clear and the protein bands are well-defined.

2.7.6 Protein detection

After transferring, the membrane was blocked for 1 h at RT using blocking buffer (5% skim milk powder (70166, Sigma-Aldrich, St Louis, MO, USA) in TBST buffer). The TBST buffer was prepared by mixing 2.42 g Trizma base, 8.0 g NaCl (Merck) in 1000 ml distilled water (pH=7.6) and adding 1 ml of Tween® 20 (P1379, Sigma-Aldrich, St Louis, MO, USA). Consequently, the membrane was incubated overnight at 4°C with the appropriate primary antibodies diluted in blocking buffer as described in *Table2-7*.

Table 2-7: Dilution of the antibodies used in this study.

Antigen	Antibody	Dilution
CXCR4	Anti-CXCR4, rabbit anti-human, polyclonal, ab2074, Abcam Inc, Cambridge, UK	1:1,000
CXCL12	Anti-SDF-1 α, rabbit anti-human, polyclonal, ab9797, Abcam Inc, Cambridge, UK	1:1,000
GAPDH	Anti-GAPDH, mouse anti-human, monoclonal, ab8245, Abcam Inc, Cambridge, UK	1:10,000

The next day the membrane was washed three times for 10 min with TBST solution to remove the excess of the first antibody. The horseradish peroxidise (HRP)-conjugated secondary antibodies were also prepared in the blocking buffer (*Table 2-8*) and added to the PVDF membrane, which

was then incubated for 1 hr at RT. The membrane was again washed three times for 10 min with TBST.

Table 2-8: Secondary antibodies used in this study and their dilution.

Antigen	Antibody	Dilution
Rabbit	Gaot anti-rabbit IgG, ab97200, Abcam Inc, Cambridge, UK	1:5,000
Mouse	Goat anti-mouse IgG, 130043, KPL, Gaitherburg, USA	1:10,000

Consequently, the enhanced chemiluminescent (ECL) substrate was prepared by mixing solution A and solution B (ratio 1:1) of Pierce™ ECL Western Blotting Substrate (32106, Thermo Scientific, Waltham, USA) and applied to the blot for 2 min. The excess reagent was drained off. The membrane was covered with transparent plastic wrap and then placed in an X-ray film cassette. In the dark, the membrane was exposed to Medical X-Ray Film 100NIF (Fujifilm Europe GmbH, Düsseldorf, Germany) and various exposure times were used to achieve optimal results. The film was then developed with a Medical Film Processor, CAT SRX-101A (Konica Minolta Medical, Tokyo, Japan).

2.7.7 Protein quantification

In order to quantify the amount of each targeted protein, developed films were scanned using a transparency scanner (CanoScan 8800 F, Canon, Tokyo, Japan) with a resolution of 600 dpi. The protein quantification was conducted with Adobe Photoshop CS5 software (Adobe, San Jose, USA). The mode of the original image was then changed to “Grayscale”. The region of interest (ROI) of each protein band was then defined and the number of the pixel value (p) and the grey mean value of each band (b) were determined. In addition, the grey mean value of the background (bg) was too detected in the vicinity of the corresponding band and then subtracted from the band value. To get the absolute intensity of each band, the difference of the grey mean values was multiplied by the number of pixels. Furthermore, to obtain comparable results, the intensities of the bands were compared with the one of the housekeeping gene (GAPDH). Finally, in order to obtain the relative intensity with respect to the standard, the quotient of both was calculated using the following formula:

$$relative\ intensity of\ the band = \frac{p.(b - bg)}{p_{GAPDH}.(b_{GAPDH} - bg_{GAPDH})} \qquad (2.3)$$

2.8 Mechanical testing of AAA wall

The mechanical testings were conducted in the institute of "Mechanics and High Performance Computing Group, Technische Universität München", as part of a cooperation project. The tensile test of the complete aortic wall was performed to explore the wall thickness, elastic properties, and failure load of the AAA wall. Therefore, AAA wall samples were first cleaned from non-vessel wall components, and cut into individual rectangular specimen suitable for uniaxial tensile testing (typically 20mm x 8mm). Specimen thickness was averaged from five measuring points using a Mitutoyo "Quick-Mini Series 700" digital thickness gauge (Mitutoyo, Kawasaki, Japan). Elastic properties and failure load were investigated using a Bose ElectroForce 3100 tensile test machine (Bose Corporation, Eden Prairie, USA). First, the tissue samples were exposed to a cyclic sinusoidal preconditioning at frequency of 0.5 Hz with a loading up to approximately 0.20 MPa (depending on specimen thickness). After applying 19 cycles of preconditioning the data of the 20th cycle was used for the evaluation of stiffness parameters. Following the cyclic testing, specimens underwent destructive testing in order to measure the failure load. In both cases, the applied force and the clamp displacement were recorded (see Appendix A and B for detailed description).

The parameters α [N/mm^2] and β [N/mm^2] of the constitutive law applied in the finite element stress and strain analysis (2.4) were determined from the cyclic experiments using a Levenberg-Marquardt curve fitting algorithm, a method to solve non-linear least squares problems. Wall strength [N/mm^2] and failure tension [N/mm] were derived from destructive testing (Reeps et al., 2009 and 2013; Maier, 2012):

$$strength = \frac{F_{\max}}{A_0} \tag{2.4}$$

$$failure\,tension = \frac{F_{\max}}{specimen\,width} \tag{2.5}$$

with the maximum measured force $F_{\max}$ and the initial cross-sectional area A_0 of each specimen. For a more detailed description of the experimental setup, the reader is referred to (Reeps et al., 2009, Maier, 2012).

2.9 Finite element analysis of patients-specific AAAs

As well as part of a cooperation work, the finite element analysis (FEA) were conducted in the institute “Mechanics and High Performance Computing Group, Technische Universität München”. FEA was performed as described in detail in the studies of Reeps and Maier (Reeps et al., 2013; Maier et al., 2010; Maier, 2012).

Prior to surgical intervention, all patients underwent clinical examination, followed by multi-slice computed tomography angiography (CTA). Using the commercial segmentation software Mimics (Materialise, Leuven, Belgium), CTA data were commuted for reconstruction of 3-dimensional (3D) AAA geometry including intraluminal thrombus (ILT) for later finite element analysis (FEA). Moreover, the 3D images were used to record the sample excision site and the orientation of the harvested AAA wall specimens during surgery.

Finite element models of the 3D reconstructions were created using Harpoon (Sharc Ltd., Manchester, UK). The corresponding patient-specific nonlinear quasi-static structural finite element simulations were carried out using our in-house research Software BACI (Wall and Gee, 2014). A hyperelastic constitutive law was used for the AAA wall based on a strain energy function (SEF) proposed by Raghavan and Vorp (2000):

$$\Psi = \alpha\left(\pi(C)-3\right)+\beta\left(\pi(C)-3\right)^2 \tag{2.6}$$

where $\pi(C)$ denotes the trace of the right Cauchy-Green deformation tensor as a measure of strain. The two parameters α and β can be interpreted as stiffness in the small strain and large strain regime, respectively (see Appendix B for detailed explanation). For the intraluminal thrombus (ILT) the constitutive model proposed by Gasser et al. (2008) was used. Additionally, local AAA diameter at the sample excision site and normalized local diameter NORD [-] at the sample excision site were determined from the 3D reconstruction of the AAA. For patients with an infrarenal abdominal aortic aneurysm NORD was standardized by dividing the local diameter by the subrenal aortic diameter. For juxtarenal aortic aneurysm, we standardized as follows: in case the aneurysm reached renal arteries, the aortic diameter between celiac and superior mesenteric artery minus 2.5 mm was used instead. The correction term of 2.5 mm was the average difference in diameter for these two positions in the complete population of infrarenal AAAs.

2.10 Statistical analysis

The data obtained in the present work were fist analysed by one sample Kolmogorov Smirnov test to prove, whether an assumption for normal distribution can be accepted. In the case the conditions for normal distribution were complied with ($p>0.05$), the samples were assumed to be normal distributed and the student's *t*-test was applied for n=2, or ANOVA test for n>2. In the case of $p<0.05$, the hypothesis of normal distribution was rejected and the samples were analysed with non-parameter tests. These data were then analysed by Mann-Whitney *U*-test for n=2 or by Kruskal Wallis test for n>2. For categorical variables, such as gender, smoking history, hypertension, diabetes and coronary disease, comparison between groups was achieved using a Chi-square (χ^2) test. Continuous data in RT-PCR results are presented as mean ± SD. The two groups were tested by homogeneity of variances, after which the differences between groups were compared by repeated measurements using One-way ANOVA. Correlations between continuous variables were quantified by using Spearman's rank correlation coefficient (ρ). All statistical tests were two-sided. *P*-values of <0.05 were considered significant. The analyses were performed using SPSS version 20.0 (SPSS Inc., Chicago, IL, USA).

Chapter 3 Results

This thesis is divided into four different studies: (3.1) Impact of extracellular matrix components on biomechanical properties in abdominal aortic aneurysm, (3.2) Gene expression and biomechanical properties of abdominal aortic aneurysm wall, (3.3) Role of the chemokine receptor CXCR4 and its ligand CXCL12 in the pathogenesis of abdominal aortic aneurysm, (3.4) Chronic kidney disease affects mechanical properties of abdominal aortic aneurysm wall.

3.1 Impact of extracellular matrix components on biomechanical properties of AAA wall

3.1.1 Patient characteristics

In this study 54 tissue samples were collected from 31 patients (30 males and one female), who underwent an open surgical repair. Study patients were a mean age of 70.1 ± 7.9 years. The mean maximum diameter of AAA was 59.8 ± 14.2 mm. Almost 21% of the patients suffered from chronic kidney disease (CKD) and diabetes mellitus (DM) and 44.8% from coronary heart disease (CHD). Moreover, 62.1% had hypertonia and 70.4% were smokers. Detailed patient characteristics are summarized in *Table 3-1*.

Table 3-1: Baseline characteristics of study patients for both studies: (i) Impact of ECM components on biomechanical properties of AAA wall and (ii) Gene expression and biomechanical properties in AAA.

Number of patients	**31 (30 males, 1 female)**
Age	70.1 ± 7.9 years
Max AAA diameter	59.8 ± 14.2 mm
Associate disease	**n / %**
Hypertonia	19 / 62.1%
Smokers	22 / 72.4%
Chronic kidney disease	6 / 20.7%
Coronary heart disease	14 / 44.8%
Diabetes mellitus	6 / 20.7%

Medication	%
ASA	69.0%
Statins	48.3%
ACE inhibitors	31.0%
Beta-blocker	62.1%

ASA-Aspirin; ACE-Angiotensin converting enzyme.

3.1.2 Histopathology

Figure 3-1 shows selected examples of the staining used in this study. Sirius red and Alcian blue were chemical staining procedures, collagen type I and type III and Elastin were stained using immunohistochemistry. Sirius red staining, detecting the total collagen, did not show any significant differences in the collagen distribution between control aorta and AAA tissue. However, in contrast to healthy vessel, the staining was very heterogeneous with many areas without any collagen. Similar results were observed also for collagen type I and type III. Interestingly, collagen type I in contrast to collagen type III was not detected in adventitia. The staining of proteoglycans showed marked differences between healthy aorta and AAA tissue. The distribution of proteoglycans was very broad. In most cases, an increased amount of proteoglycans was observed in the vessel wall layers near the lumen. The most differences between control vessels and AAA were found for elastin. Whereas in healthy tissue samples the elastin fibres were regularly distributed throughout the media, in AAA specimens very little elastin was detected, mainly loosely scattered throughout the aneurysmal wall.

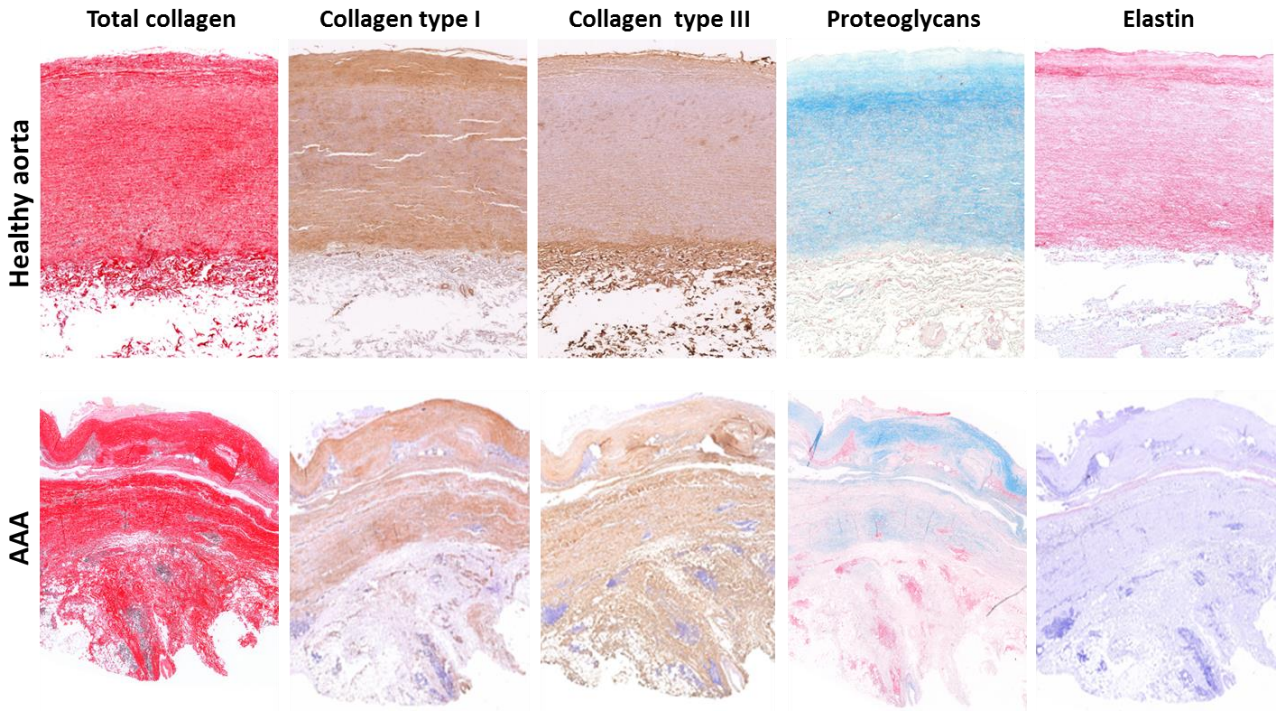

Figure 3-1: Representative stainings of the individual components of ECM in AAA and healthy aortae tissue specimens: collagen type I and type III as well as elastin were determined by immunohistochemistry, total collagen by sirius red and proteoglycans by alcian blue.

3.1.3 ECM composition in AAA wall

The total amount of the individual components of ECM within the aortic wall was expressed as a relative percentage as described in sections 2.5.2. The following results were observed: the average amount of collagen type I was 44.75% (2.8-78.07) and collagen type III was 62.18% (36.69-83.75). Total collagen was 57.46% (35.18-87.22), elastin was only 0.68% (0-14.99) and proteoglycans were 37.19% (1.7-79.8) of the total area (*Figure* 3-2).

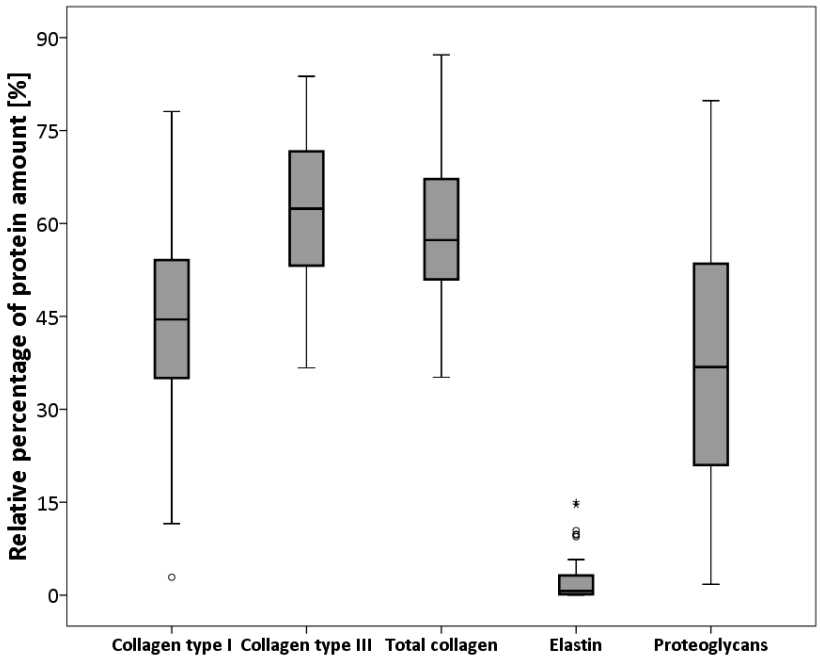

Figure 3-2: Box and whisker plots of the content of collagen type I and type III, total collagen, proteoglycans, and elastin. The content of each ECM component was determined by quantitative area measurement and displayed as a relative percentage of the total vessel area.

3.1.4 ECM components versus AAA geometrical parameters

Interestingly, the content of the different collagens within the AAA vessel wall (*Figure 3-3*) was correlated negatively with intraluminal thrombus thickness (collagen type I and type III, and total collagen; ρ=-0.399, -0.315, and -0.331; P=0.003, 0.020, and 0.015, respectively). No correlations were observed between thrombus thickness and elastic fibres or proteoglycans. Additionally, local and normalized local AAA diameter correlated significantly negative with the amount of elastin (ρ=-0.370 and -0.409, P=0.006 and 0.002, respectively) (*Figure 3-4*). The other components of ECMs did not show any significant relationships with the diameter.

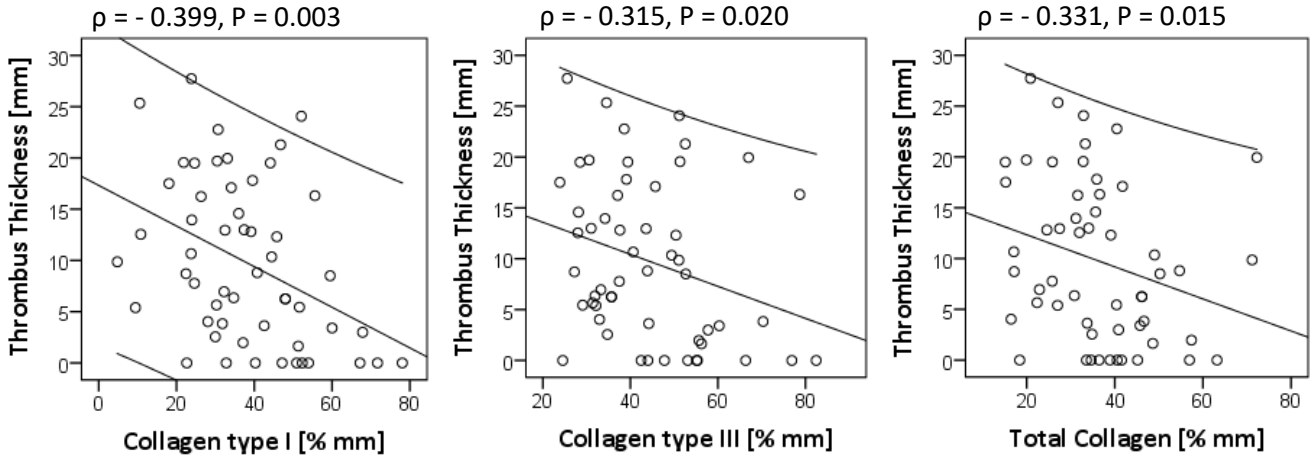

Figure 3-3: Scatter plots of significant correlations between local thrombus thickness at the sample excision site and collagen. Collagen type I and type III, and total collagen content were multiplied with the wall thickness. 95% confidence intervals are displayed.

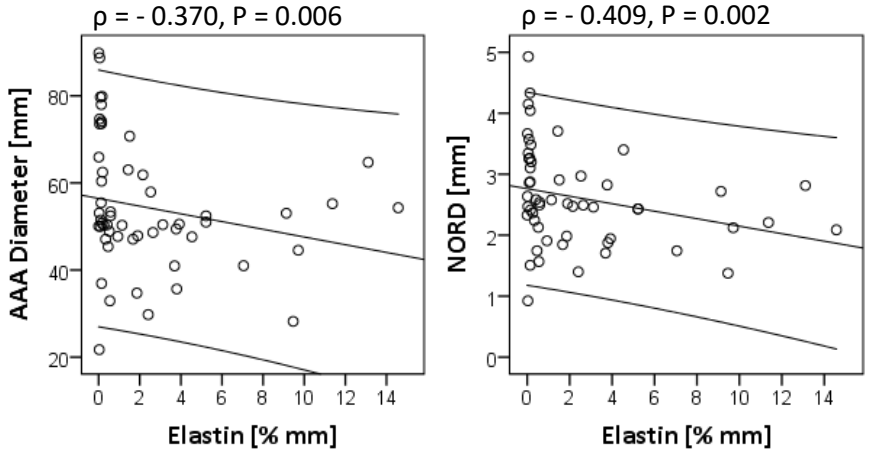

Figure 3-4: Scatter plots of significant correlations between local AAA diameter, NORD and elastic fibres. 95% confidence intervals are displayed. Wall thickness scaling was performed as described in Figure 3-3.

3.1.5 ECM components versus mechanical properties of AAA wall

The macroscopic mechanical properties of AAA wall, assessed by cyclic sinusoidal and destructive tensile testing, revealed a positive correlation corresponding to ECM composition. Collagen I, total collagen and proteoglycans were positively correlated with the failure tension of AAA wall obtained by destructive testing (ρ=0.302, 0.301 and 0.329, P=0.037, 0.038 and 0.022, respectively) (*Figure 3-5*). Further correlations were observed between collagen I, III as well as total collagen and α-stiffness of AAA wall (ρ=0.361, 0.298 and 0.374, P=0.011, 0.038 and 0.008 respectively), while proteoglycans correlated only with β-Stiffness (*ρ*=0.313, P=0.028) (*Figure 3-6*).

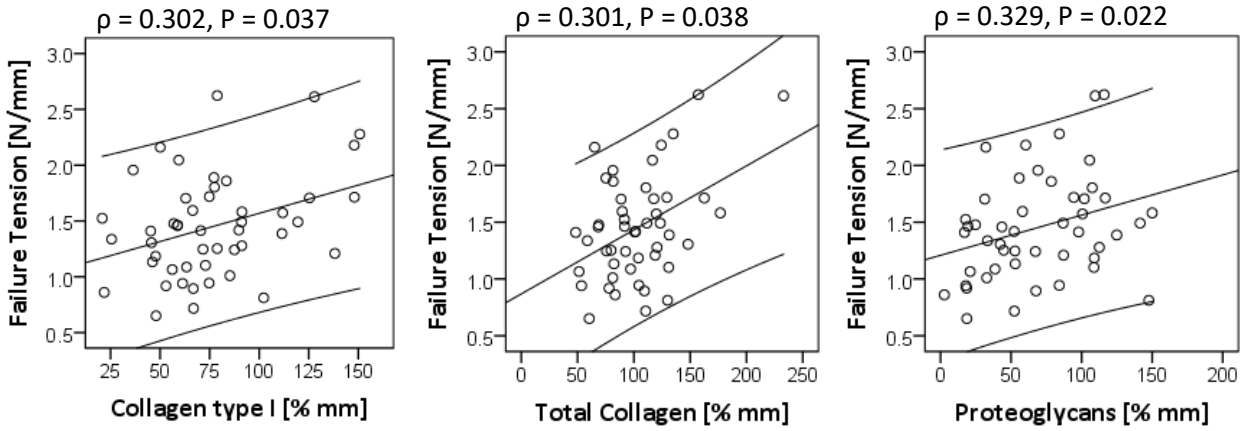

Figure 3-5: Scatter plots of significant correlations between failure tension and collagen type I, total collagen and proteoglycans. 95% confidence intervals are displayed. Wall thickness scaling was performed as described in Figure 3-3.

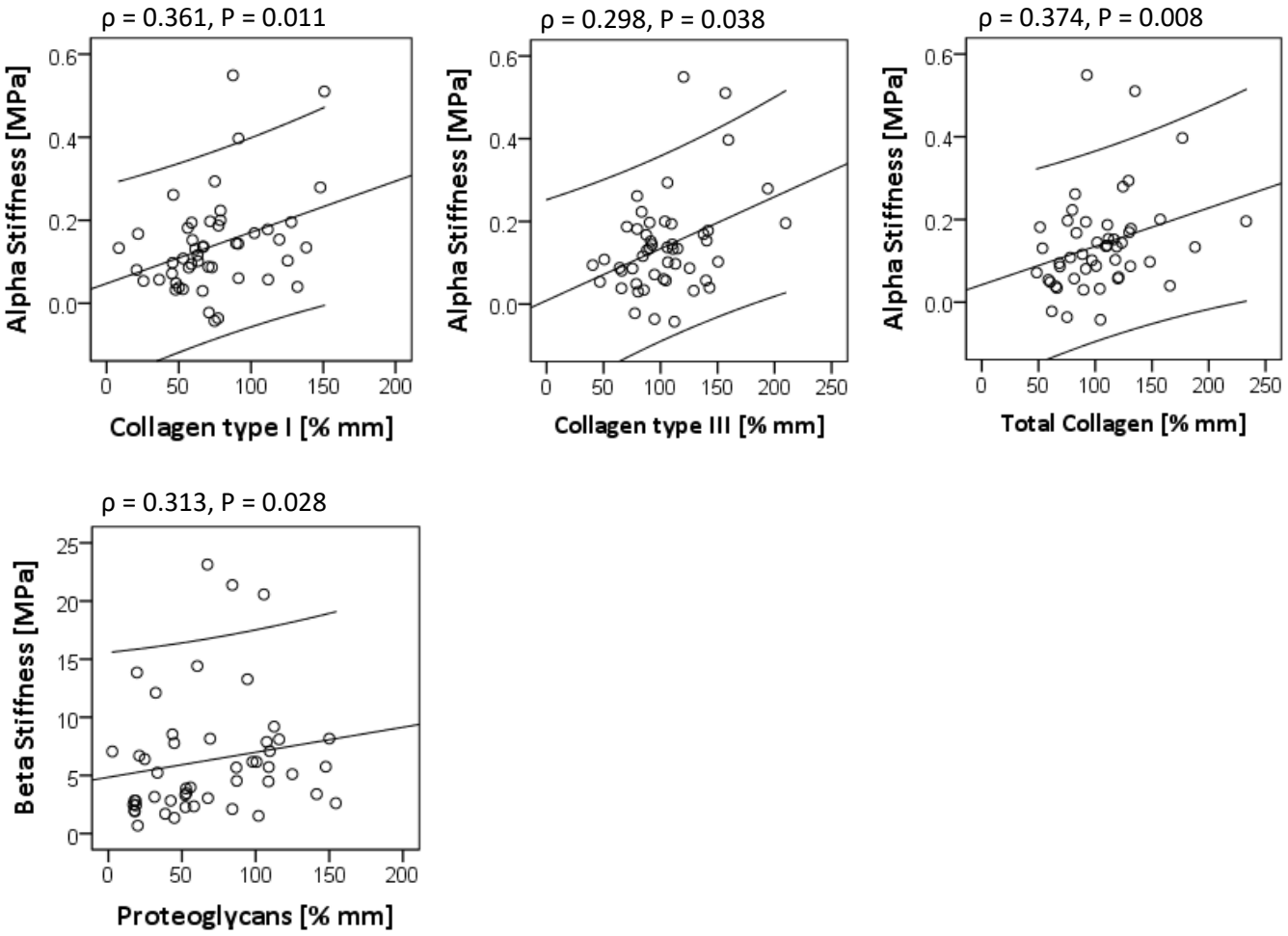

Figure 3-6: Scatter plots of significant correlations between alpha-stiffness and collagen type I and type III and total collagen and beta-stiffness with proteoglycans. 95% confidence intervals are displayed. Wall thickness scaling was performed as described in Figure 3-3.

3.1.6 ECM components versus finite element analysis in AAA wall

For the investigation of potential mechano-biological interactions, the total amount of the individual components of ECM was compared with local strain and stress (also mentioned as calculated von Mises strain and von Mises stress, respectively) state of the AAA vessel wall obtained from FE simulation at the sample excision site (*Figure 3-7*). Interestingly, content of collagen type I and type III and total collagen correlated positively with calculated von Mises stress (ρ=0.405, 0.323 and 0.296, P=0.002, 0.017 and 0.030, respectively) and likewise with von Mises strain (ρ=0.406, 0.338 and 0.315, P=0.002, 0.012 and 0.020, respectively).

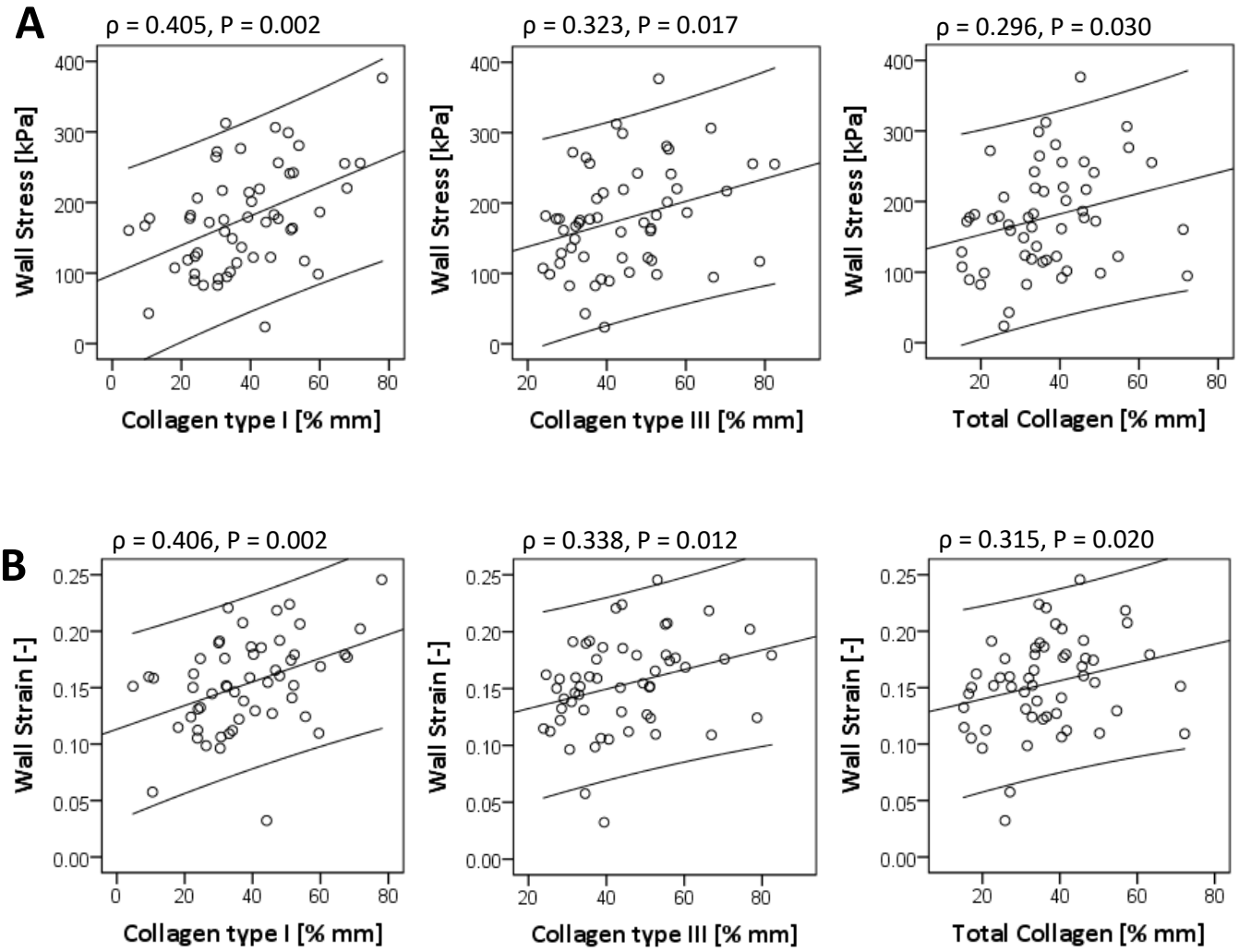

Figure 3-7: **A:** Scatter plots of significant correlations between local von Mises stress and collagen I, III and total collagen. **B:** Scatter plots of significant correlations between von Mises strain and collagen I, III and total collagen. 95% confidence intervals are displayed. Wall thickness scaling was performed as described in Figure 3-3.

3.2 Gene expression and biomechanical properties of AAA wall

3.2.1 Transcript analysis of representative markers of AAA progression

First, the gene expression of selected well known markers as representatives for AAA progression towards rupture with regard to inflammation such as leukocytes and their common surface marker CD45, macrophages with their common surface scavenger receptor MSR1, enzymes of proteolytic degradation such as MMP-2, -9, and their inhibitor TIMP-1, was analysed in this study. Furthermore, as common structural proteins responsible for AAA wall stability, the gene expression of collagen type I and type III was evaluated. The gene expression of these destabilising markers was detected in all AAA tissue samples (*Figure 3-8*). The expression of both collagen, type

I and type III, appeared to be similar (interrelated difference between collagen type I and type III was 0.77, P=0.381). In contrast, the expression of CD45 was 6.02-fold higher than that of MSR1 (P>0.001). The same tendency as for collagen was observed also for MMP-2 and -9 (interrelated difference 1.87, P=0.097). Regarding the relationship between the expression of MMPs analysed in this study and TIMP-1, the expression of their inhibitor was significantly higher, 2.23-fold for MMP-2 (P<0.001) and 1.93-fold for MMP-9 (P<0.001).

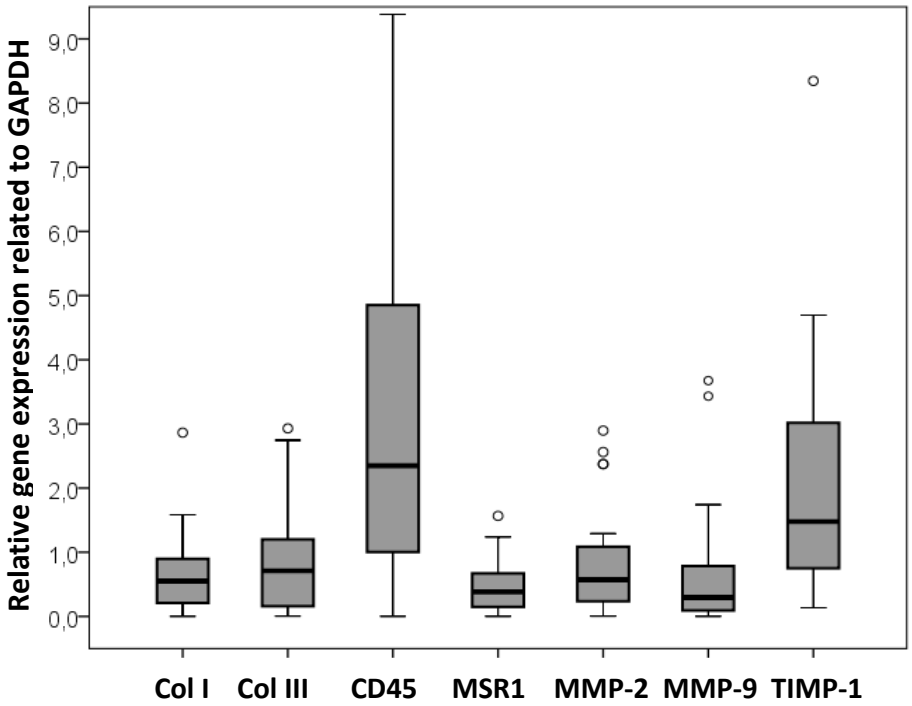

Figure 3-8: Gene expression of structural proteins in AAA wall: collagen (Col) type I and type III, inflammatory factors CD45 and MSR1, proteolytic enzymes MMP-2 and MMP-9, and their inhibitor TIMP-1 in AAA wall. RNA was extracted from FFPE AAA tissue samples adjacent to the histological and mechanical part. All values show relative expression of the individual factors related to the expression of the house-keeping gene GAPDH, which means that values at y-axis show the x-fold expression related to the expression of GAPDH.

3.2.2 Analysis of gene expression and underlying pathohistology

To analyse whether the gene expression at mRNA level is associated with histopathological changes in AAA wall, the mRNA expression was also correlated semi-quantitatively with the assessed histological findings such as infiltrates and neovessels (*Table 3-2*). As expected, the infiltration rate as well as the appearance of neovessels within the AAA wall correlated significantly with the mRNA level of CD45 and MSR1 (ρ=0.496 and ρ=0.548, P<0.001 for infiltrates; ρ=0.375 and ρ=0.540, P<0.01 and P<0.001 for neovessels). Interestingly, the mRNA level of collagen type III was related to the abundance of inflammatory cells and neovessels (ρ=0.308 and ρ=0.445, P<0.05 and P<0.001, respectively). Furthermore, the gene expression of MMP-2 was

significantly associated with the grade of inflammation within the aortic wall (ρ=0.559, P<0.001). In contrast, no association was found for the expression of MMP-9. Further, no correlation was observed between the semi-quantitatively determined amounts of collagen type I and type III in the tissue samples and the gene expression of collagen type I and type III.

It is to note that an analysis of the expression of elastin was omitted, because the histological analyses revealed very low amounts of elastic fibres in AAA tissue specimens mainly under 5%, in most cases even under 1% as shown in *section 3.1.3*.

Table 3-2: Correlation between semi-quantitatively assessed histology and gene expression. Significance *P<0.05; **P<0.01; ***P<0.001; -=no correlation (P>0.05).

	Infiltrates	Neovessels
Collagen I	-	-
Collagen III	**0.308***	**0.445*****
CD45	**0.496*****	**0.375****
MSR1	**0.548*****	**0.540*****
MMP-2	**0.559*****	**0.520*****
MMP-9	-	-
TIMP1	**0.314***	**0.409****

3.2.3 Correlation of gene expression with FEA

To identify the potential induction mechanisms of entirely mechanical conditions on biological processes, the computationally calculated wall stress and strain at the sample excision site were compared with the mRNA expression of the above mentioned inflammatory, proteolytic, and ECM-proteins. Thereby, no significant correlations of local calculated von Mises stress or von Mises strain (e.g. wall stress and strain) were observed with these parameters (*Table 3-3*).

Table 3-3: Correlation between gene expression, morphology and biomechanics for all patients included in this study. Significance *P<0.05; **P<0.01; ***P<0.001; -=no correlation (P>0.05). [+]Wall strength was measured using tensile tests, [++]Wall stress and Wall strain are calculated von Mises stress and strain.

	Thrombus	Diameter	Wall strength[+]	Wall Stress[++]	Wall strain[++]	Alpha	Beta
Collagen I	-	-	-	-	-	-	-
Collagen III	-	-	-	-	-	**-0.348***	-
CD45	-	**0.285***	-	-	-	-	-
MSR1	-	**0.551*****	-	-	-	-	-
MMP-2	-	-	**-0.438****	-	-	-	**-0.593****
MMP-9	-	-	-	-	-	-	-
TIMP1	-	**0.328***	-	-	-	-	-

3.2.4 Correlation of gene expression with geometrical and mechanical properties of AAA wall

To compare biological and mechanical properties of the AAA wall, the gene expression of the destabilising factors was correlated with measured tensile mechanical properties and pathomorphological features of the aortic wall (*Table 3-3*). Significant positive correlations were observed between the AAA diameter at the sample excision site (local diameter) and the expression of inflammatory factors CD45 and MSR1 (ρ=0.285 and ρ=0.551, P<0.05 and P<0.001, respectively). Respecting the constitutive parameters obtained from tensile tests, the expression of collagen type III correlated significantly negative with the parameter α (ρ=-0.348, P<0.05) and in addition MMP-2 with the parameter β and wall strength (ρ=-0.593 and ρ=-0.438, P<0.01, respectively). No other significant correlations were found for the expression of other biological parameters with mechanical quantities.

Moreover, because accompanied diseases such as diabetes mellitus (DM) or chronic kidney disease (CKD) may also influence the gene expression within the AAA wall, additional correlation analysis was performed after excluding patients with the above mentioned diseases (*Table 3-4*). The results following exclusion of patients with DM or CKD confirmed the data including all individuals of this study. Further correlations were observed for the gene expression of collagen type III with the local diameter and for the stiffness parameter β following exclusion of CKD

patients (both P<0.05). Finally, an additional correlation was found between MMP-2 and the diameter excluding DM patients.

Table 3-4: Correlation between gene expression, morphology and biomechanics excluding patients with chronic kidney disease (upper values) or with diabetes mellitus (lower values). Significance *P<0.05; **P<0.01; ***P<0.001; -=no correlation (P>0.05). [+]Wall strength was measured using tensile tests, [++]Wall stress and Wall strain are von Mises stress and strain.

	Thrombus	Diameter	Wall strength[+]	Wall Stress[++]	Wall strain[++]	Alpha	Beta
Collagen I	-	-	-	-	-	-	-
	-	-	-	-	-	-	-
Collagen III	-	**0.321***	-	-	-	**-0.351***	**-0.402***
	-	-	-	-	-	**-0.324***	-
CD45	-	**0.314***	-	-	-	-	-
	-	**0.326***	-	-	-	-	-
MSR1	-	**0.501*****	-	-	-	-	-
	-	**0.564*****	-	-	-	-	-
MMP-2	-	-	**-0.469****	-	-	-	**-0.686*****
	-	**0.360***	**-0.414***	-	-	-	**-0.467****
MMP-9	-	-	-	-	-	-	-
	-	-	-	-	-	-	-
TIMP1	-	**0.350***	-	-	-	-	-
	-	-	-	-	-	-	-

3.3 Role of the chemokine receptor CXCR4 and its sole ligand CXCL12 in the pathogenesis of AAA

3.3.1 Characterisation of AAA patients and control group

All AAA tissue samples (n=32) were harvested, based on CT data, from the anterior or lateral AAA sac at the maximum dilatation area of the AAA during elective open surgical repair. The average age of the experimental group (26 males and 6 females) was 66.8 ± 11.2 years. The maximum AAA diameter derived from preoperative CT scans was 64.4 ± 17.0 mm. The demographic data of the study patients, including patients' age, sex, smoking history, associated diseases and medications are summarized in *Table 3-5*.

As control group, 12 non-aneurysmal aortic specimens (10 males and 2 females; 45 ± 17 years), obtained from human organ donors of the Department of Transplant surgery, Klinikum rechts der Isar, were included. Moreover, due to the anonymity of donors, no additional information regarding the medical history of the control group was obtained.

Table 3-5: Demographic data of patients used in the study of "Role of the chemokine CXCR4 and its ligand CXCL12 in the pathogenesis of AAA".

Number of patients	**32 (26 males, 6 females)**
Age	76.8 ± 11.2 years
Max AAA diameter	64.4 ± 17.0 mm
Associate disease	**n / %**
Hypertonia	26 / 81.25%
Smokers	8 / 25%
Chronic kidney disease	12 / 37.5%
Coronary heart disease	6 / 18.75%
Diabetes mellitus	6 / 18.75%
Medication	**%**
ASA	71.87
Beta-blocker	62.5
Statins	56.25
ACE inhibitors	40.62
Diuretics	40.62

3.3.2 Expression of CXCR4/CXCL12 at mRNA level

Using quantitative real-time RT-PCR, the mRNA levels of the chemokine receptor CXCR4 and its ligand CXCL12, as well as the inflammatory markers for T-and B- lymphocytes and macrophages were detected in the AAA wall excised from the anterior or lateral sack at the maximum dilatation site as well as in the control tissue samples (*Figure 3-9*). Following standardization to the expression of GAPDH, AAA samples showed significantly increased mRNA expression levels for CXCR4 compared to control aorta by 9.6-fold ($P<0.0001$). The expression of CXCL12 was increased by 4.6-fold ($P<0.0001$), CD45 by 6.3-fold ($P<0.0001$), CD3 by 10.3-fold ($P=0.014$), and MSR1 by 16.6-fold ($P<0.0001$) in comparison with the control subjects.

Furthermore, because the study groups (AAA vs. control aortae) were not age-matched, additional correlation analysis was performed between age and the gene expression of *CXCR4* and *CXCL12* in the AAA patients and in the control group calculating the Spearman rang correlation coefficient. No significant relationships were observed (AAA-group: $\rho=-0.38$; $P=0.849$ for CXCR4 and $\rho=0.104$; $P=0.570$ for CXCL12; control group: $\rho=0.447$; $P=0.168$ for CXCR4 and $\rho = 0.451$; $P=0.190$ for CXCL12).

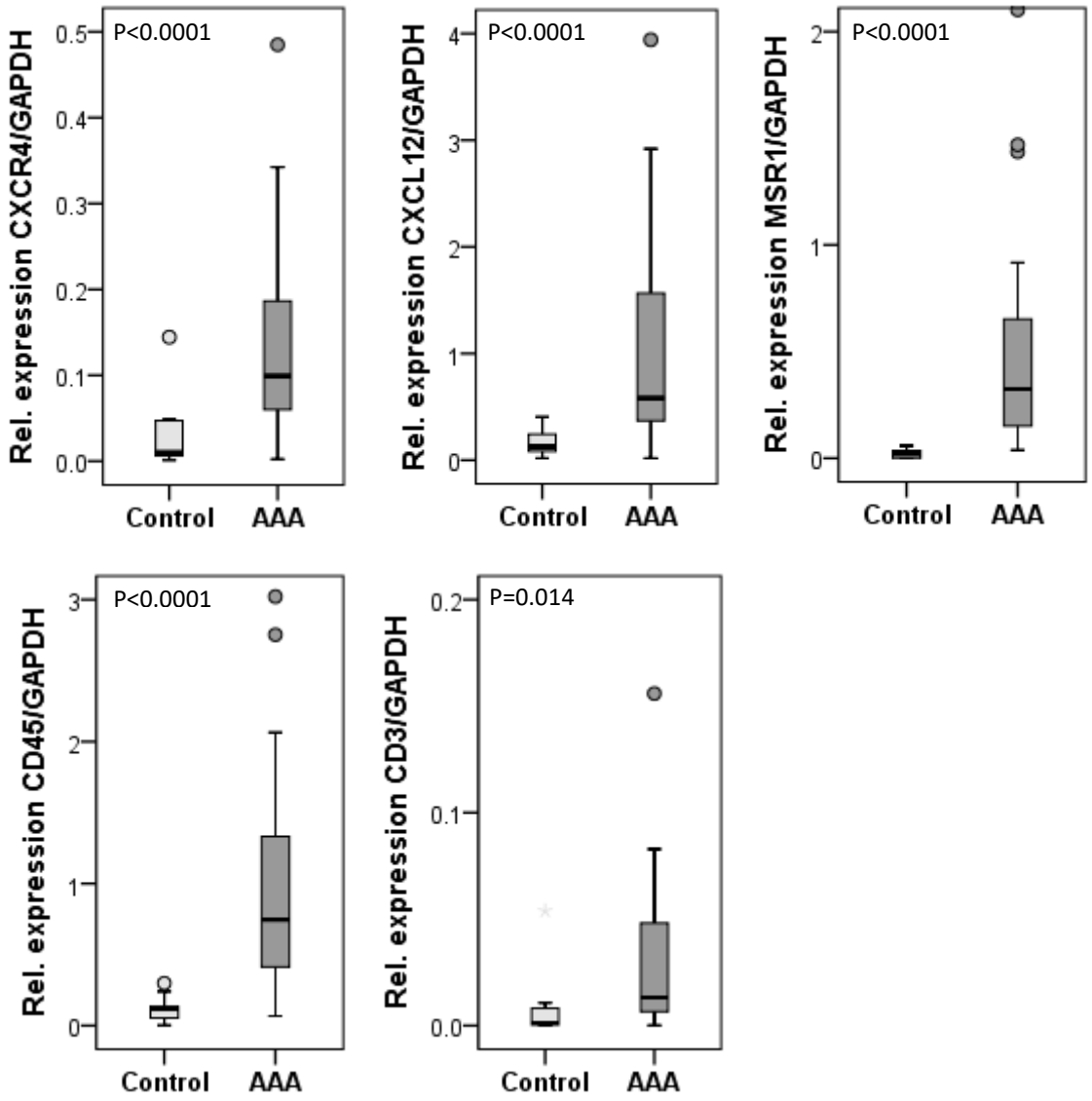

Figure 3-9: Expression of CXCR4, CXCL12 and inflammatory markers: MSR1, CD45, CD3 at the mRNA level in the AAA tissue samples (n=32) compared with the healthy control tissues (n=12) analysed by quantitative real-time PCR and SYBR green fluorescence dye; the expression levels were standardized to GAPDH. Mann-Whitney U-test was used. AAA, abdominal aortic aneurysm; CD, cluster of differentiation; MSR1, macrophages scavenger receptor 1; GAPDH, glyceraldehyde 3-phosphate dehydrogenase.

3.3.3 Relationship between the gene expression of CXCR4, CXCL12 and inflammation

As the chemokine receptor CXCR4 is known to be involved in lymphocytes activation, differentiation and trafficking at the site of inflammation, it had to be resolved, whether any relationship exists between CXCR4, CXCL12 and inflammatory cells in AAA wall (*Table 3-6*). Positive correlations were observed between the expression of CXCR4 and the expression of CXCL12, MSR1, CD45 and CD3 (ρ=0.761, ρ=0.532, ρ=0.746 and ρ=0.535; P<0.001, P=0.002, P<0.001 and P=0.002, respectively). Furthermore, CXCL12 was significantly correlated with the inflammatory

markers MSR1, CD45, and CD3, too (ρ=0.712, ρ=0.822 and ρ=0.549; P<0.001, P<0.001, and P=0.001, respectively).

Table 3-6: Correlation between the expression of CXCR4 and CXCL12 at mRNA level and inflammatory markers analysed within the AAA wall. Correlations were calculated using the Spearman rank correlation coefficient (ρ). Significance: *P<0.05; **P<0.01, ***P<0.001.

	CXCR4	CXCL12	MSR1	CD45	CD3
CXCR4	-				
CXCL12	**0.761****	-			
MSR1	**0.532****	**0.712****	-		
CD45	**0.746****	**0.822****	**0.663****	-	
CD3	**0.535****	**0.549****	**0.414***	**0.581****	-

3.3.4 Expression of CXCR4/CXCL12 at protein level

Following expression analysis at the mRNA level, the expression of CXCR4 and CXCL12 in the AAA tissue samples was determined at the protein level using western blot analysis (*Figure 3-10*). The expression of CXCR4 was found in the AAA group, as well as in the control group at the expected protein size (43 kDa). In contrast, the expression of CXCL12 at protein level could not be detected. An example of the protein bands is shown in *Figure 3-10*. The protein level of CXCR4 in AAA tissue samples in comparison with the control subjects was increased by 3.2-fold (P<0.0001). In contrast to CXCR4, the western blot analysis did not lead to any detection of protein bands for CXCL12.

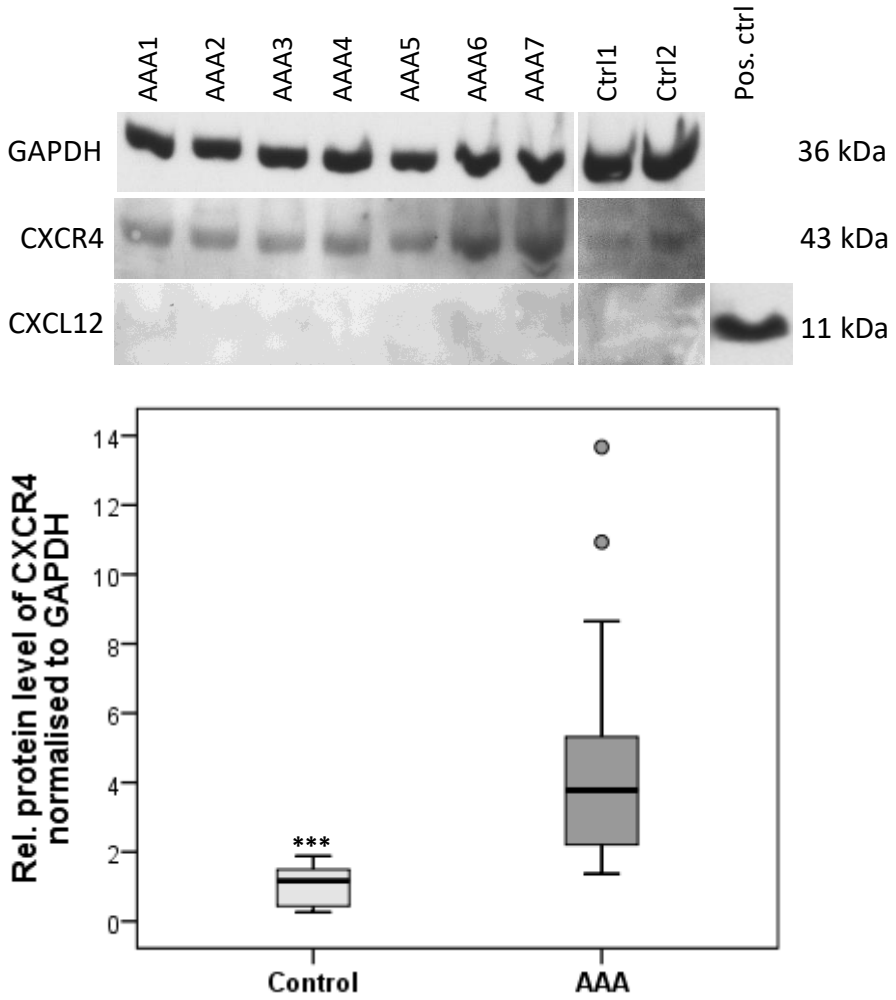

Figure 3-10: Expression of CXCR4 and CXCL12 at the protein level in AAA tissue samples (n=32) compared with healthy control tissues (Ctrl, n=12) analysed by western blot. Recombinant CXCL12 protein (Abcam) was used as positive control (Pos. ctrl, 0.1µg/lane). CXCL12 protein could not be detected either in AAA or in healthy aorta. The intensities of the bands following blotting and chemiluminescence detection were standardized to GAPDH. Mann-Whitney U test was used. *** P<0.0001.

3.3.5 Cellular localization of CXCR4 in AAA and healthy aortae determined by IHC

Histological and immunohistochemical analyses were performed to associate the expression of CXCR4 and CXCL12 to the different cell types within the AAA wall. The most abundant cells detected in AAA samples, were smooth muscle cells (SMCs) and inflammatory cells such as lymphocytes and macrophages, as already shown in a previous work (Reeps et al., 2009). The IHC analyses of the chemokine receptor CXCR4 and its ligand CXCL12 are shown in *Figure 3-11*. CXCR4 staining was positive for B- and T-lymphocytes, as well as for macrophages, indicating that these cells exhibited the highest expression of CXCR4. With regard to CXCL12, IHC analysis revealed only positive staining for plasma cells (*Figure 3-12*). All other cells in AAA wall as well as in the control aorta were negative for CXCL12.

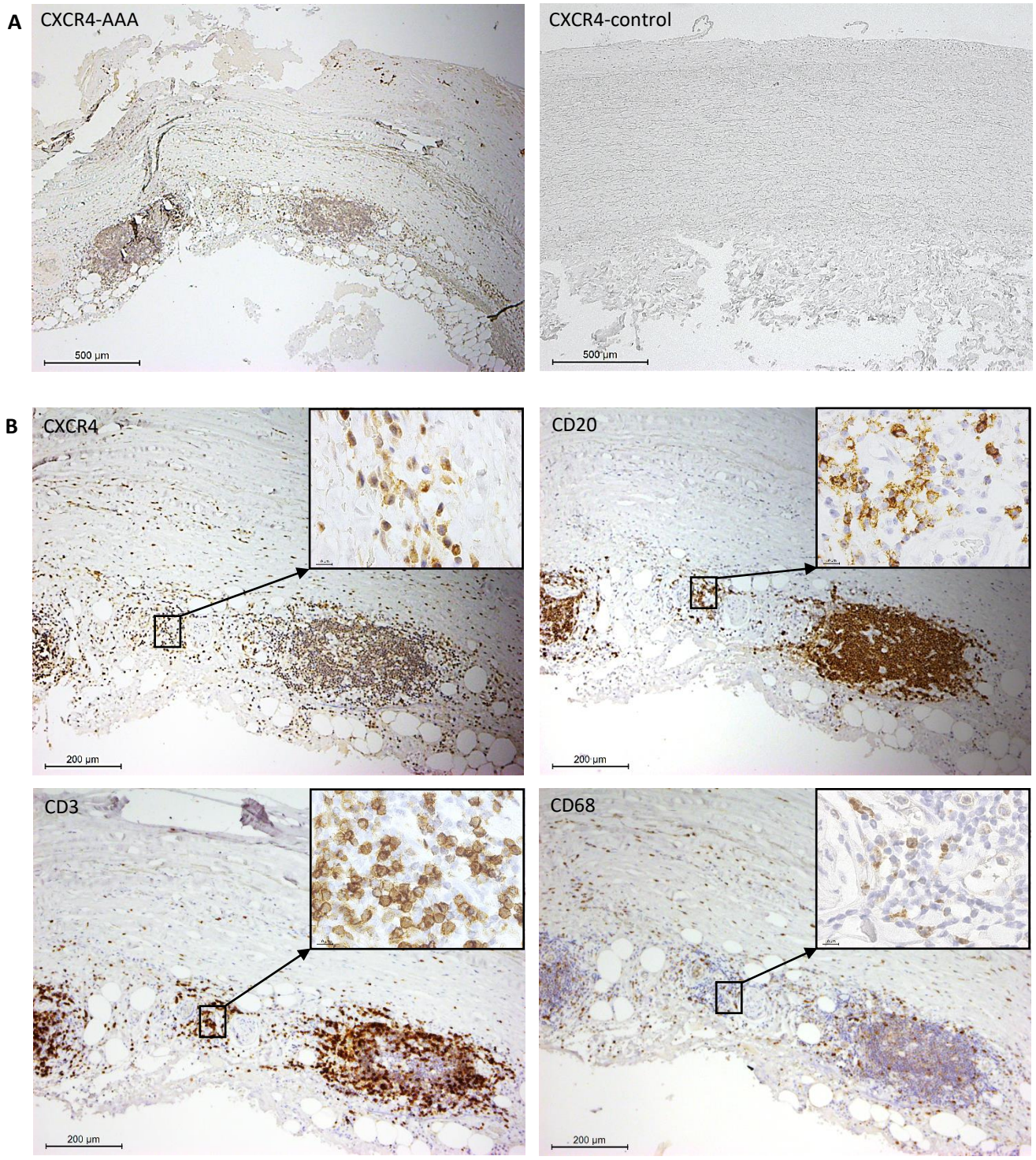

Figure 3-11: **A.** Immunohistochemical analyses of CXCR4 in AAA tissues samples and in healthy tissues. **B.** Selective immunohistochemical staining of CXCR4, CD68, CD3 and CD20 within the AAA tissues samples. Positive cells are brown and counterstained with haematoxylin and eosin, showing cell nucleus in blue. Scale bars are 200 µm. The inserts are high-power images of the selected regions. Scale bars are 10 µm.

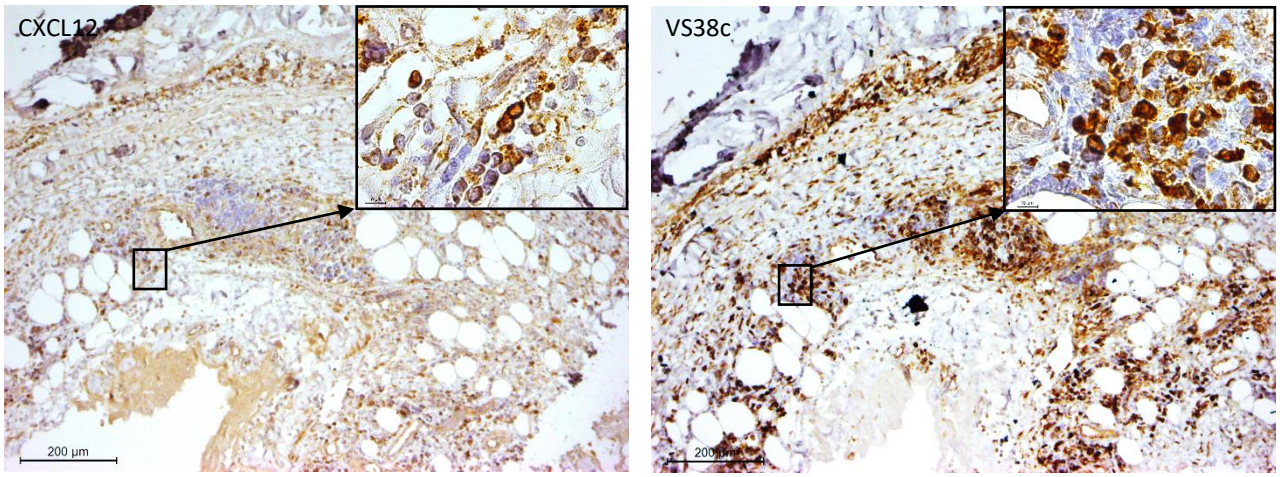

Figure 3-12: Immunohistochemical staining of CXCL12 and VS38c (plasma cells marker) within the AAA tissue samples. Positive cells are brown, the cells are counterstained with haematoxylin and eosin, showing cell nucleus in blue. Scale bar are 200 µm. The inserts are high-power images of the selected regions. Scale bar are 10 µm.

3.4 Chronic kidney disease affects mechanical properties of AAA wall

3.4.1 Patient characteristics

The basic demographic data of the study patients, including patients age, sex, smoking history, associated diseases such as coronary heart disease (CHD), hypertension, diabetes mellitus (DM), hyperlipidaemia, medications (aspirin, beta-blocker, statins, use of ACE (angiotensin converting enzyme) inhibitors, diuretics) as well as laboratory parameters e.g. high sensitivity C-reactive protein (hsCRP), creatinine, creatine kinase, blood calcium, potassium, sodium and urea nitrogen are summarised in *Table 3-7*. The study criterion for patient grouping was an estimated glomerular filtration rate (eGFR) according to the Kidney Disease Improving Global Outcomes (Kidney Disease: Improving Global Outcomes (KDIGO) CKD-MBD Work Group, 2009). Study individuals with eGFR<60 ml/min were considered as CKD patient.

Study patients were of a mean age of 69.25 ± 6.75 years. No differences were observed in the medical treatment between patients with or without CKD. In addition, there were no significant differences between the study groups in age, gender, maximum thrombus thickness and subrenal aortic diameter, as well as concerning diabetes, hyperlipidaemia and smoking, hsCRP, creatine kinase, calcium and sodium. The only differences were observed for hypertonia and coronary heart disease (P=0.009 and P=0.05, respectively), creatinine, potassium and urea (P=0.0001, P=0.022 and P=0.0001, respectively).

Table 3-7: Patient characteristics used in this study, including associated diseases, laboratory parameters and medical treatment. *Statistically significant differences between the groups.

Parameters	CKD (n=14)	No CKD (n=35)	P-values
Age, years	71.1 ± 4.7 (63-79)	67.4 ± 8.8 (48-90)	0.108
Male sex	14 (100%)	32 (91.4%)	0.548
Associated disease	**%**	**%**	
Hypertonia	92.8	51.4	**0.0009***
Hyperlipidaemia	50	45.7	0.752
Smoking status	50	60	0.542
Coronary heart disease	57.1	28.6	**0.05***
Diabetes mellitus	21.4	20	1.000
Laboratory parameters	**Mean**	**Mean**	
hsCRP(mg/l)	2.62 ± 3.77	1.76 ± 2.86	0.613
Creatinine (mg/dl)	1.65 ± 0.57	0.92 ± 0.13	**0.0001***
Creatine kinase (U/l)	89.83 ± 27.57	111.76 ± 75.29	0.624
Calcium (mmol/l)	2.14 ± 0.42	2.22 ± 0.25	0.579
Potassium (mmol/l)	4.82 ± 0.52	4.44 ± 0.51	**0.022***
Sodium (mmol/l)	141.36 ± 4.48	139.44 ±2.85	0.163
Urea (mg/dl)	34.38 ± 14.29	17.79 ± 5.30	**0.0001***
Medication	**%**	**%**	
ASA	71.4	62.8	0.503
Beta-blocker	57.1	48.5	0.530
Statins	64.3	40	0.111
ACE inhibitors	35.7	31.4	0.739
Diuretics	35.7	20	0.269

3.4.2 Biomechanics of AAA wall in patients with and without CKD

First, a direct comparison of all values was performed between patients with and without CKD. Significant differences observed in our study between the study groups are shown in *Figure 3-13*. Thrombus thickness was significantly increased in AAA patients suffering from CKD by factor 2.29 (range for the thrombus 0-29.5 mm) (P=0.001). In contrast, the diameter of AAA was decreased in the diseased patients by 1.21-fold (range 0.42-1.89) (P<0.0001), indicating that patients with CKD have a smaller diameter than patients without CKD. Furthermore, the wall thickness and failure tension were reduced in patients with CKD by factor 1.21 (range 0.33-3.68) and 1.30 (range 0.29-7.65) (P<0.0001 and *P*=0.021, respectively). Patients with CKD had also significant decrease of von Mises stress and von Mises strain (e.g. wall stress and strain) by 1.22-fold (range 0.08-10.92) (P<0.0001) and 1.21-fold (range 0.14-5.00) (P<0.0001), compared to patients without CKD.

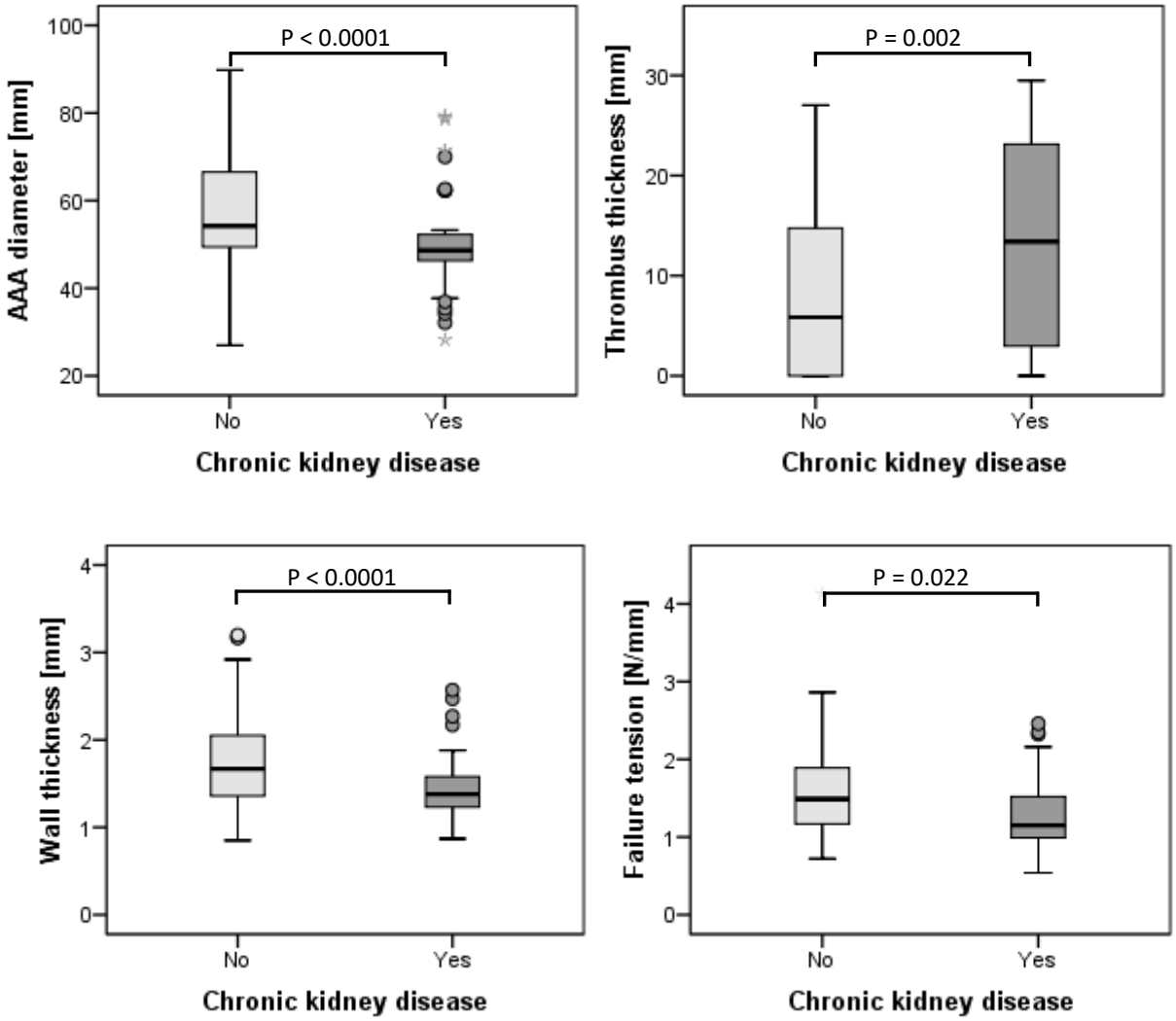

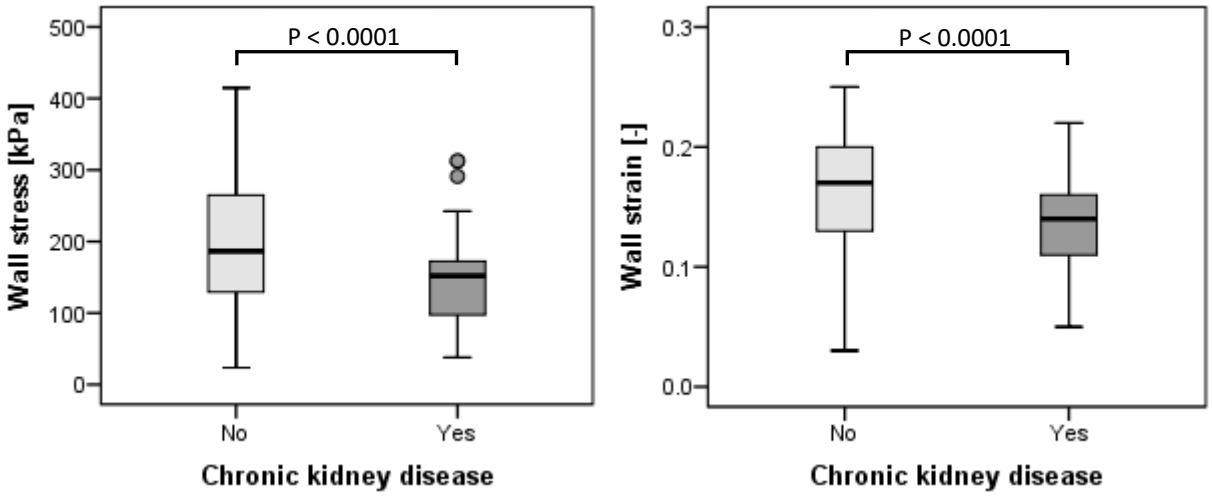

Figure 3-13: Box and whisker plots showing significant differences between AAA patients with or without chronic kidney disease (CKD). Mann-Whitney U-test was used.

3.4.3 Biomechanics of AAA wall and parameters associated with CKD

Next, correlation analyses were performed between various parameters associated with CKD and mechanical properties of the AAA wall determined by tensile tests and FEA (*Table 3-8*). Significant correlations are shown in addition as scatter plots in *Figures 3-14* to *3-18*.

Table 3-8: Correlations between mechanical properties of AAA wall and patients characteristics with focus on factors associated with CKD. Significance: *P<0.05; **P<0.01.

	Wall strength	Failure Tension	Alpha Stiffness	Beta Stiffness	Wall thickness	Wall stress	Wall strain
Max. AAA diameter	-	-	-	-	-	**0.474****	**0.498****
Subrenal aortic diameter	-	-	**0.270****	**0.287****	-	-	-
Ma. Thrombus thickness	-	-	-	-	-	**-0.338****	**-0.339****
Local thrombus thickness	-	-	-	**0.169***	**-0.182***	**-0.782****	**-0.761****
AAA calcification	-	-	**0.239****	**0.306****	-	**-0.155***	-

	Wall strength	Failure Tension	Alpha Stiffness	Beta Stiffness	Wall thickness	Wall stress	Wall strain
hsCRP	**0.251***	-	-	-	-	-	-
Creatinine	-	-	-	-	-	-	-
Creatine kinase	-	-	-	-	-	-	-
Calcium	-	-	-	-	-	-	-
Potassium	**-0.234****	**-0.280****	-	**-0.193***	-	**-0.165***	**-0.166***
Sodium	-	-	-	**0.225****	**-0.236****	**-0.204****	**-0.231****
Urea	-	-	-	**-0.229****	-	-	-

3.4.4 Tensile tests of AAA wall and parameters associated with CKD

The wall strength was significantly associated with hsCRP and indirect proportional with potassium determined from patient blood (ρ=0.251 and ρ=-0.234, P=0.020 and P=0.006, respectively) as shown in *Figure 3-14 A*. Failure tension of AAA wall correlated with blood values of potassium (ρ=-0.280, P=0.001) and urea (ρ=-0.238, P=0.008) as presented in *Figure 3-14 B*. Remarkably, AAA wall thickness was negatively associated with local thrombus thickness (ρ=-0.182, P=0.021) and sodium concentration in blood (ρ=0.236, P=0.003) as shown in *Figure 3-14 C*.

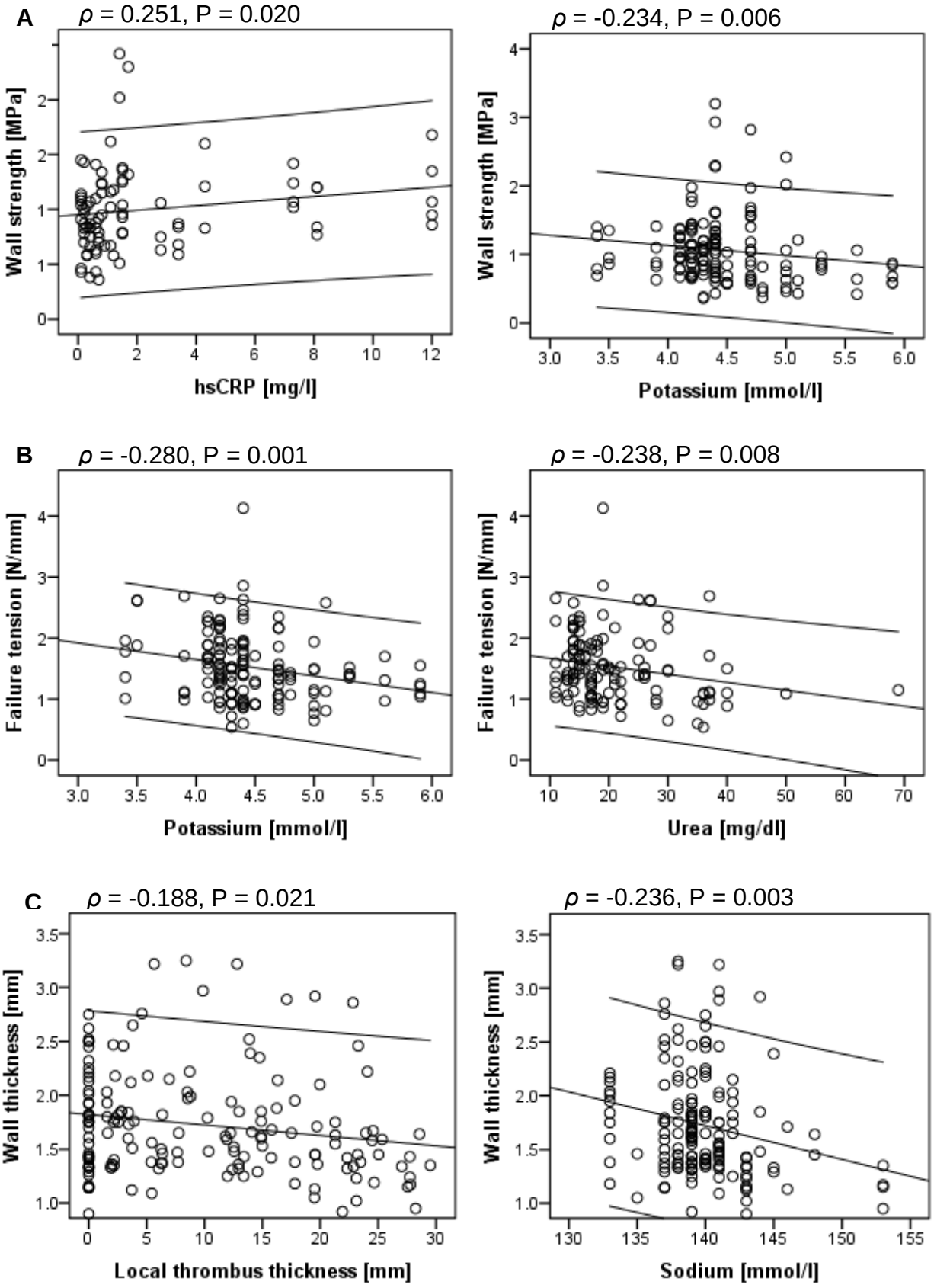

Figure 3-14: **A.** Scatter plots showing significant correlations between AAA wall strength and laboratory parameters, hsCRP and potassium. **B.** Scatter plots showing significant correlations between failure tension and potassium and urea. **C.** Scatter plots showing significant correlations between AAA wall thickness and local thrombus thickness and sodium.

Alpha and beta stiffness revealed significant correlations with the degree of calcification within the AAA wall specimens (ρ=0.239 and ρ=0.306, P=0.004 and P=0.0001), the subrenal aortic diameter (ρ=0.270 and ρ=0.287, P=0.001 and P=0.001, respectively) and urea (ρ=-0.230 and ρ=-0.229, P=0.009 and P=0.010). Additionally, beta stiffness showed significant correlations to local thrombus thickness (ρ=0.169, P=0.046) and potassium content in blood (ρ=-0.193, P=0.024) as shown in *Figures 3-15* and *3-16*.

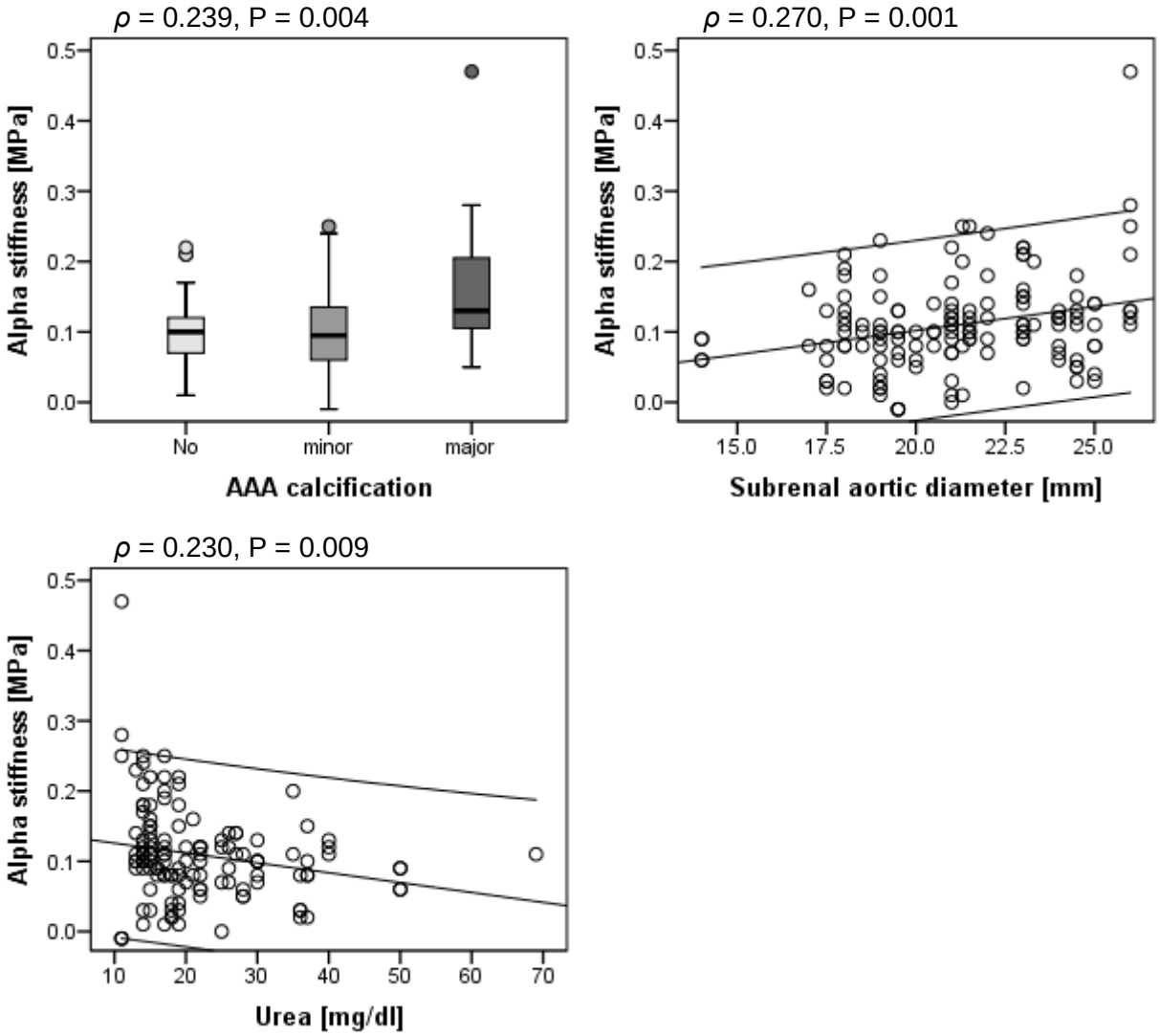

Figure 3-15: Box and whisker plot showing significant difference between alpha stiffness and extent of AAA calcification. Scatter plots showing significant correlations between alpha stiffness and subrenal aortic diameter and urea.

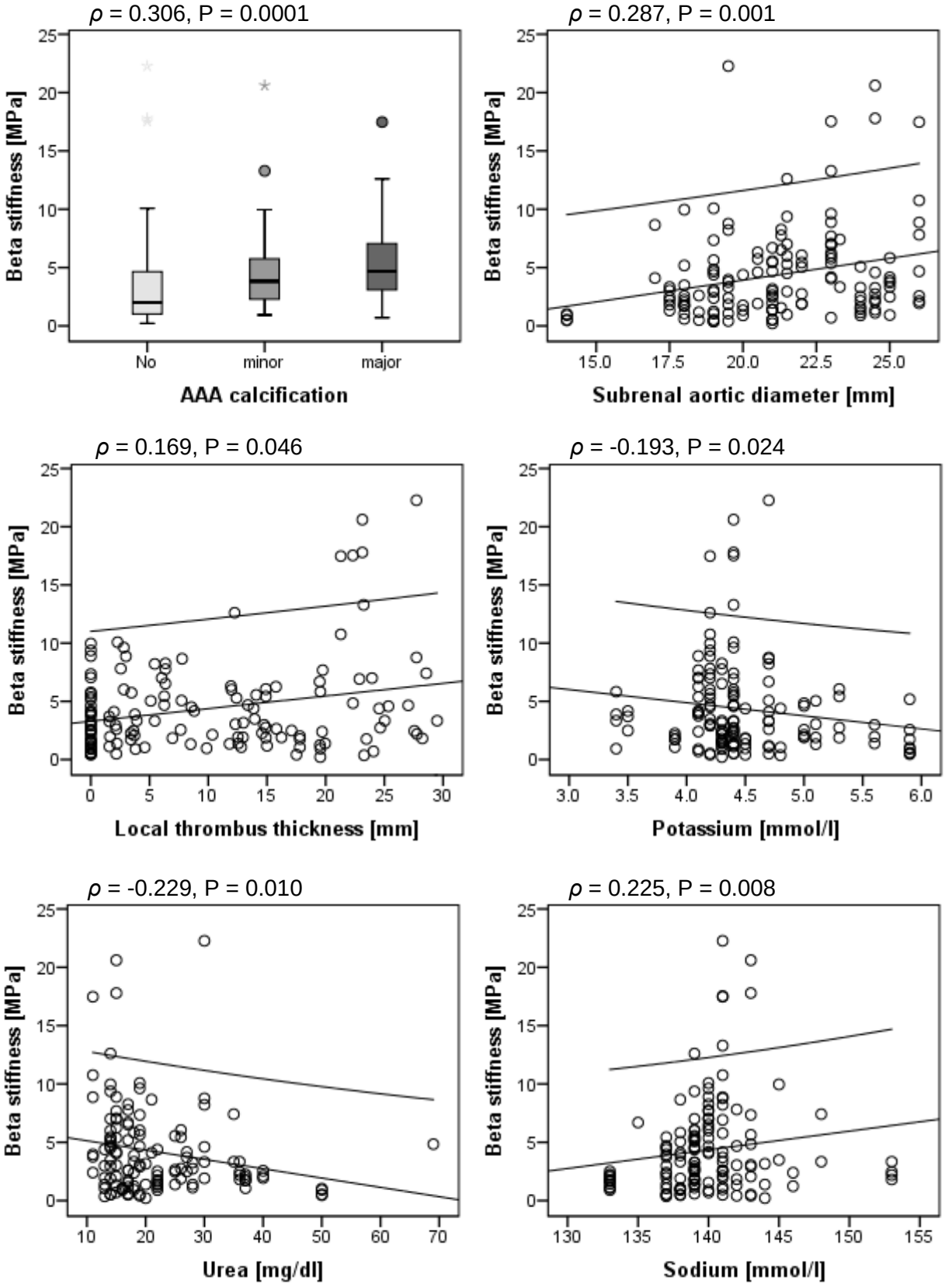

Figure 3-16: Box and whisker plot showing significant difference between beta stiffness and the extent of AAA calcification. Scatter plots showing significant correlations found between beta stiffness and subrenal aortic diameter, local thrombus thickness, potassium, urea and sodium.

3.4.5 Finite element analysis of AAA wall and parameters associated with CKD

For the determination of potential mechanisms of mechanical loads on patients' parameters, the computationally calculated von Mises stress and strain were compared to the parameters of the AAA wall at the sample excision site. Wall stress and strain showed significant correlations to maximum AAA diameter (ρ=0.474 and ρ=0.498, P=0.0001 and P=0.0001, respectively), maximum thrombus thickness (ρ=-0.338 and ρ=-0.339, P=0.0001 and P=0.0001, respectively), local thrombus thickness (ρ=-0.782 and ρ=-0.761, P=0.0001 and P=0.0001, respectively), blood potassium (ρ=-0.165 and ρ=-0.166, P=0.037 and P=0.036, respectively) and blood sodium (ρ=-0.204 and ρ=-0.231, P=0.010 and P=0.003) as shown in *Figures 3-17* and *3-18*.

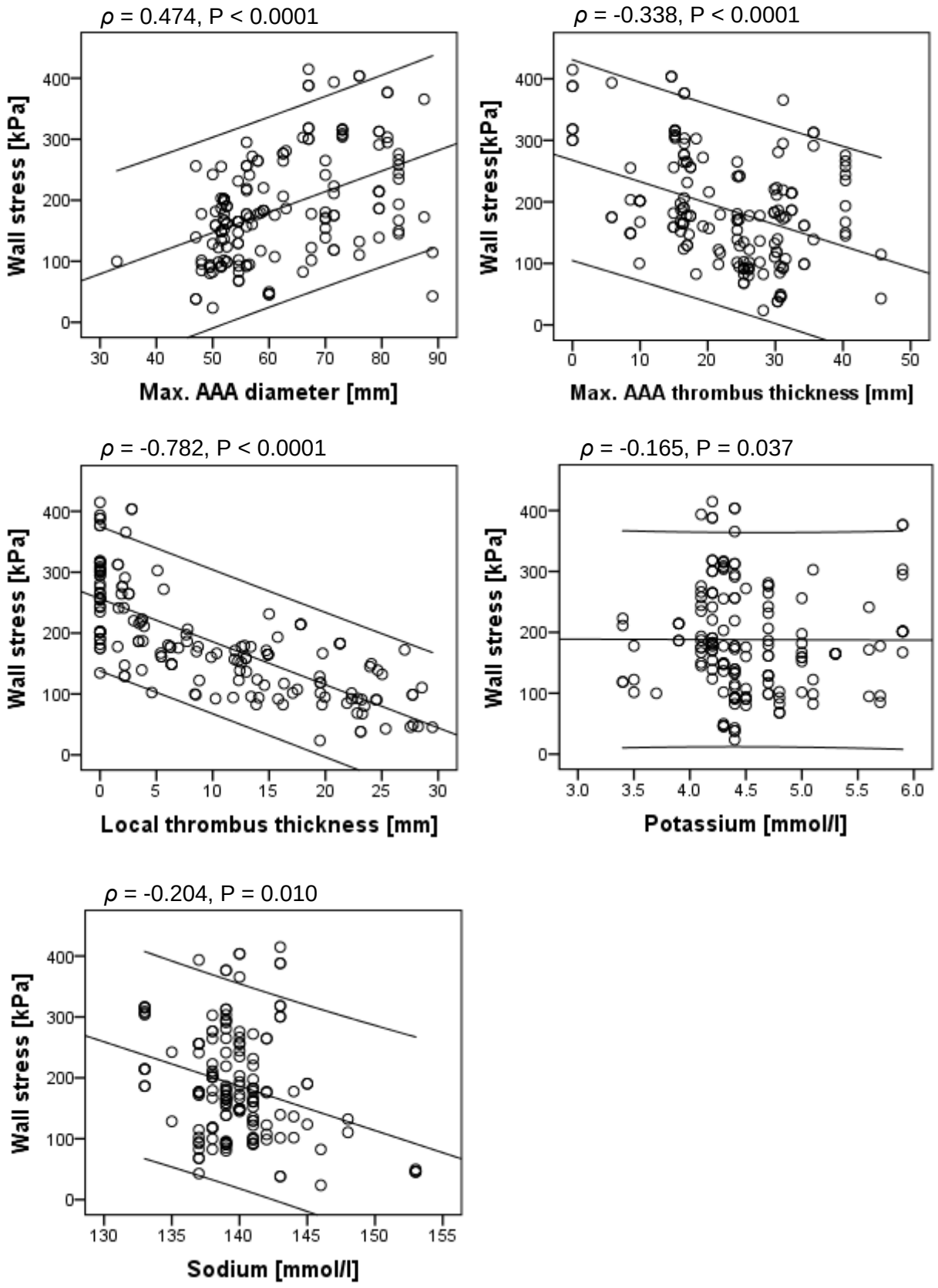

Figure 3-17: Scatter plots showing significant correlations found between AAA wall stress and maximal AAA diameter, maximal AAA thrombus thickness, local thrombus thickness, potassium and sodium.

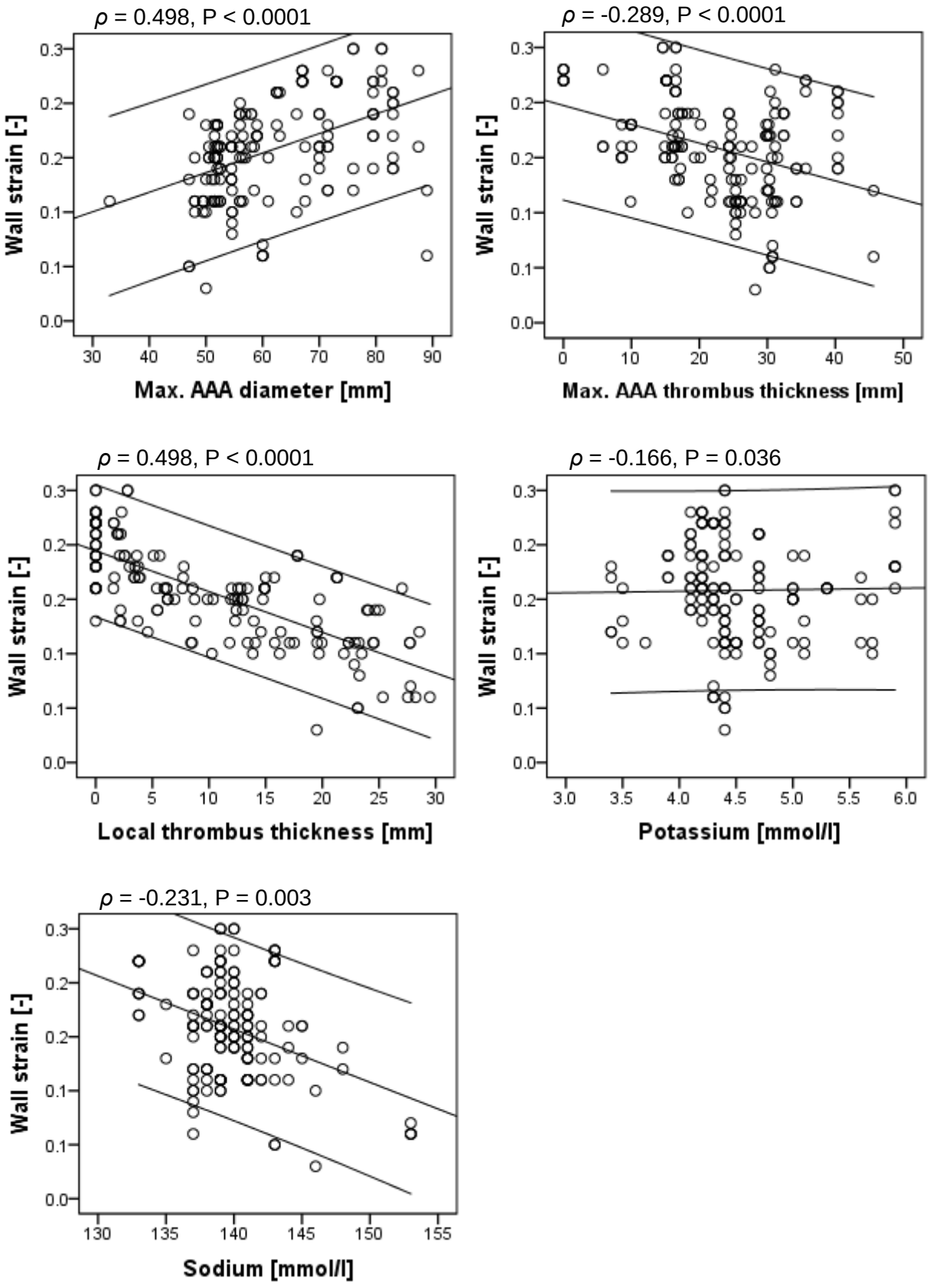

Figure 3-18: Scatter plots showing significant correlations found between AAA wall strain and maximal AAA diameter, maximal AAA thrombus thickness, local thrombus thickness, potassium and sodium.

Chapter 4 Discussion

4.1 Interplay between ECM composition and biomechanical properties in human AAAs

It is acknowledged that the development of AAA is a complex biological process with permanent remodelling of ECM, maintained by mechanical forces acting continuously on the aortic wall. Previously published studies have focused either on the mechanical or on the biological properties of abdominal aortic aneurysms (Maier et al., 2010; Di Martino et al., 2006; Vande Geest et al., 2006; Vorp et al., 2001; Vande Geest et al., 2006), but did not consider both aspects in one work. The only study showing tensile tests and histological features of the diseased aorta was the work of Pierce et al. (2015). However, the authors did not quantify their histological findings and did not correlate mechanical and biological properties of the AAA wall. For that reason, in the first part of the thesis the interdependencies of vascular collagen and other ECM proteins with the calculated mechanical loads in the AAA vessel wall were evaluated to better understand the interactions between mechanical parameters and biological components of aneurysm wall and successively of remodelling processes in AAA. The most relevant components of ECM such as collagens, proteoglycans, and elastic fibres were analysed by quantitative histology and immunohistochemistry and their amount was compared with the mechanical properties and biomechanical conditions of the corresponding AAA tissue samples.

Remarkably, significant correlations were observed between collagen amounts (collagen type I and type III and total collagen) and computational stress and strain as well as AAA wall failure tension. These findings indicate the high relevance of mechanical loads for collagen synthesis in vivo as a consequence of compensatory tissue repair mechanisms in the AAA wall until rupture occurs, when significantly increased wall stress finally exceeds the stability of the withstanding AAA wall (Reeps et al., 2013; Reeps et al., 2010). In agreement with previously published studies (Sakalihasan et al. 1993; Osakabe et al., 2000; White et al., 1993), only few elastic fibres were detected, whereas collagens, namely type I and III, were the predominant structural components

of the AAA wall with about 30-40% each (White et al., 1993; Mayne, 1986). These results underline the importance of collagen synthesis to countervail the mechanical stresses and maintain the integrity of the aortic wall (van der Rest et al., 1991; Rizzo et al., 1989; Menashi et al., 1897), but collagen does not grant the physiological wall elasticity, which is given only by elastic fibres.

Moreover, proteoglycans were reduced in AAA tissue samples analysed in this part of the thesis. These results are in agreement with previous studies, where the reduction of proteoglycans and their components such as biglycan and decorin were observed in the AAA wall compared to normal aorta (Theocharis et al., 2001; Theocharis et al., 2002; Kowalewski et al., 2006; Tamarina et al., 1998). Furthermore, the degradation of proteoglycans is mediated by the activation of matrix metalloproteinase (MMPs), especially MMP-3 and MMP-7, as already shown in a previous study (Reeps et al., 2009). It has already been demonstrated in vitro that the amount of proteoglycans differs with mechanical loads (Culav et al., 1999). Thus, the observed reduction of proteoglycans could be associated with a significantly decreased failure tension and wall stiffness in material testing. Consequently, these changes in the composition of ECM might be a sign of aortic wall destabilization, accelerated progression, and increased risk of rupture.

In the matter of the analysed geometrical parameters of AAAs, the thickness of thrombus was negatively correlated with the collagen content (type I and type III and total collagen), suggesting that thrombus may partially withstand the direct impact of hemodynamic tractions on the aortic vessel wall, thus reducing the necessity of compensatory collagen synthesis. These results are congruent with the previous study, showing a relevant reduction of aortic wall stress by thrombus (Maier et al., 2010). Furthermore, it has been mentioned that ILT may contribute to wall hypoxia and the decrease of collagen synthesis up-regulates the activation of MMP (Erdozain et al., 2011). Moreover, AAA local and normalized local diameter (NORD) correlated negatively with elastin, but not with collagens. This expected result indicates that elastin does not contribute to repair processes due to the almost non-existent level of synthesis of new elastin in the adult aorta (Tsamis et al., 2008).

Failure tension of the AAA wall obtained from the destructive tests was significantly increased with increasing collagen amount (collagen type I and total collagen) and also with proteoglycans, as expected. Similarly, alpha (α) and beta (β) stiffness representing the elastic properties of the AAA wall show similar correlations. The α-stiffness, describing the initial stiffness of the specimen

in the low-strain regime, correlated positively with the amount of collagen type I and type III and total collagen, while the β-stiffness, representing the stiffness in the high strain regime correlated only with proteoglycans. These findings reflect that proteoglycans and collagens are in close association with each other and proteoglycans stabilize the structure of collagen fibres (Culav et al., 1999; Kowalewski et al., 2006). Consequently, these facts emphasize the important role of compensatory collagens and proteoglycans synthesis to maintain the structural integrity and stability of the aortic wall during AAA progression as a reaction to increased mechanical loads.

4.2 Relationships between gene expression and biomechanical properties in human AAAs

In this study, a new aspect of the pathogenetic evaluation of AAA was approached by comparing mechanical properties of the diseased aortic wall with the corresponding gene expression of relevant biological factors responsible for AAA progression towards rupture, such as proteases (especially matrix metalloproteases, MMPs), inflammation, and important structural proteins of the ECM.

The gene expression of all these potentially destabilising factors of AAA analysed in the present study was detected in the aneurysmatic arterial wall. The mRNA level of collagen type I and type III was found to be expressed at a similar level, suggesting that both types of collagen might be equally important for the maintenance of AAA wall stability or aneurysm wall remodelling. Among the different collagens in vessel wall, type I and type III are the major fibrillar collagens with 60% and 30% of the total aortic wall protein content, respectively (Mayne, 1986; van der Rest et al., 1991). Their proper function is essential for maintaining the stability of the aortic wall (Rizzo et al., 1989; Keeling et al., 2005). On the other hand, former studies have already shown that MMPs may contribute to the development and progression of AAA by proteolysis of ECM (Vande Geest et al., 2006; Thompson et al., 2006; Longo et al., 2002; Choke et al., 2005; Reeps et al., 2009; Tamarina et al., 1997). In the vascular wall, elastases and collagenases such as MMPs are secreted from activated smooth muscle cells (SMC), or from infiltrating leukocytes, as well as from macrophages (Jacob et al., 2003). Therefore, it is to be assumed that the expression of collagen type I and type III alone is not adequate to illustrate biologically the stability of the vessel wall.

Concerning inflammation, the expression of surface markers of leukocytes (CD45) and macrophages (MSR1, scavenger receptor) at mRNA level was analysed, as representatives of the potentially destabilizing factors of inflammation in AAA wall. As anticipated and previously published (Choke et al., 2005; Sakalihasan et al., 2005; Lindholt et al., 2006), both markers of inflammation, were up-regulated and were significantly correlated with the amount of inflammatory cells (perivascular leucocytes and macrophages) as well as neovessels in the AAA wall (*Table 3-2*). During the formation of aneurysm, extensive infiltration of inflammatory cells and neovascularization is observed, in particular that of macrophages and lymphocytes (Shimizu et al., 2005; Sakalihasan et al., 2005, Linholdt et al., 2006). Upon activation, leukocytes express a variety of cytokines and consequently promote expression of MMPs and may thus further contribute to the proteolysis of the AAA wall with a consecutive expansion of the diseased aorta. The results assume that especially due to inflammatory cytokines the overall expression of both protective and promoting factors are increased during AAA progression (Choke et al., 2005; Reeps et al., 2009). Nonetheless, due to an imbalance of these factors, the progression of the AAA may further proceed.

In addition, because accompanying diseases such as diabetes mellitus (DM) and chronic kidney disease (CKD) can also influence gene expression (Dwivedi et al., 2011; Kitada et al., 2010), these patients were excluded and additional correlation analysis was performed. The results mainly confirmed the data with all individuals included in the current study. In addition, following the exclusion of patients suffering from CKD, two additional correlations were observed for collagen type III and AAA diameter as well as for collagen type III and the mechanical parameter β-stiffness. Furthermore, an additional correlation was found between MMP-2 and AAA diameter excluding patients with DM. So these diseases might be considered as additional factors affecting the aortic wall stability. Nevertheless, because the correlation data with or without exclusion of patients with the above mentioned accompanying disease were mostly akin, there is a supposition that the affect is negligible or rather low.

The most important results of the present study are the interdependencies between mechanical conditions, AAA geometry, gene expression and material properties of the AAA wall as depicted in *Table 3-3*. Significant correlations were observed between local aortic diameter and the expression of both inflammatory factors CD45 and MSR1. One possible explanation is that with

increasing diameter, the total volume of vessel wall increases and so does the amount of inflammatory cells and consequently, the expression of the inflammatory factors. However, in this case, the mRNA level of all factors analysed should have increased. Another explanation would be that the increased expression of the inflammatory factors may simply reflect the biological progression of the vessel disease at larger diameters. The third and possibly more reasonable explanation is that along the law of Laplace the enlargement of aortic diameter leads to higher mechanical stress acting on the vessel wall, thus activating mechanoreceptors and cytoskeleton on the endothelial layer or resident cells (Chatzizisis et al., 2007). In contrary to these assumptions, no significant correlation was found between the computationally assessed calculated local stresses and strains and the mRNA expression of inflammatory markers, MMPs, and collagens in corresponding tissue samples. These results may be explained by the comparison of long term acting parameters such as mechanical conditions with short time regulation mechanisms such as mRNA expression. There can be other unknown influences on the specific mRNA synthesis. Moreover, time and threshold phenomena can be discussed in this context. Mechano-biological interactions may only lead to notably increased reactive mRNA expressions of inflammatory and proteolytic factors or collagen synthesis at the initiation of an AAA and in case of strongly misbalanced mechano-biological vessel wall homeostasis.

Furthermore, the role of mRNA expression of inflammatory cells, MMP-proteolysis, and collagen synthesis was analysed in comparison to the material properties of AAA wall. As expected, the increasing expression of MMP strongly correlated to the decreasing AAA wall strength and β-stiffness. Interestingly, independent from local diameter this correlation was only observed for MMP-2 but not for MMP-9. Moreover, the α-stiffness of the AAA wall was negatively correlated with the expression of collagen type III. These results may be explained as a response of aortic wall to the reduced wall elasticity by elastic fibre degradation. Collagen type III is prominent in the initial stage of healing, where it provides early mechanical strength to the newly synthesised ECM (Culav et al., 1999). In contrast, collagen type I possesses the ability to carry a higher mechanical load and is found in mature scar tissue with low ECM turnover. This reasoning might explain the missing correlation of collagen type I mRNA expression with the mechanical properties of AAA walls.

Furthermore, no correlation was observed between the expressions of MMP-2 or -9 and the AAA diameter, as already described by previous studies (Dilmé et al., 2014; Papalambros et al., 2003; Petersen et al., 2002). These discrepancies can be explained in several manners. First, it could be due to the low number of patients used in our study. Furthermore, most researchers analysed the level of MMP-2 and -9 in the blood of these patients in comparison with AAA diameter (Lauhio et al., 2011; Flondell-Sité et al., 2010). So far only few studies evaluated the expression of MMP-2 and -9 directly in AAA tissue samples and the achieved results are conflicting, inconclusive or controversial. Dilmé et al. (2014) compared three different groups of patients, with small AAA diameter (<5.5 cm), moderate AAA diameter (5.5-6.99 cm), and large AAA diameter (≥7.0 cm). No differences were observed for MMP-2 and MMP-9 displayed the maximum expression level in the moderate-diameter group. Papalambros et al. (2003) observed no relationships between MMP-2 activity and AAA size as well; MMP-9 was significantly higher in larger AAAs (> 6.0 cm). Petersen et al. (2002) found significant differences for MMP-2 levels in large AAAs (> 7.0 cm) in comparison to the medium-sized AAAs (5.0-7.0 cm) and MMP-9 expression was significantly increased in medium-sized compared to large AAAs. Furthermore, these authors did not perform direct correlation analysis between AAA diameter and expression of MMPs, but rather compared various groups with different AAA sizes. In the current study, such sizing of AAA patients by AAA diameter was not performed because of the relatively small number of patients.

4.3 The function of CXCR4 and CXCL12 in human AAAs

This study demonstrates that the expression of CXCR4 and its ligand CXCL12 is significantly upregulated in human AAAs compared to non-aneurysmal aortic tissue. Furthermore, CXCR4 is mainly localized in inflammatory cells, in particular in B- and T-lymphocytes as well as in macrophages.

As mentioned before, AAA is a complex degenerative disease, characterized by accumulation of infiltrating cells such as macrophages and lymphocytes (Shimizu et al., 2006; Curci et al., 2004; Choke et al., 2009). The inflammatory processes within AAA wall are initiated by multiple factors, including various proinflammatory cytokines, chemokines and their receptors. A special focus has recently been devoted to the chemokine receptor CXCR4 and intensively investigated in various tumours, cancer (Burger et al., 2006; Teicher et al., 2010) and brain disorders (Réaux-Le Goazigo et al., 2013; Guyon,2014), as well as in atherosclerosis (Bot et al., 2014), which is also known to be

associated with AAA progression. CXCR4 has been shown to be critical for adhesion and/or migration by mediating trafficking and activation of lymphocytes, suggesting the involvement of CXCR4 in tumour progression, invasion and metastasis (Oberlin et al., 1996; Loetscher et al., 2000; Burger et al., 2006; Teicher et al., 2010; Réaux-Le Goazigo et al., 2013). Interestingly, only few groups have analysed so far the chemokine receptor CXCR4 and its ligand in human AAA in order to examine their role in lymphoid recruitment (Ocaña et al., 2008) and to evaluate the expression of CXCL12/CXCR4 in aneurysmal aortic wall and during AAA progression in a mouse model (Michineau et al., 2014). The current study focused on the expression of CXCR4 and its ligand CXCL12 in the aortic wall of AAA patients and non-aneurysmal tissue subjects at the protein and mRNA level and on the association of their expression in the individual cells within the AAA wall.

First, to evaluate the presence of CXCR4 and CXCL12 in AAA tissue samples, the mRNA level was determined. The gene expression of CXCR4 and CXCL12 was detected in all AAA samples as well as in non-aneurysmal aortas. Nevertheless, the expression of CXCR4 was 9.6-fold, the expression of CXCL12 4.6-fold significantly increased in AAA tissue samples compared to non-aneurysmal aortae. These results were in accordance with the previous published study from Lenk et al., who used Affymetrix and Illumina arrays on ten AAA tissue samples and ten control aortae (Lenk et al, 2007). They observed a significantly increased expression of CXCR4 in AAA attributed to leukocytes. Furthermore, another study analysed 15 AAA and 15 control aortic tissues using a custom-designed AAA chip and observed 38 differentially expressed genes between AAA and control samples. One of these genes was CXCR4 with a 6.9-fold increase in AAA walls (Hinterseher et al., 2013). Both studies were carried out with control samples obtained from age-, sex-, and ethnicity-matched individuals and they were all from the infrarenal region of the aorta. Consequently, we confirmed upregulation of CXCR4 expression in AAA versus healthy aortae, even if our control group was not matched. Because both factors are associated with the activation of inflammatory cells, their gene expression was correlated with the expression of the following inflammatory cells markers: MSR1, CD45, and CD3. Interestingly, significantly positive correlations were observed between the gene expression of CXCR4, CXCL12 and all these inflammatory markers (Table 3-6), indicating that the gene expression of CXCR4 and CXCL12 is concomitant with inflammatory cells within the AAA wall. These results were in agreement with previous studies that showed that CXCR4 and CXCL12 is upregulated in human (Ocaña et al., 2008) and in mouse AAAs (Michineau et al., 2014). Remarkably, CXCR4 transcription was detected also in the healthy aorta, although the

CXCR4 expression was associated mainly with inflammatory cells. This discrepancy might be explained by using the elderly individuals as controls, which had already slightly enlarged intima containing monocytes and by the presence of inflammatory cells in the adventitia.

The results of this study showed an unambiguous increase in the expression of CXCR4 also at protein level. Interestingly, even if the expression of CXCL12 at mRNA level was found in all samples, no protein could be detected. These results were in discordance with the findings of Ocaña, who detected CXCL12 in adventitia of the AAA wall. This apparent disagreement could be explained by differences in the methodology applied in both studies. Ocaña et al. (2008) analysed the expression of CXCL12 by immunohistochemical staining, we in contrast evaluated the expression via western blot, which is often less sensitive than immunohistochemistry. Using recombinant CXCL12 protein, the limit of detection was 0.1 µg/µl. Consequently, if the protein concentration was lower, it was not detectable in the performed western blot analysis. Since the CXCL12 positive cells in the study of Ocaña expressed neither CD45 marker of inflammatory cells, nor smooth muscle actin or CD34, the precise source of CXCL12 could not be identified (Ocaña et al, 2008). This part of the thesis focused especially on inflammatory cells within AAAs, which were negative for CXCL12 as well as in the study of Ocaña et al. (2008). However, CXCL12 positive cells could be associated only with plasma cells. This can be interpreted in the way that these cells might be activated by an autoimmune response in the AAA wall as result of chronic inflammation (Calame et al., 2001). Whether plasma cells are capable of expressing CXCL12 has to be further elucidated. Furthermore, the lack of detection of CXCL12 at protein level could be also due to following reasons. First, protein and mRNA expression levels are known to be independent from each other (Greenbaum et al., 2003). Second, the half-life of the proteins is often different from that of the corresponding mRNA (Glickman et al., 2002). In accordance, CXCR4 as a transmembrane receptor is a stable protein. In contrast, the half-life of CXCL12 was described to be rather short (Kirkpatrick et al., 2010). Thus, the instability of CXCL12 might be the other reason, why the expression of this ligand was not detectable at the protein level.

Finally, to determine the cells within the AAA wall that express CXCR4 or CXCL12, consecutive immunohistological staining was performed for B- and T- lymphocytes and macrophages. These cells have already been classified as an important source of inflammatory processes, which invade the aortic vessel wall during the pathogenesis of the AAA (Reeps et al., 2009; Shimizu et al., 2006).

The results indicated that B- and T-lymphocytes as well as macrophages express CXCR4. In particular, the strongest staining intensity was observed in B- and T-lymphocytes. Furthermore, similarly to CXCL12, CXCR4 was detected also in plasma cells. These cells differentiate from B-cells and produce antibodies from the precursor B-cell. The presence of plasma cells and B-lymphocytes in aneurysm (Reeps et al., 2009), together with the expression of CXCR4/CXCL12, further support the assumption that immunological reaction is involved in AAAs and play a crucial role in disease progression. Additionally, CXCR4 and CXCL12 positive cells were not detected in healthy aorta tissues. These findings confirm once again the critical role of inflammation, which participates in a negative remodelling of extracellular matrix throughout the arterial wall leading to vessel wall instability, AAA progression and finally to rupture (Reeps et al., 2009; Newby, 2005; Halloran and Baxter, 1995; Guo et al., 2006; Wassef et al., 2007; Kuivaniemi et al., 2008). Additionally, these results are in accordance with a recent study demonstrating that CXCL12/CXCR4 pathway in the development and progression of AAAs is triggered through the accumulation of macrophages within the diseased aortic wall (Michineau et al., 20104). Moreover, Bot et al. (2014) provide clear evidence that blockade of CXCR4/SDF-1α on leucocytes induces atherosclerotic plaque progression in mice. Taken together, these results emphasize that the expression and appearance of CXCR4 may correspond with the AAA progression and might be a potential target for detection of inflammatory activity in AAA patients.

4.4 The impact of mechanical properties in AAA patients with CKD

Although multiple etiological features have been suggested to contribute to AAA, its progression and the factors leading to rupture are still not completely understood. The results of this present study show that geometry of AAA and hemodynamic forces acting upon the aortic wall are not the only criteria defining the development and risk of rupture of AAA. There are also other factors distressing the aorta such as e.g. the patients' medical history, especially chronic kidney disease, which leads to pathological changes of blood parameters such as calcium, phosphate, potassium, sodium or urea nitrogen (Moody et al., 2013; Keith et al., 2004; Pelisek et al., 2011; Pelisek et al., 2010; Levey and Coresh, 2012). These changes in turn affect the biological features of the AAA wall and consequently the material properties of the diseased aorta (Lim et al., 2011; Choke et al., 2005; Brown et al., 1999).

Regarding the geometry of the AAA wall, the results revealed that patients with CKD had smaller AAA diameters and thinner aortic walls compared to patients without CKD, whereas the local thrombus thickness in the CKD patients was significantly increased. The reasons for these findings might be as follows. It has already been described that CKD patients have various metabolic abnormalities that lead to a malformed remodelling of arterial wall and accelerate the disease progression (Briet et al., 2012). Calcification and augmented inflammation of the vessel wall are the main causes of complications associated with CKD (Briet et al., 2012; Shanahan et al., 2011). Calcification is well known e.g. to increase the apoptosis of SMCs (Briet et al., 2012; Proudfoot et al., 2000) by activation of various osteogenic bone morphogenic proteins (BMPs), especially BMP-2 and -4 (Proudfoot et al., 2000; Hruska et al., 2005). These BMPs, particularly BMP-2, induce also transdifferentiation of vascular smooth muscle cells into osteoblast-like cells, which further facilitate the calcium deposition within the arterial and aortic wall (Villa-Bellosta et al., 2011). Furthermore, SMCs are the only reliable source of the components of extracellular matrix (ECM). The increased SMCs apoptosis leads consequently to an inadequate synthesis of ECM proteins, which finally weakens the aorta. These circumstances could be one of the reasons explaining thinner AAA wall observed in patients suffering from CKD.

Animal models with impaired kidney function show a decrease in elastin content, an increase in the amount of collagen and augmented calcification (Ng et al., 2011). These abnormalities lead to increased arterial stiffness and might be the reason for augmented stiffness in AAA patients with CKD, as was observed in this study. Furthermore, increased stiffness inevitably decelerates the progression of AAA, executing higher resistance against the hemodynamic forces acting upon the diseased aorta. Thus, the reduced aortic elasticity might be the cause of the smaller aortic diameter in CKD patients due to the lesser extension of AAA. Nevertheless, the diseased aortic wall of CKD patients is still less stable than that of AAA individuals without CKD, due to the abnormal vascular remodelling (Briet et al., 2012).

The mechanisms leading to an extended pathological remodelling and endothelial dysfunction in AAA patients with CKD involve also other pathways including inflammation and oxidative stress (Briet et al., 2012). Oxidative stress is augmented due to the imbalance between the production of free radicals, reactive oxygen species (ROS) and insufficient elimination of these products (Del Vecchio et al., 2011). Low-grade inflammation plays an important role in arterial wall calcification.

Furthermore, there is a link between calcification and inflammation, because endothelial cells in CKD patients synthesise more BMP-2 and -4 in responses to inflammatory cytokines or ROS and BMPs are known to be key modulators of vascular calcification (Boström et al., 2011). Inflammatory processes participate in the calcification of aortic wall e.g. by releasing various proteolytic enzymes such as MMPs (Irwin et al., 2009), which are the actual culprits of vessel wall remodelling and degradation (Briet et al., 2012). The vessel wall calcification shares several characteristics with the biology of bone development and MMPs, which are known to have an important function during differentiation of SMCs into osteoblast-like cells.

The increased endothelial dysfunction in patients suffering from CKD is associated with hypertrophic remodelling and oxidative stress (Amiri et al., 2004). Endothelial dysfunction leads also to an increased arterial stiffness (Briet et al., 2012), which is regulated by the endothelial cells through the release of nitric oxide. Endothelial dysfunction in patients with CKD in large arteries such as aorta has already been associated with poor outcome in these patients (Verbeke et al., 2011; Stam et al., 2006). The augmented endothelial dysfunction facilitates also binding and activation of platelets to the arterial wall, initiating blood coagulation and leading finally to thrombus formation. These circumstances may explain the increased thrombus thickness in AAA patients suffering from CKD, as observed in the present study.

In addition, significant correlations were observed between mechanical properties of AAA walls, such as wall stress and strain, failure tension and stiffness with blood parameters such as potassium, sodium and urea nitrogen. These results confirm close association between CKD and AAA wall function. The liver and to lesser extent also the kidney produce urea as a waste product of the digestion of proteins. Insufficiency of the urea metabolisms occurs in various liver disorders and in patients with CKD. Blood urea nitrogen is therefore one of the common clinical biomarkers of kidney disease. Consequently, urea might serve also as a marker of AAA progression in patients suffering from CKD due to the association of urea nitrogen and mechanical properties of the diseased aortic wall. Population studies have already demonstrated an association between dietary sodium chloride as well as dietary potassium and blood pressure (Cook et al., 2009; Saint-Remy et al., 2012). In addition, most patients with CKD have hypertension. The relationship between sodium and potassium intake, blood pressure and cardiovascular disease has already been described (Kimura et al., 2010). Higher sodium and potassium salt concentration in the blood

of CKD patients causes an increase in blood pressure. Patients with CKD are frequently salt sensitive and the increased concentration of sodium and potassium in their blood not only leads to an increase in blood pressure but also plays a role in endothelial dysfunction, kidney disease progression and cardiovascular morbidity and mortality (Aaron and Sanders, 2013). Furthermore, CKD patients often respond to increased salt intake with increased glomerular filtration fraction and proteinuria. Significant negative correlation was found between sodium and potassium concentration in blood and mechanical properties of AAA wall, suggesting these salts as an indirect marker of abnormal changes within the AAA wall of CKD patients.

Patients with CKD have in general significant cardiovascular comorbidities and reduced long-term survival in proportion to the severity of renal disease (Go et al., 2004; Norwood et al., 2004). Furthermore, the presence of severe CKD in patients considered for AAA repair is associated with significantly increased mortality (Patel et al., 2012). Some clinical studies have already shown marked changes in aortic stiffness following renal transplantation, confirming an important role of proper kidney function for accurate aortic wall elasticity (Covic et al., 2003; Zoungas et al., 2004; Bachelet-Rousseau et al., 2011). Furthermore, malicious changes in aortic wall have already been associated with other organ damages such as heart, kidney or brain (Safar and Btruijker-Boudier, 2010).

Chapter 5 Conclusions and Outlook

Abdominal aortic aneurysm (AAA) is a common disease of older people and often stays unnoticed due to the absence of symptoms. The great danger for those affected is the rupture of the aneurysm, which leads to death in the majority of cases. In clinical practice, the decision for a therapeutical approach is commonly based on aneurysm size. A maximum diameter >5.5 cm is a well-accepted criterion for elective operative repair or endovascular intervention. However, smaller AAA may rupture unexpectedly and larger AAA may remain stable for a long time and thus, these patients will be unnecessarily subjected to the risks of prophylactic surgery. Currently, the lack of an accurate AAA rupture risk index remains an important issue in the clinical management of this disease. Nevertheless, the occurrence of AAA and its development are influenced by variability of local hemodynamic factors along the aorta. It is generally recognized that AAA can continuously expand, dissect and even potentially rupture, when the stress acting on the wall exceeds the strength of the wall. Moreover, the key processes of AAA pathogenesis are characterized by chronic inflammation, degradation of extracellular matrix, loss of smooth muscle cells of the media, as well as the neovascularization. In particular, the degradation of the connective tissue of the aortic vessel wall leads to the destabilization and rupture of the aneurysm.

Therefore, the focus of this thesis was to improve the prediction of the rupture risk stratification of AAA based on the evaluation of histological, biological and mechanical characterization of the AAA wall and their correlation with the patient specific clinical data.

In the first study, the results could confirm the key role of major ECM components in AAA in macroscopically observable mechanical wall properties by comparing histological findings with mechanical tests. Collagens, especially type I, are important for vessel stability and corresponded accordingly with von Mises strain and stress of the aortic wall. Furthermore, thrombus seems to reduce the forces acting on the vessel wall and leads to decreased collagen synthesis. Thereby, proteoglycans appear to act in the same manner as collagens and improve the vessel wall stability.

The results of the second study show some interesting relationships regarding the expression of relevant destabilizing factors of AAA and its mechanical properties, which might play a potential relevant role in the maintenance of aortic wall stability, such as MMP-2 and collagen III. Regarding biomechanical parameters, expression of inflammatory factors correlated significantly with AAA diameter at the sample excision site. No significant correlation of computationally assessed local stresses and strains was found with the mRNA expression of inflammatory markers, MMPs, and collagens in the underlying tissue samples.

The outcomes of the third study demonstrated that CXCR4 is abundantly expressed in AAA tissue samples at both RNA and protein level compared to non-aneurysmal tissues. CXCR4 is particularly co-localized with inflammatory cells in the AAA wall. Thus, CXCR4 may serve as a potential target to detect non-invasively inflammatory activity in the diseased aortic wall.

The results of the fourth study showed that associated diseases of AAA might also play a key role in its pathogenesis, especially CKD, which is a complex disease characterized by various pathological features such as arterial wall calcification, low-grade inflammation, oxidative stress and abnormal vessel wall remodelling. These processes lead to increased aortic wall stiffness, smaller diameter and reduction of wall thickness, decrease of failure tension, wall stress, and strain, which in turn increase the risk of rupture in AAA patients. Furthermore, in a clinical practice, these features could signal an increased rupture risk at already smaller AAA diameter. Moreover, these results demonstrated that estimation of the risk of rupture in AAA patients should also consider the patient's medical history such as e.g. CKD.

In summary, data provided in this thesis revealed a number of new results and allow a better understanding of AAA disease and its rupture risk stratification, which might improve the clinical management of aneurysm patients.

References

Aaron KJ, Sanders PW. Role of dietary salt and potassium intake in cardiovascular health and disease: a review of the evidence. Mayo Clin Proc. 2013;88(9):987-95.

Ailawadi G, Eliason JL, Upchurch GR Jr. Current concepts in the pathogenesis of abdominal aortic aneurysm. J Vasc Surg. 2003;38 (3):584-588.

Amiri F, Virdis A, Neves MF, Iglarz M, Seidah NG, Touyz RM, Reudelhuber TL, Schiffrin EL. Endothelium-restricted overexpression of human endothelin-1 causes vascular remodeling and endothelial dysfunction. Circulation 2004;110(15):2233-40.

Ashton JH, Vande Geest JP, Simon BR, Haskett DG. Compressive mechanical properties of the intraluminal thrombus in abdominal aortic aneurysms and fibrin-based thrombus mimics. J. Biomech. 2009;42(3):197-201.

Bachelet-Rousseau C, Kearney-Schwartz A, Frimat L, Fay R, Kessler M, Benetos A. Evolution of arterial stiffness after kidney transplantation. Nephrol Dial Transplant. 2011;26(10):3386-3391.

Basu R, Kassiri Z. Extracellular matrix remodelling and abdominal aortic aneurysm. J Clin Exp Cardiolog. 2013;4(8):1-8.

Bengtsson H, Ekberg O, Aspelin P, Källerö S, Bergqvist D. Ultrasound screening of the abdominal aorta in patients with intermittent claudication. Eur J Vasc Surg. 1989;3(6):497–502.

Blanchard JF, Armenian HK, Friesen PP. Risk factors for abdominal aortic aneurysm: results of a case-control study. Am J Epidemiol. 2000;151(6):575-583.

Bleul CC, Fuhlbrigge RC, Casasnovas JM, Aiuti A, Springer TA. A highly efficacious lymphocyte chemoattctant, stromal cell derived factor 1 (SDF-1). J Exp Med. 1996;184(3):1101-1109.

Boddy AM, Lenk GEM, Lillvis JH, Nischan J, Kyo Y, Kuivaniemi H. Basic research studies to understand aneurysm disease. Drug News Perspect. 2008;21:142-148.

Boström KI1, Rajamannan NM, Towler DA. The regulation of valvular and vascular sclerosis by osteogenic morphogens. Circ Res 2011;109(5):564-77.

Bot I, Daissormont IT, Zernecke A, van Puijvelde GH, Kramp B, de Jager SC, Sluimer JC, Manca M, Hérias V, Westra MM, Bot M, van Santbrink PJ, van Berkel TJ, Su L, Skjelland M, Gullestad L, Kuiper J, Halvorsen B, Aukrust P, Koenen RR, Weber C, Biessen EA. CXCR4 blockade induces atherosclerosis by affecting neutrophil function. J Mol Cell Cariol. 2014;74:44-52.

Brewster DC, Cronenwett JL, Hallett JW, Johnston K.W, Krupski WC, Matsumura JS. Guideline for the treatment of abdominal aortic aneurysms. Report of a subcommittee of the Joint Council of the American Association for Vascular Surgery and Society for Vascular Surgery. J. Vasc Surg. 2003;37(5):1106-17.

Brewster DC, Geller SC, Kaufman JA, Cambria RP, Gertler JP, LaMuraglia DM, Atamian S, Abott WM. Initial experience with endovascular aneurysm repair: comparision of early results with outcome of conventional open repair. J Vasc Surg. 1998;27(6):1004-5.

Briet M, Burns KD. Chronic kidney disease and vascular remodelling: molecular mechanisms and clinical implications. Clin Sci (Lond). 2012;123(7):399-416.

Brown LC and Powell JT. Risk factors for aneurysm rupture in patients kept under ultrasound surveillance. Ann Surg. 1999;230(3):289-297.

Brown PM, Zelt DT, Sobolev B. The risk of rupture in untreated aneurysms: the impact of size, gender, and expansion rate. J Vasc Surg. 2003;37(2):280-284.

Burger JA, Kipps TJ. CXCR4: a key receptor in the crosstalk between tumor cells and their microenvironment. Blood 2006;107(5):1761-1767.

Cabellon S, Jr, Moncrief CL, Pierre DR, Cavanaugh DG. Incidence of abdominal aortic aneurysms in patients with atheromatous arterial disease. Am J Surg. 1983;146(5):575–6.

Calame K.L. Plasma cells: finding new light at the end of B cell development. Nature Immunol. 2001;2(12):1103-1108.

Campa JS, Greenhalgh RM, Powell JT. Elastin degradation in abdominal aortic aneurysms. Atherosclerosis 1987;65(1-2):13-21.

Chaikof EL, Brewster DC, Dalman RL, Makaroun MS, Illig KA, Sicard GA, Timaran CH, Upchurch GR Jr, Veith F. The care of patients with an abdominal aortic aneurysm: the Society for Vascular Surgery practice Guidelines. J Vasc Surg. 2009;50(4 Suppl):S2-49.

Chandana R, Mythri RB, Mahadevan A, Shankar SK, Srinivas Bharath MM. Biochemical analysis of protein stability in human brain collected at different post-mortem intervals. Indian J Med Res. 2009;129(2):189-99.

Charo IF, Ransohoff RM. The many roles of chemokines and chemokines receptors in inflammation. N Eng J Med. 2006;354(6):610-21.

Chatzizisis YS, Coskun AU, Jonas M, Edelman ER, Feldman CL, Stone PH. Role of endothelial shear stress in the natural history of coronary atherosclerosis and vascular remodeling: molecular, cellular, and vascular behavior. J Am Coll Cardiol. 2007;49(25):2379-93.

Choke E, Cockerill G, Wilson WR, Sayed S, Dawson J, Loftus I, Thompson MM. A review of biological factors implicated in abdominal aortic aneurysm rupture. Eur J Vasc Endovasc Surg. 2005;30(3):227-44.

Choke E, Cockerill GW, Laing K, Dawson J, Wilson WR, Loftus IM, Thompson MM. Whole genome-expression profiling reveals a role for immune and inflammatory response in abdominal aortic aneurysm rupture. Eur J Vasc Endovasc Surg. 2009;37(3):305-310.

Choksy SA, Wilmink AB, Quick CR. Ruptured abdominal aortic aneurysm in the Huntingdon district: a 10-year Experience. Ann R Coll Surg Engl. 1999;81(1):27-31.

Clifton MA. Familial abdominal aortic aneuryms. Br J Surg. 1977;64(11):765-766.

Collin J. UK small aneurysm trial. Lancet 1999;353(9150):407-8.

Conrad MF, Crawford RS, Pedraza JD, Brewster DC, Lamuraglia GM, Corey M, Abbara S, Cambria RP. Long-term durability of open abdominal aortic aneurysm repair. J Vasc Surg. 2007;46(4):669-675.

Cook NR, Obarzanek E, Cutler JA, Buring JE, Rexrode KM, Kumanyika SK, Appel LJ, Whelton PK. Joint effects of sodium and potassium intake on subsequent cardiovascular disease: the Trials of Hypertension Prevention follow-up study. Arch Intern Med 2009;169(1):32-40.

Cornuz J, Pinto CS, Tevaearai H, Egger M. Risk factors for asymptomatic Abdominal Aortic Aneurysm: systematic review and meta-analysis of population-based screening studies. Eur J Public Health. 2004;14(4):343–349.

Covic A, Goldsmith DJ, Gusbeth-Tatomir P, Buhaescu I, Covic M. Successful renal transplantation decreases aortic stiffness and increases vascular reactivity in dialysis patients. Transplantation 2003;76(11):1573-1577.

Crawford ES, Cohen ES. Aortic Aneurysm: a multifocal disease. Arch. Surg. 1982;117(11):1393-1400.

Culav EM, Clark CH, Merrilees MJ. Connective tissues: matrix composition and its relevance to physical therapy. Phys Ther. 1999;79(3):308-19.

Curci JA, Thompson RW. Adaptive cellular immunity in aortic aneurysms: cause, consequence, or context? J Clin Invest. 2004;114(2):168-171.

Darling RC, Messina CR, Brewster DC, Ottinger LW. Autopsy study of unoperated abdominal aortic aneurysms: The case for early resection. Circulation 1977;56(3 Suppl):II161-4.

Daugherty A, Cassis LA. Mechanisms of abdominal aortic aneurysm formation. Curr Atheroscler Rep. 2002;4(3):222-7.

De Putter S, Wolters BJ, Rutten MC, Breeuwer M, Gerritsen FA, van de Vosse FN. Patient-specific initial wall stress in abdominal aortic aneurysms with a backward incremental method. J Biomech. 2007;40(5):1081-1090.

Defawe OD, Colige A, Lambert CA, Munaut C, Delvenne P, Lapiere CM, Limet R, Nusgens BV, Sakalihasan N. TIMP-2 and PAI-1 mRNA levels are lower in aneurysmal as compared to athero-occlusive abdominal aortas. Cardiovasc Res. 2003;60(1):205-213.

Del Vecchio L, Locatelli F, Carini M. What we know about oxidative stress in patients with chronic kidney disease on dialysis--clinical effects, potential treatment, and prevention. Semin Dial. 2011;24(1):56-64.

Di Martino ES, Bohra A, Vande Geest JP, Gupta N, Makaroun MS, Vorp DA.–Biomechanical properties of ruptured versus electively repaired abdominal aortic aneurysm wall tissue. J Vasc Surg. 2006;43(3):570-6.

Dilmé JF, Bellmunt S, Camacho M, Solà-Villà D, Romero JM, Escudero JR, Vila L. Influence of Cardiovascular Risk Factors on Levels of Matrix Metalloproteinases 2 and 9 in Human Abdominal Aortic Aneurysms. Eur J Vasc Endovasc Surg. 2014; pii:S1078-5884(14)00307-4.

Dingemans KP, Teeling P, Lagendijk JH, Becker AE. Extracellular matrix of the human aortic media: an ultrastructural, histochemical and immunohistochemical study of the adult aortic media. Anat Rec. 2000;258(1):1-14.

Dua MM, Miyama N, Azuma J, Schultz GM, Sho M, Morser J, Dalman RL. Hyperglycemia modulates plasminogen activator inhibitor-1 expression and aortic diameter in experimental aortic aneurysm disease. Surgery 2010;148(2):429-435.

Dwivedi RS, Herman JG, McCaffrey TA, Raj DS. Beyond genetics: epigenetic code in chronic kidney disease. Kidney Int. 2011;79(1):23-32.

Eckstein H-H, Böckler D, Flessenkämper I, Schmitz-Rixen T, Debus S, Lang W. Ultrasonographic screening for the detection of abdominal aortic aneurysms. Dtsch Arztbl Int. 2009;106(41):657-663.

Eckstein H-H, Reeps C, Zimmermann H, Söllner H. Ultraschallscreening auf abdominale Aortenaneurysmen (AAA): Evidenz aus randomisierten Studien. Gefäßchirurgie 2014;19:515-527.

Erdozain OJ, Pegrum S, Winrow VR, Horrocks M, Steens CR. Hypoxia in abdominal aortic aneurysm supports a role for HIF-1α and Ets-1 as driers of matrix metalloproteinase upregulation in human aortic smooth muscle cells. J Vasc Res. 2011; 48:163-170.

Evans PC, Kwak BR. Biomechanical factors in cardiovascular disease. Cardiovasc Res. 2013;99(2):229-231.

Fillinger MF, Marra SP, Raghavan ML, Kennedy FE. Prediction of rupture risk in abdominal aortic aneurysm during observation: wall stress versus diameter. J Vasc Surg. 2003;37(4):7249-732.

Fillinger MF, Raghavan ML, Marra SP, Croonenwett, Kennedy FE: In vivo analysis of mechanical wall stress and abdominal aortic aneurysm rupture risk. J Vasc Surg. 2002;36:589-597.

Fleming C, Whitlock EP, Beil TL, Lederle FA. Screening for abdominal aortic aneurysm: A best-evidence systematic review for the US Preventive Services Task Force. Ann Intern Med. 2005;142(3):203-11.

Flondell-Sité D, Lindblad B, Kölbel T, Gottsäter A. Markers of proteolysis, fibrinolysis, and coagulation in relation to size and growth rate of abdominal aortic aneurysms. Vasc Endovascular Surg. 2010;44(4):262-8.

Galland RB, Whiteley MS, Magee TR. The fate of patients undergoing surveillance of small abdominal aortic aneurysms. Eur J Vasc Endovasc Surg. 1998;16(2):104-9.

Gasser TC, Auer M, Labruto F, Swedenborg J, Roy J. Biomechanical rupture risk assessment of abdominal aortic aneurysms: model complexity versus predictability of finite element simulations. Eur J Vasc Endovasc Surg. 2010;40(2):176-85.

Gasser TC, Görgülü G, Folkesson M, Swedenborg J. Failure properties of intraluminal thrombus in abdominal aortic aneurysm under static and pulsating mechanical loads. J Vasc Surg. 2008;48(1):179-88.

Giugliano G, Laurenzano E, Rengo C, De Rosa G, Brevetti L, Sanino A, Perrino C, Chiariotti L, Schiattarella GG, Serino F, Ferrone M, Scudiero F, Carbone A, Sorropago A, Amato B, Trimarco B, Esposito G. Abdominal aortic aneurysm in patients affected by intermittent claudiation: prevalence and clinical predictors. BMC Surg. 2012;12 (Supl 1):S17.

Glickman MH, Ciechanover A. The ubiquitin-proteasome proteolytic pathway: destruction for the sake of construction. Physiol Rev. 2002;82(2):373-428.

Go AS, Chertow GM, Fan D, McCulloch CE, Hsu CY. Chronic kidney disease and the risks of death, cardiovascular events, and hospitalization. N Engl J Med. 2004;351(13):1296-305.

Golledge A, Walker P, Norman P, Golledge J. A systematic review of studies examining inflammation associated cytokines in human abdominal aortic aneurysm samples. Dis Markers. 2009;26(4):181-8.

Greenbaum D, Colangelo C, Williams K, Gerstein M. Comparing protein and mRNA expressions levels on a genomic scale. Genome Biol. 2003;4(9):117.

Greenhalgh RM, Brown LC, Kwong GP, Powell JT, Thompson SG. Comparison of endovascular aneurysm repair with open repair in patients with abdominal aortic aneurysm (EVAR trial-1). 30-day operative mortality results randomised controlled trial. Lancet 2004;364(9437):843-848.

Greenhalgh RM, Forbes JF, Fowkes FG, Powell JT, Ruckley CV, Brady AR, Brown LC, Thompson SG. Early elective open surgical repair of small abdominal aortic aneurysms is not recommended: results of the UK small aneurysm trial. Eur J Vasc Endovasc Surg. 1998;16(6):462-464.

Guo DC, Papke CL, He R, Milewicz DM. Pathogenesis of thoracic and abdominal aortic aneurysms. Ann NY Acad Sci. 2006;1085:339-352.

Gurvan M, Tonon T, Scornet D, Cock JM, Kloareg B. The cell wall polysaccharide metabolism of the brown alga Ectocarpus siliculosus. Insight into the evolution of extracellular matrix polysaccharides in Eukaryotes. New Phytologist. 2010;188(1):82-97.

Gussmann A, Kühn J, Weise U. Leitlinien zum Bauchaortenaneurysma und Beckenarterienaneurysma. Deutsche Gesellschaft für Gefäßchirurgie 2008.

Guyon A. CXCL12 chemokine and its receptor as major players in the interactions between immune and nervous system. Front Cell Neurosci. 2014;8:65.

Halloran BG, Baxter BT. Pathogenesis of aneurysms. Semin Vasc Surg. 1995;8:85-92.

Hance KA, Tataria M, Ziporin SJ, Lee JK, Thompson RW. Monocyte chemotactic activity in human abdominal aortic aneurysms: role of elastin degradation peptides and 67-kD cell surface elastin receptor. J Vasc Surg. 2002;35(2):254-261.

Heider P, Wolf O, Reeps C, Hanke M, Zimmermann A, Berger H, Eckstein H-H. Aneurysms and dissections of the thoracal and abdominal aorta. Chirurg. 2007;78(7):602-6, 608-10.

Hellenthal FA, Buurman WA, Wodzig WK, Schurink GW. Biomarkers of AAA progression. Part 1: Extracellular matrix degeneration. Nature Rev Cardiol. 2009;6(7):464-74.

Henderson EL, Geng YJ, Sukhova GK, Whittemore AD, Knox K, Libby P. Death of smooth muscle cells and expression of mediators of apoptosis by T lymphocytes in human abdominal aortic aneurysms. Circulation 1999;99(1):96-104.

Heng MS, Fagan MJ, Collier JW, Desai G, McCollum PT, Chetter IC. Peak wall stress measurement in elective and acute abdominal aortic aneurysms. J Vasc Surg. 2008, 47(1):17-22.

Heron M. National Vital Statistics Reports: from the centers for disease control and prevention, national center for health statistics. National Vital Statistics System 2011;59:1-95.

Hinnen JW, Rixen DJ, Koning OH, van Bockel JH, Hamming JF. Development of fibrinous thrombus analogue for in-vitro abdominal aortic aneurysm studies. J Biomech. 2007;40(2):289-295.

Hinterseher I, Erdman R, Elmore JR, Stahl E, Pahl MC, Derr K, Golden A, Lillvis JH, Cindric MC, Jackson K, Bowen WD, Schworer CM, Chernousov MA, Franklin DP, Gray JL, Garvin RP, Gatalica Z, Carey DJ, Tromp G, Kuivaniemi H. Novel pathways in the pathobiology of human abdominal aortic aneurysm. Pathobiology 2013;80(1):1-10.

Hirsch AT, Haskal ZJ, Hertzer NR, Bakal CW, Creager MA, Halperin JL, Hiratzka LF, Murphy WR, Olin JW, Puschett JB, Rosenfield KA, Sacks D, Stanley JC, Taylor LM Jr, White CJ, White J, White RA, Antman EM, Smith SC Jr, Adams CD, Anderson JL, Faxon DP, Fuster V, Gibbons RJ, Hunt SA, Jacobs AK, Nishimura R, Ornato JP, Page RL, Riegel B; American Association for Vascular Surgery; Society for Vascular Surgery; Society for Cardiovascular Angiography and Interventions; Society for Vascular Medicine and Biology; Society of Interventional Radiology; ACC/AHA Task Force on Practice Guidelines Writing Committee to Develop Guidelines for the Management of Patients With Peripheral Arterial Disease; American Association of Cardiovascular and Pulmonary Rehabilitation; National Heart, Lung, and Blood Institute; Society for Vascular Nursing; TransAtlantic Inter-Society Consensus; Vascular Disease Foundation. ACC/AHA 2005 Practice Guidelines for the management of patients with peripheral arterial disease (lower extremity, renal, mesenteric, and

abdominal aortic): A collaborative report from the American Association for Vascular Surgery/Society for Vascular Surgery, Society for Cardiovascular Angiography and Interventions, Society for Vascular Medicine and Biology, Society of Interventional Radiology, and the ACC/AHA Task Force on Practice Guidelines (Writing Committee to Develop Guidelines for the Management of Patients With Peripheral Arterial Disease): Endorsed by the American Association of Cardiovascular and Pulmonary Rehabilitation; National Heart, Lung, and Blood Institute; Society for Vascular Nursing; Trans-Atlantic Inter-Society Consensus; and Vascular Disease Foundation. Circulation. 2006;113(11):e463–e654.

Hruska KA, Mathew S, Saab G. Bone morphogenetic proteins in vascular calcification. Circ Res. 2005;97(2):105-14.

Hua J, Mower WR. Simple geometric characteristics fail to reliably predict abdominal aortic aneurysm wall stresses. J Vasc Surg. 2001;34(2):308-315.

Humphrey JD, Taylor CA. Intracranial and abdominal aortic aneurysms: Similarities, differences, and need for a new class of computational models. Ann Rev Biomed Eng 2008, 10(1):221-246.

Humphrey JD. Cardiovascular Solid Mechanics: Cells, Tissues, and Organs. Springer New York Berlin Heidelberg, 2002.

Irwin CL, Guzman RJ. Matrix metalloproteinases in medial arterial calcification: potential mechanisms and actions. Vascular 2009;17 Suppl 1:S40-4.

Jacob MP. Extracellular matrix remodeling and matrix metalloproteinases in the vascular wall during aging and in pathological conditions. Biomed Pharmacother. 2003;57(5-6):195-202.

Johnston KW, Rutherford RB, Tilson MD, Shah DM, Hollier L, Stanley JC. Suggested standards for reporting on arterial aneurysms. J. Vasc. Surg. 1991;13(3):452-458.

Keeling WB, Armstrong PA, Stone PA, Bandyk DF, Shames ML. An overview of matrix metalloproteinases in the pathogenesis and treatment of abdominal aortic aneurysms. Vasc Endovasc Surg. 2005;39(6):457-64.

Keith DS, Nichols GA, Gullion CM, Brown JB, Smith DH. Longitudinal follow-up and outcomes among a population with chronic kidney disease in a large managed care organization. Arch Intern Med. 2004;164:659-663.

Kidney Disease: Improving Global Outcomes (KDIGO) CKD-MBD Work Group. KDIGO clinical practice guideline for the diagnosis, evaluation, prevention, and treatment of chronic kidney disease-mineral and bone disorder (CKD-MBD). Kidney Int Suppl. 2009;113:S1-130.

Kim LG, Ra PS, Ashton HA, Thompson SG. A sustained mortality benefit from screening for abdominal aortic aneurysm. Ann Intern Med. 2007;146(10):699-706.

Kimura G, Dohi Y, Fukuda M. Salt sensitivity and circadian rhythm of blood pressure: the keys to connect CKD with cardiovascular events. Hypertens Res. 2010;33(6):515-20.

Kirkpatrick B, Nguyen L, Kondrikova G, Herberg S, Holl WD. Stability of human stromal-derived factor-1α after blood sampling. Ann Clin Lab Sci. 2010;40(3):257-260.

Kitada M, Zhang Z, Mima A, King GL. Molecular mechanisms of diabetic vascular complications. J Diabetes Investig. 2010;1(3):77-89.

Kniemeyer HW, Kessler T, Reber PU, Ris HB, Hakki H, Widmer MK. Treatment of ruptured abdominal aortic aneurysm, a permanent challenge or a waste of resources? Prediction of outcome using a multi-organ-dysfunction score. Eur J Vasc Endovasc Surg. 2000;19(2):190-6.

Koch AE, Kunkel SL, Pearce WH, Shah MR, Parikh D, Evanoff HL, Haines GK, Burdick MD, Strieter RM. Enhanced production of the chemotactic cytokines interleukin-8 and monocyes chemoattractant protein-1 in human abdominal aortic aneurysms. Am J Pathol. 1993;142(5):1423-1431.

Kowalewski R, Sobolewski K, Małkowski A, Wolańska M, Gacko M. Evaluation of enzymes involved in proteoglycan degradation in the wall of abdominal aortic aneurysms. J Vasc Res. 2006; 43(1):95-100.

Krettek A, Sukhova GK, Libby P. Elastogenesis in human arterial disease: a role for macrophages in disordered elastin synthesis. Arterioscler Thromb Vasc Biol. 2003;23(4):582-7.

Kuivaniemi H, Platsoucas CD, Tilson MD III. Aortic aneurysms: an immune disease with a strong genetic component. Circulation 2008;117(2):242-252.

Kuivaniemi H, Shibamura H, Arthur C, Berguer R, Cole CW, Juvonen T, Kline RA, Limet R, Mackean G, Norrgard O, Pals G, Powell JT, Rainio P, Sakalihasan N, van Vlijmen-van Keulen C, Verloes A, Tromp G. Familial abdominal aortic aneurysms: collection of 233 multiplex families. J Vasc Surg. 2003;37(2):340-345.

Kurvers H, Veith FJ, Lipsitz EC, Ohki T, Gargiulo NJ, Cayne NS, Suggs WD, Timaran CH, Kwon GY, Rhee SJ, Santiago C. Discontinuous, staccato growth of abdominal aortic aneurysms. J Am Coll Surg. 2004;199(5):709-715.

Lagerström MC, Schioth HB. Structural diversity of G protein-coupled receptors and significance for drug discovery. Nat Rev Drug Discov. 2008;7(4):339-57.

Laheij RJ, Buth J, Harris PL, Moll FL, Stelter WJ, Verhoeven EL. Need for secondary interventions after endovascular repair of abdominal aortic aneurysms. Intermediate-term follow-up results of a European collaborative registry (EUROSTAR). Br J Surg. 2000;87(12):1666-1673.

Lapiere CM, Courtois A, Nusgens B. Extracellular matrix proteins in normal and aneurysmal aorta. In: Sakalihasan N, Kuivaniemi H, Michel JB (eds.) Aortic Aneurysms, New Insights into an Old Problem, pp 67-83. Les Editions de l'Université de Liège, Liège (2008).

Lauhio A, Hästbacka J, Pettilä V, Tervahartiala T, Karlsson S, Varpula T, Ruokonen E, Sorsa T, Kolho E. Serum MMP-8, -9 and TIMP-1 in sepsis: high serum levels of MMP-8 and TIMP-1 are

associated with fatal outcome in a multicentre, prospective cohort study. Hypothetical impact of tetracyclines. Pharmacol Res. 2011;64(6):590-4.

Lederle FA. The strange relationship between diabetes and abdominal aortic aneurysm. Eur J Vasc Endovasc Surg 2012;43(3):254-256.

Lederle FA, Johnson GR, Wilson SE, Ballard DJ, Jordan WD Jr, Blebea J, Littooy FN, Freishclag JA, Bandyk D, Rapp JH, Salam AA. Rupture rate of large abdominal aortic aneurysms in patients refusing or unfit for elective repair. JAMA 2002;287(22):2968-2972.

Lederle FA, Johnson GR, Wilson SE, Chute EP, Hye RJ, Makaroun MS, Barone GW, Bandyk D, Moneta GL, Makhoul RG. The aneurysm detection and management study screening program: Validation cohort and final results. Aneurysm Detection and Management Veterans Affairs Cooperative Study Investigators. Arch Intern Med. 2000;160(10):1425-30.

Lederle FA, Johnson GR, Wilson SE, Chute EP, Littooy FN, Bandyk D, Krupski WC, Barone GW, Ballard DJ. Prevalence and associations of abdominal aortic aneurysm detected through screening. Aneurysm Detection and Management (ADAM) Veterans Affairs Cooperative Study Group. Ann Intern Med. 1997;126(6):441-9.

Lederle FA, Johnson GR, Wilson SE. Aneurysm Detection and Management Veterans Affairs Cooperative Study. Abdominal aortic aneurysm in women. J Vasc Surg. 2001;34:122-6.

Lee SM, Schelcher C, Gashi S, Schreiber S, Thasler RM, Jauch KW, Thasler WE. RNA stability in human liver: comparison of different processing times, temperatures and methods. Mol Biotechnol. 2013;53(1):1-8.

Lenk GM, Tromp G, Weinsheimer S, Galtalica Z, Berguer R, Kuivaniemi H. Whole genome expression profiling reveals a significant role for immune function in human abdominal aortic aneurysms. BMC Genomics. 2007;8:237.

Levey AS and Coresh J. Chronic kidney disease. Lancet 2012;379:165-80.

Li PF, Dietz R, von Harsdorf R. Reactive oxyge species induce apoptosis of vascular smooth muschle cell. FEBS Lett. 1997;404(2-3):249-252.

Lim ST, Kim YK, Hwang JK, Kim SD, Park SC, Won YS, Park JS, Kim JI, Yun SS, Moon IS. A clinical consideration of abdominal aortic aneurysm rupture. Korean J Vasc Endovasc Surg 2011;27(3):103-107.

Limet R, Nusgens B, Verloes A, Sakalihasan N. Pathogenesis of abdominal aortic aneurysm (AAA) formation. Acta Chir Belg. 1998;98(5):195-8.

Limet R, Sakalihasan N, Albert A. Determination of the expansion rate and the incidence of rupture of abdominal aortic aneurysms. J Vasc Surg. 1991;14(4):540-548.

Lindholt JS, Shi GP. Chronic inflammation, immune response, and infection in abdominal aortic aneurysms. Eur J Vasc Endovasc Surg. 2006;31(5):453-63.

Lindholt JS, Vammen S, Juul S, Henneberg EW, Fasting H. The validity of ultrasonographic scanning as screening method for abdominal aortic aneurysm. Eur J Vasc Endovasc Surg. 1999;17(6):472-475.

Loetscher P, Moser B, Baggiolini M. Chemokines and their receptors in lymphocyte traffic and HIV infection. Adv Immuol. 2000;74:127-180.

Longo GM, Xiong W, Greiner TC, Zhao Y, Fiotti N, Baxter BT. Matrix metalloproteinases 2 and 9 work in concert to produce aortic aneurysms. Journal Clin Invest. 2002;110(5):625-32.

Lopez-Candales A, Hokmes DR, Liao S, Scott MJ, Wickline SA, Thompson RW. Decreased vascular smooth muscle cell density in medial degeneration of human abdominal aortic aneurysms. Am J Pathol. 1997;150(3):993-1007.

Lovegrove RE, Javid M, Magee TR, Galland RB. A meta-analysis of 21, 178 patients undergoing open or endovascular repair of abdominal aortic aneurysm. Br J Surg. 2008;95(6):677-684.

Maier A, Gee MW, Reeps C, Pongratz J, Eckstein HH, Wall WA. A comparison of diameter, wall stress, and rupture potential index for abdominal aortic aneurysm rupture risk prediction. Ann Biomed Eng. 2010;38(10):3124-3134.

Maier A. Computational modeling of rupture risk in abdominal aortic aneurysms. PhD Thesis, Lehrstuhl für Numerische Mechanik, Technische Universität München, Germany. 2012. ISBN 978-3-8439-1066-8.

Marini G, Maier A, Reeps C, Eckstein HH, Wall WA, Gee MW. A continuum description of the damage process in the arterial wall of abdominal aortic aneurysms. Int J Numer Meth Bio. 2012;28(1):87-99.

May J, White GH, Yu W, Ly CN, Waugh R, Stephen MS, Arulchelvam M, Harris JP. Concurrent comparison of endoluminal versus open repair in the treatment of abdominal aortic aneurysm: analysis of 303 patients by life table method. J Vasc Surg. 1998;27(2):213-20; discussion 220-1.

Mayne R. Collagenous proteins of blood vessels. Arteriosclerosis 1986;6(6):585-93.

McFarlane MJ. The epidemiologic necropsy for abdominal aortic aneurysm. JAMA. 1991;265(16):2085-8.

Menashi S, Campa JS, Greenhalgh RM, Powell JT. Collagen in abdominal aortic aneurysm: Typing, content, and degradation. J Vasc Surg. 1987;6(6):578-582.

Michel J, Ventura J, Egido J, Sakalihasan N, Treska V, Lindholt J, Allaire E, Thorsteinsdottie U, Cockerill G, Swedenborg J, FAD EU consortium. Novel aspects of the pathogenesis of Aneurysms of the Abdominal Aorta in humans. Cardiovasc Res. 2011;90(1):18-27.

Michineau S, Franck G, Wagner-Ballon O, Dai J, Allaire E, Gervais M. Chemokine (C-X-C Motif) receptor 4 blockade by AMD3100 inhibits experimental abdominal aortic aneurysm

expansion through anti-inflammatory effects. Arterioscler thromb Vasc boil. 2014;34(8):1747-55.

Moody WE, Edwards NC, Chue CD, Ferro CJ, Townend JN. Arterial disease in chronic kidney disease. Heart 2013;99(6):365-372.

Moore JE Jr, Ku DN, Zarins CK, Glagov S. Pulsatile flow visualization in the abdominal aorta under differing physiologic conditions implication for increased susceptibility to atherosclerosis. J Biomech Eng. 1992;114(3):391-7.

Morris GE, Hubbard CS, Quick CR. An abdominal aortic aneurysm screening programme for all males over the age of 50 years. Eur J Vasc Surg. 1994;8(2):156-160.

Murdoch C, Finn A. Chemokine receptors and their role in infectious diseases. Blood 2000;95(10):3025-3043.

Newby AC. Dual role of matrix metalloproteinases (matrixins) in intimal thickening and atherosclerotic plaque rupture. Physiol Rev. 2005;85:1-31.

Newman KM, Jean Claude J, Li H, Ramey WG, Tilson MD. Cytokines that activate proteolysis are increased in abdominal aortic aneurysms. Ciruculation 1994; 90(5 Pt 2):II224-7.

Ng K, Hildreth CM, Phillips JK, Avolio AP. Aortic stiffness is associated with vascular calcification and remodelling in a chronic kidney disease rat model. Am J Physiol Renal Physiol. 2011;300(6):F1431-6.

Nordon IM, Hinchliffe RJ, Loftus IM, Thompson MM. Pathophysiology and epidemiology of abdominal aortic aneurysms. Nat Rev Cardiol. 2011;8:92-102.

Norwood MG, Polimenovi NM, Sutton AJ, Bown MJ, Sayers RD. Abdominal aortic aneurysm repair in patients with chronic renal disease. Eur J Vasc Endovasc Surg. 2004;27(3):287-91.

Oberlin E, Amara A, Bachelerie F, Bessia C, Virelizier JL, Arenzana-Seisdedos F, Schwartz O, Heard JM, Clark-Lewis I, Legler DF, Loetscher M, Baggiolini M, Moser B. The CXC chemokine SDF-1 is the ligand for LESTR/fusin and prevents infection by T-cell-line-adapted HIV-1. Nature 1996;382(6594):833-835.

Ocaña E; Pérez-Requena J; Bohórquez JC; Brieva JA; Rodríguez C. Chemokine receptor expression on infiltrating lymphocytes from abdominal aortic aneurysm. Role of CXCR4-CXCL12 in lymphoid recruitment. Atherosclerosis 2008;200:264-270.

Okamoto R, Wagenseil J, DeLong W, Peterson S, Kouchoukos N, Sundt T. Mechanical Properties of Dilated Human Ascending Aorta. Ann Biomed Eng. 2002;30(5):624-635.

Osakabe T, Okada N, Wachi H, Sato A, Sasaki S, Wada N, Seyama Y. Quantitative changes of elastin, fibrillin and collagen in abdominal aortic aneurysms. Nihon Ronen Igakkai Zasshi. 2000;37(12):979-83.

Papaharilaou Y, Ekaterinaris JA, Manousaki E, Katsamouris AN. A decoupled fluid structure approach for estimating wall stress in abdominal aortic aneurysms. J Biomech. 2007;40(2):36-377.

Papalambros E, Sigala F, Georgopoulos S, Menekakos C, Giatromanolaki A, Bastounis E, Sivridis E. Immunohistochemical expression of metalloproteinases MMP-2 and MMP-9 in abdominal aortic aneurysms: correlation with symptoms and aortic diameter. Int J Mol Med. 2003;12(6):965-8.

Patel VI, Lancaster RT, Mukhopadhyay S, Aranson NJ, Conrad MF, LaMuraglia GM, Kwolek CJ, Cambria RP. Impact of chronic kidney disease on outcomes after abdominal aortic aneurysm repair. J Vasc Surg. 2012;56(5):1206-13.

Pelisek J, Assadian A, Sarkar O, Eckstein HH, Frank H. Carotid plaque composition in chronic kidney disease: a retrospective analysis of patients undergoing carotid endarterectomy. Eur J Vasc Endovasc Surg. 2010;39(1):11-16.

Pelisek J, Hahntow I, Eckstein HH, Ockert S, Reeps C, Heider P, Luppa PB, Frank H. Impact of chronic kidney disease on carotid plaque vulnerability. J Vasc Surg. 2011;54(6):1643-9.

Petersen E, Wågberg F, Angquist KA. Proteolysis of the abdominal aortic aneurysm wall and the association with rupture. Eur J Vasc Endovasc Surg. 2002;23(2):153-7.

Pierce DM, Maier F, Weisbecker H, Viertler C, Verbrugghe P, Famaey N, Fourneau I, Herijgers P, Holzapfel GA. Human thoracic and abdominal aortic aneurysmal tissues: Damage experiments, statistical analysis and constitutive modeling. J Mech Behav Biomed Mater. 2015;41:92-107.

Pleumeekers HJ, Hoes AW, van der Does E, van Urk H, Hofman A, de Jong PT, Grobbee DE. Aneurysm of the abdominal aorta in older adults. The Rotterdam Study. Am J Epidemiol. 1995;142(12):1291-9.

Powell JT, Brown LC, Forbes JF, Fowkes FG, Greenhalgh RM, Ruckley CV, Thompson SG. Final 12-year follow up of surgery versus surveillance in the UK Samll Aneurysm Trial. Br. J Surg. 2007;94(6):702-708.

Powell JT, Greenhalgh RM. Clinical practice. Small abdominal aortic aneurysms. N Engl J Med. 2003;348(19):1895-1901.

Proudfoot D, Skepper JN, Hegyi L, Bennett MR, Shanahan CM, Weissberg PL. Apoptosis regulates human vascular calcification in vitro: evidence for initiation of vascular calcification by apoptotic bodies. Circ Res. 2000;87(11):1055-62.

Raghavan ML, Fillinger MF, Marra SP, Naegelein BP, Kennedy FE. Automated methodology for determination of stress distribution in human abdominal aortic aneurysm. J Biochem Eng-Trans ASME 2005;127(5):868-71.

Raghavan ML, Hanaoka MM, Kratzberg JA, de Lourdes Higuchi M, da Silva ES. Biomechanical failure properties and microstructural content of ruptured and unruptured abdominal aortic aneurysms. J Biomech. 2011;44(13):2501-2507.

Raghavan ML, Vorp DA: Toward a biomechanical too to evaluate rupture potential of abdominal aortic aneurysm: identification of a finite strain consecutive model and evaluation of its applicability. J Biomech. 2000;33(4):475-482.

Raines EW. The extracellular matrix can regulate vascular cell migration, proliferation, and survival relationships to vascular disease. Int J Exp Pathol. 200;81(3):173-182.

Rausch SM, Martin C, Bornemann PB, Uhlig S, Wall WA. Material model of lung parenchyma based on living precision-cut lung slice testing. J Mech Behav Biomed Mater. 2011;4(4):583-92.

Réaux-Le Goazigo A, Van Steenwinckel J, Rostène W, Mélik Parsadaniantz S. Current status of chemokines in the adult of CNS. Prog Neurobiol. 2013;104:67-92.

Reed WW, Hallett JW, Damiano MA, Ballard DJ. Learning from the last ultrasound. A population-based study of patients with abdominal aortic aneurysm. Arch Intern Med. 1997;157(18):2064-2068.

Reeps C, Gee M, Maier A, Gurdan M, Eckstein HH, Wall WA. The impact of model assumptions on results of computational mechanics in abdominal aortic aneurysm. J Vasc Surg. 2010;51(3):679-88.

Reeps C, Gee MW, Pelisek J, Gurdan M, Wall WA, Schwaiger M, Eckstein HH, Essler M: The glucose metabolism in the vessel wall correlates with mechanical instability and inflammatory changes in a patient with a growing aneurysm of the abdominal aorta. Circ Cardiovasc Imaging 2009, 2(6):507-9.

Reeps C, Maier A, Pelisek J, Härtl F, Grabher-Meier V, Wall WA, Essler M, Eckstein HH, Gee MW. Measuring and modeling patient-specific distributions of material properties in abdominal aortic aneurysm wall. Biomech Model Mechanobiol. 2013;12(4):717-733.

Reeps C, Pelisek J, Seidl S, Schuster T, Zimmermann A, Kuehnl A, Eckstein HH. Inflammatory infiltrates and neovessels are relevant sources of MMPs in abdominal aortic aneurysm wall. Pathobiology 2009;76(5):243-52.

Rizzo RJ, McCarthy WJ, Dixit SN, Lilly MP, Shively VP, Flinn WR, Yao JS. Collagen types and matrix protein content in human abdominal aortic aneurysms. J Vasc Surg. 1989;10:365-373.

Safar ME, Struijker-Boudier HA. Cross-talk between macro- and microcirculation. Acta Physiol (Oxf). 2010;198(4):417-30.

Saint-Remy A, Somja M, Gellner K, Weekers L, Bonvoisin C, Krzesinski JM. Urinary and dietary sodium and potassium associated with blood pressure control in treated hypertensive kidney transplant recipients: an observational study. BMC nephrology 2012;13:121

Sakalihasan N, Heyeres A, Nusgens BV, Limet R, Lapière CM. Modifications of the extracellular matrix of aneurysmal abdominal aortas as a function of their size. Eur J Vasc Surg. 1993;7(6):633-7.

Sakalihasan N, Kuivaniemi H, Nusgens B, Durieux R, Defraigne JO. Aneurysm: Epidemiology Aetiology and Pathophysiology. In: McGloughlin T (ed.) Biomechanics and Mechanobiology of Aneurysms: Studies in Mechanobiology, Tissue Engineering and Biomaterials, pp 1-33. Springer Berlin Heidelberg, 2011.

Sakalihasan N, Limet R, Defawe OD. Abdominal aortic aneurysm. Lancet 2005;365(9470):1577-1589.

Salo JA, Soisalon-Soininen S, Bondestam S, Matilla PS. Familial occurrence of abdominal aortic aneurysm. Ann Intern Med. 1999;130(8):637-42.

Sandford RM, Bown MJ, Sayers RD, Fishwick G, London NJ, Nasim A. Endovascular abdominal aortic aneurysm repair: 5-year follow-up results. Ann Vasc Surg. 2008;22(3):372-378.

Schurink GW, Aarts NJ, van Bockel JH. Endoleak after stent-graft treatment of abdominal aortic aneurysm: a meta-analysis of clinical studies. Br J Surg. 1999;86(5):581-7.

Scott RA, Wilson NM, Ashton HA, Kay DN. Influence of screening on the incidence of ruptured abdominal aortic aneurysm: 5year results of a randomized controlled study. Br J Surg. 1995;82(8):1066-1070.

Shah PK. Inflammation, metalloproteinases, and increased proteolytic: an emerging pathophysiological paradigm in aortic aneurysm. Circulation 1997;96(7):2115-2117.

Shanahan CM, Crouthamel MH, Kapustin A, Giachelli CM. Arterial calcification in chronic kidney disease: key roles for calcium and phosphate. Circ Res. 2011;109(6):697-711.

Shimizu K, Libby P, Mitchell RN. Local cytokine environments drive aneurysm formation in allografted aortas. Trends in Cardiovasc Med. 2005;15(4):142-8.

Shimizu K, Mitchell RN, Libby P. Inflammation and cellular immune responses in abdominal aortic aneurysms. Arterioscler Thromb Vasc Biol. 2006;26(5):978-94.

Siegel CL, Cohan RH, Korobkin M, Alpern MB, Courney DL, Leder RA. Abdominal aortic aneurysms morphology: CT features in patients with ruptured and nonruptured aneurysms. AJR Am J Roentgenol. 1994;6(7):464-74.

Singh K, Bonaa KH, Jacobsen BK, Bjork L, Solberg Sl. Prevalence of and risk factors for abdominal aortic aneurysms in a population-based study: The Tromso Study. Am J Epidemiol. 2001;154(3):236-244.

Stam F, van Guldener C, Becker A, Dekker JM, Heine RJ, Bouter LM, Stehouwer CD. Endothelial dysfunction contributes to renal function-associated cardiovascular mortality in a population with mild renal insufficiency: the Hoorn study. J Am Soc Nephrol. 2006;17(2):537-45.

Stonebridge PA, Draper T, Kelman J, Howlett J, Allan PL, Prescott R, Ruckley CV. Growth rate of infrarenal aortic aneurysms. Eur J Vasc Endovasc Surg. 1996;11(1):70-73.

Sweeting MJ, Thompson SG, Brown LC, Powell JT, RESCAN collaborators. Meta-analysis of individual patient data to examine factors affecting growth and rupture of small abdominal aortic aneurysms. Br J Surg. 2012;99(5):655-665.

Takagi H, Manabe H, Kawai N, Goto SN, Umemoto T. Serum high-density and low-density lipoprotein cholesterol is associated with abdominal aortic aneurysm presence: a systematic review and meta-analysis. Int Angiol. 2010;29(4):371-375.

Tamarina NA, Grassi MA, Johnson DA, Pearce WH. Proteoglycan gene expression is decreased in abdominal aortic aneurysms. J Surg Res. 1998;74(1):76-80.

Tamarina NA, McMillan WD, Shively VP, Pearce WH. Expression of matrix metalloproteinases and their inhibitors in aneurysms and normal aorta. Surgery 1997;122(2):264-72.

Teicher BA, Fricker SP. CXCL12 (SDF-1)/CXCR4 pathway in cancer. Clin Cancer Res. 2010;16:2927-2931.

Thanos J, Rebeira M, Shragge BW, Urbach D. Vascular ultrasound screening for asymptomatic abdominal aortic aneurysm. Health Policy 2008;4(2):75-83.

Theocharis AD, Karamanos NK. Decreased biglycan expression and differential decorin localization in human abdominal aortic aneurysms. Atherosclerosis 2002;(2):221-30.

Theocharis AD, Tsolakis I, Hjerpe A, Karamanos NK. Human abdominal aortic aneurysm is characterized by decreased versican concentration and specific downregulation of versican isoform V(0). Atherosclerosis 2001;154(2):367-76.

Thompson M, Cockerill G. Matrix metalloproteinase-2. The forgotten enzyme in aneurysm pathogenesis. Annals NY Acad Sci. 2006;1085:170-4.

Thompson RW, Parks WC. Role of matrix metalloproteinases in abdominal aortic aneurysms. Ann N Y Acad Sci. 1996;800(1):157-74.

Töpel I, Norger N, Steinbauer M. Inflammatory disease of the aorta: Part 1: Non-infectious aortitis. Gefäßchirugie 2014; 19:169-180.

Trenner M, Haller B, Söllner H, Storck M, Umscheid T, Niedermeier H, Eckstein H-H. Twelve years of the quality assurance registry abdominal aortic aneurysm of the German vascular society (DGG)-Part 1: trends in therapy and outcome of non-ruptured abdominal aortic aneurysms in Germany between 1999 and 2010. Gefäßchirurgie 2013;18:206-2013.

Truijers M, Pol JA, Schultzekool LJ, van Sterkenburg SM, Fillinger MF, Blankensteijn JD. Wall stress analysis in small asymptomatic, symptomatic and ruptured abdominal aortic aneurysms. Eur J Vasc Endovasc Surg. 2007;33(4):401-407.

Tsamis A, Stergiopulos N. Arterial remodelling in response to increased blood flow using a constituent-based model. J Biomech. 2008;42(4):531-6.

United Kingdom Small Aneurysm Trial Participants (2002) Long-term outcomes of immediate repair compared with surveillance of small abdominal aortic aneurysms. N Engl J Med. 2002;346(19):1445–1452.

Valentine RJ, Decaprio JD, Castillo JM, Modrall JG, Jackson MR, Clagett GP. Watchful waiting in cases of small abdominal aortic aneurysms appropriate for all patients? J Vasc Surg. 2000;32(3):441-448.

Vallabhaneni SR, Gilling-Smith GL, How TV, Carter SD, Brennan JA, Harris PL. Heterogeneity of tensile strength and matrix metalloproteinase activity in the wall of abdominal aortic aneurysms. J Endovasc Ther. 2004;11(4):494-502.

van Dam EA, Dams SD, Peters GW, Rutten MC, Schurink GW, Buth J, van de Vosse FH. Non-linear viscoelastic behaviour of abdominal aortic aneurysm thrombus. Biomech Model Mechanoniol. 2008;72(2):127-137.

van der Rest M, Garrone R. Collagen family of proteins. FASEB J. 1991;5(13):2814-23.

Vande Geest JP, Di Martino ES, Bohra A, Makaroun MS, Vorp DA. A biomechanics-based rupture potential index for abdominal aortic aneurysm risk assessment: demonstrative application. Ann N Y Acad Sci. 2006; 1085:11-21.

Vande Geest JP, Sacks MS, Vorp DA. The effects of aneurysm on the biaxial mechanical behavior of human abdominal aorta. J Biomech. 2006;39(13):1324-34.

Vande Geest JP, Wang DH, Wisniewski SR, Makaroun MS, Vorp DA. Towards a noninvasive method for determination of patient-specific wall strength distribution in abdominal aortic aneurysms. Annals of Biomedical Engineering 2006; 34:1098–1106.

Vega de Céniga M, Gómez R, Estallo L, de la Fuente N, Viviens B, Barba A. Analysis of expansion patterns in 4-4.9 cm abdominal aortic aneurysms. Ann Vasc Surg. 2008;22(1):34-44.

Vega de Céniga M, Gómez R, Estallo L, Rodriguez L, Baquer M, Barba A. Growth rate and associated factors in small abdominal aortic aneurysms. Eur J Vasc Endovasc Surg. 2006;31(3):231-236.

Venkatasubramaniam AK, Fagan MJ, Mehta T, Mylankal KJ, Ray B, Kuhan G, Chetter IC, McCollum PT. A comparative study of aortic wall stress using finite element analysis for ruptured and non-ruptured abdominal aortic aneurysms. Eur J Vasc Endovasc Surg. 2004;28(2):168-176.

Verbeke FH, Pannier B, Guérin AP, Boutouyrie P, Laurent S, London GM. Flow-mediated vasodilation in end-stage renal disease. Clin J Am Soc Nephrol 2011;6(8):2009-15.

Villa-Bellosta R, Millan A, Sorribas V. Role of calcium-phosphate deposition in vascular smooth muscle cell calcification. Am J Physiol Cell Physiol 2011;300(1):C210-20.

Viola A, Luster AD. Chemokines and their receptors: drug targets in immunity and inflammation. Annu Rev Pharmacol Toxicol. 2008;48:171-97.

Vorp DA, Lee PC, Wang DH, Makaroun MS, Nemoto EM, Ogawa S, Webster MW. Association of intraluminal thrombus in abdominal aortic aneurysm with local hypoxia and wall weakening. J Vasc Surg. 2001;34(2):291-9.

Wagenseil JE, Mecham RP. Vascular extracellular matrix and arterial mechanics. Physiol Rev. 2009;89(3):957-989.

Wall WA, Gee MW. BACI - a multiphysics simulation environment. Technical report, Technische Universität München, 2014.

Wang DHJ, Makaroun MS, Webster MW, Vorp DA. Effect of intraluminal thrombus on wall stress in patient-specific models of abdominal aortic aneurysm. J Vasc Surg. 2002;36(3):598-604.

Wassef M, Baxter BT, Chisholm RL, Dalman RL, Fillinger MF, Heinecke J, Humphrey JD, Kuivaniemi H, Parks WC, Pearce WH, Platsoucas CD, Sukhova GK, Thompson RW, Tilson MD, Zarins CK. Pathogenesis of abdominal aortic aneurysms: a multidisciplinary research program supported by the National Heart, Lung, and Blood Institute. J Vasc Surg. 2001;34(4):730-8.

Wassef M, Upchurch GR, Kuivaniemi H, Thompson RW, Tilson MD III. Challenges and opportunities in abdominal aortic aneurysm research. J Vasc Surg. 2007;45(1):192-198.

White JV, Haas K, Phillips S, Comerota AJ. Adventitial elastolysis is a primary event in aneurysm formation. J Vasc Surg. 1993; 17(2):371-80; discussion 380-1.

Wills A, Thompson M, Crowther M, Saysers R, Bell P. Pathogenesis of abdominal aortic aneurysms-cellular and biochemical mechanisms. Eur J Vasc Endovasc Surg. 1996;12(4):391-400.

Wolf YG, Thomas WS, Brennan FJ, Goff WG, Sise MJ, Bernstein EF. Computed tomography scanning findings associated with rapid expansion of abdominal aortic aneurysm. J Vasc Surg. 1994;20(4):529-535.

Wolters BJ, Emmer M, Rutten MC, Schurink GW, van de Vosse FN. Assessment of endoleak significance after endovascular repair of abdominal aortic aneurysms: a lumped parameter model. Med Eng Phys. 2007;29(10):1106-1118.

Yamashita A, Noma T, Nakazawa A, Saito S, Fujioka K, Zempo N, Esato K. Enhanced expression of matrix metalloproteinase-9 in abdominal aortic aneurysms. World J Surg. 2001;25(3):259-65.

Zarins CK, White RA, Schwarten D, Kinney E, Diethrich EB, Hodgson KJ, Fogarty TJ. AneuRX stent graft versus open surgical repair of abdominal aortic aneurysm: multicenter prospective clinical trial. J Vasc Surg. 1999;29(2):292-308.

Zoungas S, Kerr PG, Chadban S, Muske C, Ristevski S, Atkins RC, McNeil JJ, McGrath BP. Arterial function after successful renal transplantation. Kidney Int. 2004;65(5):1882-1889.

Appendices

Appendix A: Detailed description of the mechanical experiment

As mentioned in chapter 2, section 2.8, the mechanical testings were conducted in the institute of "Mechanics and High Performance Computing Group, Technische Universität München", as part of a cooperation project (Reeps et al., 2013; Maier, 2012).

Mechanical testing was carried out to analyse AAA wall thickness, elastic properties, and failure load. Moreover, mechanical tests were performed on the complete wall compound, rather than separating the layers for testing. Samples were cleaned from loosely adherent thrombus deposition, if applicable, and then cut into individual rectangular specimens suitable for uniaxial tensile testing (typically 20mm x 8mm). The calcification grade of specimens was observed by naked eye and during cutting process; special awareness was paid to detect hard, calcified tissue constituents. Consequently, the specimens were categorized into "no calcification", minor calcification" and "major calcification" for later statistical analysis. Specimen orientation was deduced from the sample marking and documented. If possible, circumferential orientation was preferred to longitudinal orientation, since highest principal stresses in the AAA wall are usually oriented in circumferential direction. Specimen width was measured using digital calipers. Specimen thickness was averaged from five measuring points on the specimen surface using a Mitutoyo "Quick-Mini Series 700" digital thickness gauge (Mitutoyo, Kawasaki, Japan; Constant measure force = 0.5 N, measuring anvil diameter = 5 mm, accuracy = 20 µm). Elastic properties and failure load were investigated with uniaxial tensile tests using an ElectroForce 3100 tensile test machine (Bose Corporation, Eden Prairie, USA). The machine featured a maximum tensile force of 22 N and a maximum clamp displacement of 5 mm. The resolutions were 1 mN and 1 µm, respectively. Specimens were clamped at an initial clamp distance of 7.3 mm. For the measurement of elastic properties at a physiological stress-stretch range, the specimens were exposed to cyclic sinusoidal loading at frequency of f = 0.5 Hz and up to a stress of approximately P

= 0.20 MPa (depending on specimen thickness). 19 cycles were used for preconditioning; data from the 20th cycle was used for evaluation. Applied force and clamp displacement were continuously recorded at a sampling rate of 200 Hz. Subsequent to cyclic testing; specimens underwent destructive testing in order to measure their failure load. Therefore, the clamps were moved to their maximum displacement at a speed of 0.2 mm/s. Applied force and clamp displacement were recorded at a sampling rate of 40 Hz. Failure load was assessed as the maximum tensile force measured in this experiment. Specimens that slipped from the clamps during testing were excluded from the study. Specimens that ruptured close to the clamps were not excluded from the study since their failure loads were higher than average.

Appendix B: Measurement and equations of biomechanical parameters

Assessed clamp displacements and measured forces were converted into suitable stretch and stress measure: stretch was calculated as follow:

$$stretch = \lambda = \frac{\Delta x + l_0}{l_0} = \frac{x + l_{x=o}}{x_0 + l_{x=0}} \tag{1}$$

with Δx as the clamp displacement and l_0 the initial clamp distance. Stress was calculated in terms of the First Piola-Kirchhoff (1.PK) stress in testing direction:

$$stress = P_{11} = \frac{F}{A_0} \tag{2}$$

with F as measured force and A_0 as the initial cross sectional area of the specimen.

Biological tissues emphasize non-linear stress-stretch behaviour with an initially soft response followed by stiffening of the material. To explain this nonlinearity of the material, the obtained stress-stretch curves from the cyclic testing were used to fit a hyperelastic, incompressible and isotropic material model described by the strain energy function (SEF)

$$SEF = \Psi = \frac{\alpha}{6}(I_1 - 3) + \beta(I_1 - 3)^2 \tag{3}$$

as proposed by Raghavan and Vorp (2000). However the only difference to Raghavan and Vorp is the use of $\frac{\alpha}{6}$ instead of α. α [N/mm^2] and β [N/mm^2] are the sought material parameters, symbolised *alpha stiffness* and *beta stiffness*, describing the elastic properties of the individual specimen. Moreover α can be interpreted as the initial stiffness of the specimen at the load free state, while β represents the stiffness measured at the high region after the stiffening of the material e.g. under physiological prestretch due to diastolic blood pressure.

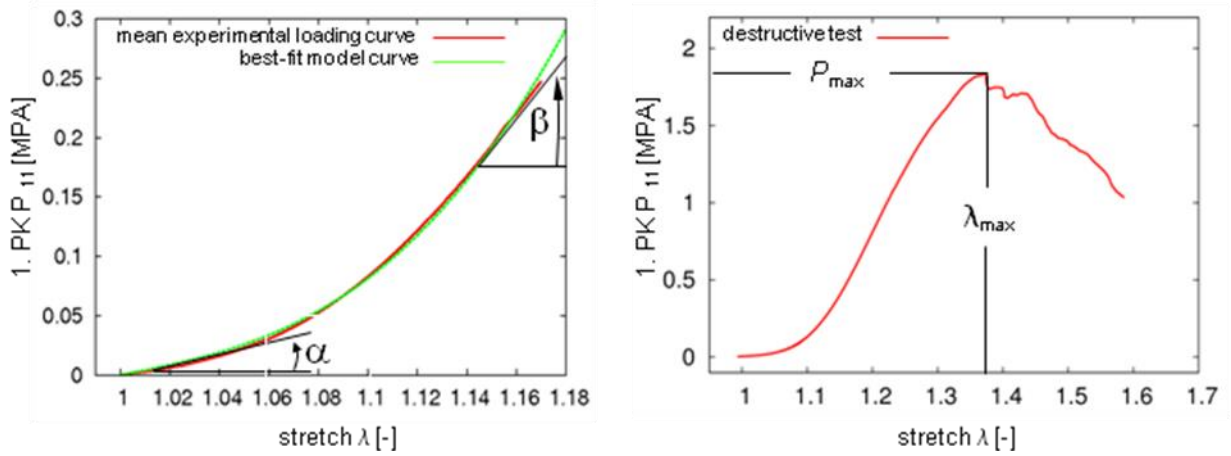

Figure B-1: Experimental stress-stretch curves of an AAA wall tissue sample assessed from tensile testing. **Left:** Curve obtained from the cyclic sinusoidal tensile test. The red curve represents the complete 20th cycle. The green curve represents the best fit model curve. It features characteristic nonlinear stress-stretch behaviour with initial soft response (alpha stiffness), followed by stiffening in the high stretch region (beta stiffness). **Right:** Curve obtained from destructive tensile test. The wall strength is defined as the maximum stress (Maier, 2012).

Following differentiation and under the assumption of an uniaxial stress state during testing, Eq. (3) can be transformed to a relation between P and λ:

$$P_{11} = \left(\frac{\alpha}{3} + 4\beta\left(\lambda^2 + 2\lambda^{-1} - 3\right)\right)\left(\lambda - \lambda^{-2}\right) \tag{4}$$

Using this formula, alpha and beta stiffness were then determined from the experimental data if each specimen utilizing a Levenberg-Marquardt curve fitting algorithm, a method to solve non-linear least squares problems.

Two failure measure, the strength and the failure tension, were derived from destructive testing. Specimen strength was assessed as maximum stress during the destructive test. $P_{\max}$ indicates the strength in terms of the 1. PK stresses:

$$strength = P_{\max} = \frac{F_{\max}}{A_0} \tag{5}$$

with $F_{\max}$ as the maximum force and A_0 as the initial cross sectional area of the specimen. The use of a strength formula for AAA rupture risk prediction is only reasonable if the actual wall thickness of a specific AAA is known. With an unknown wall thickness, e.g. the AAA geometry is obtained from the CT images, a strength measure that is independent of the actual wall thickness has to be used. To overcome this inadequacy, Raghavan et al. (2011) introduced the failure tension $T_{\max}$ as a second useful failure measure for AAA wall:

$$failure\,tension = T_{\max} = \frac{F_{\max}}{b_0} \tag{6}$$

Where b_0 is the specimen width in the undeformed configuration. Hence, the failure tension describes the resistance of the wall portion against the rupture, independent of the actual wall thickness. The stretch associated with $T_{\max}$ and $P_{\max}$ was considered as failure stretch $\lambda_{\max}$.

Accordingly, strength $\sigma_{\max}$ and failure tension $T_{\max,Cauchy}$ were obtained in terms of Cauchy stresses, respectively, as follow:

$$\sigma_{\max} = P_{\max} \cdot \lambda_{\max} \tag{7}$$

$$T_{\max,Cauchy} = T_{\max} \cdot \sqrt{\lambda_{\max}} \tag{8}$$

List of Publications

Christian Reeps, Sebastian Kehl, **Fadwa Tanios**, Jonas Biehler, Jaroslav Pelisek, Wolfgang A Wall, Hans-Henning Eckstein and Michael W Gee. Biomechanics and gene expression in abdominal aortic aneurysm. J Vasc Surg. 2014; 60(6):1640-7.

Fadwa Tanios, Michael W Gee, Jaroslav Pelisek, Sebastian Kehl, Jonas Biehler, Verena Grabher-Meier, Wolfgang A Wall, Hans-Henning Eckstein, Christian Reeps. Interaction of biomechanics with extracellular matrix components in abdominal aortic aneurysm. Eur J Vasc Endovasc Surg. 2015; 50(2):167-174.

Fadwa Tanios, Jaroslav Pelisek, Brigitta Lutz, Benedikt Reutersberg, Michael Kallmayer, Edouard Matevossian, Kristina Schwamborn, Volker Hösel, Hans-Henning Eckstein, Christian Reeps. CXCR4: a potential marker for inflammatory activity in abdominal aortic aneurysm wall. Eur J Vasc Endovasc Surg. 2015; 50 (6):745-53.

Yanshuo Han, **Fadwa Tanios**, Christian Reeps, Jian Zhang, Kristina Schwamborn, Hans-Henning Eckstein, Alma Zernecke, Jaroslav Pelisek. Histone acetylation and histone acetyltransferases show significant alteration in human abdominal aortic aneurysm. Clin Epigenetics. 2016; 8:3.

Jonas Biehler, Sebastian Kehl, Michael W Gee, **Fadwa Schmies**, Jaroslav Pelisek, Andreas Maier, Christian Reeps, Hans-Henning Eckstein, Wolfgang A Wall (2016). Probabilistic Non-Invasive Prediction of Wall Properties of Abdominal Aortic Aneurysms Using Bayesian Regression. Biomech Model Mechanobiol. 2016; 1-17.

Veronika Klaus, **Fadwa Schmies**, Christian Reeps, Matthias Trenner, Edouard Matevossian, Hans-Henning Eckstein, Jaroslav Pelisek. Association of MMP levels with collagen degradation in the context of AAA. Accepted by Eur J Vasc Endovasc Surg. January 2017.

Fadwa Schmies, Jaroslav Pelisek, Andreas Maier, Wolfgang A Wall, Michael W Gee, Hans-Henning Eckstein, Christian Reeps. Mechanical properties of abdominal aortic aneurysm wall assessed by tensile tests and finite element analysis are significantly inferior in patients with chronic kidney disease. In preparation.

Oral / Poster Presentations

Fadwa Tanios. Sind biomechanische Belastungen oder morphologische Faktoren relevant für die Genespression in der Wand des abdominalen Aortenaneurysmas? 17. Chirurgische Forschungstage 2013Frankfurt am Main, Deutschland, Oktober 4-5, 2013.

Fadwa Tanios, Michael W Gee, Verena Grabher-Meier, Jaroslav Pelisek, Andreas Maier, Jonas Biehler, Sebastian Kehl, Wolfgang A Wall, Hans-Henning Eckstein, Christian Reeps. Impact of extracellular matrix components on mechanical properties of abdominal aortic aneurysm wall. ESVS Spring Meeting, ESVS Spring Meeting, Vascular Biology, Materials & Engineering, UCL Institute of Child Health, London United Kingdom, May 16-17, 2014.

Fadwa Tanios, Jaroslav Pelisek, Brigitta Lutz, Benedikt Reutersberg, Hans-Henning Eckstein, Christian Reeps. CXCR4 activity in abdominal aortic aneurysm wall. Charing Cross, Vascular & Endovascular Controversies Update, London United Kingdom, 28 April-1 Mai, 2015.

Fadwa Tanios, Michael W Gee, Jaroslav Pelisek, Sebastian Kehl, Jonas Biehler, Verena Grabher-Meier, Wolfgang A Wall, Hans-Henning Eckstein, Christian Reeps. Interactions of biomechanics with extracellular matrix components in abdominal aortic aneurysm wall. 83rd European Atherosclerosis Society Congress, Glasgow, United Kingdom, March 22-25, 2015.

Jaroslav Pelisek, Yanshuo Han, **Fadwa Tanios**, Christian Reeps, Alma Zernecke, Hans-Henning Eckstein. Histone acetylation in human abdominal aortic aneurysm. 83rd European Atherosclerosis Society Congress, Glasgow, United Kingdom, March 22-25, 2015.